EFFECTS OF INTERNAL CONTACT SURFACES OF DENTAL IMPLANTS AND ABUTMENT SCREW SURFACE ROUGHNESS ON SCREW LOOSENING

A THESIS SUBMITTED TO
GRADUATE SCHOOL OF NATURAL AND APPLIED SCIENCES
OF
KOCAELİ UNIVERSITY

BY

ABDULRAHMAN MOHAMMED AL-SANEA

IN PARTIAL FULFILLMENT OF THE REQUIREMENTS
FOR
THE DEGREE OF MASTER OF SCIENCE
IN
BIOMEDICAL ENGINEERING

KOCAELİ 2023

EFFECTS OF INTERNAL CONTACT SURFACES OF DENTAL IMPLANTS AND ABUTMENT SCREW SURFACE ROUGHNESS ON SCREW LOOSENING

A THESIS SUBMITTED TO
GRADUATE SCHOOL OF NATURAL AND APPLIED SCIENCES
OF
KOCAELİ UNIVERSITY

BY

ABDULRAHMAN MOHAMMED AL-SANEA

IN PARTIAL FULFILLMENT OF THE REQUIREMENTS
FOR
THE DEGREE OF MASTER OF SCIENCE
IN
BIOMEDICAL ENGINEERING

Prof. Dr. Yasin KİŞİOĞLU		
Supervisor,	**Kocaeli University**	**.....**
Assoc. Prof. Dr. Talip ÇELİK		
Jury member	**Kocaeli University**	**.....**
Prof. Dr. Kadir GÖK		
Jury member	**Bakırçay University**	**.....**

Thesis Defense Date: 21/06/2023

ETHICAL STATEMENT AND RESEARCH FUND SUPPORT

In this thesis/project study, which I prepared in accordance with the thesis writing rules of Kocaeli University Graduate School of Natural and Applied Sciences,

I declare that,

- This thesis/project is my own and an original work,
- I act in accordance with scientific ethical principles and rules at all stages of my study, including preparation, data collection, analysis, and presentation of information,
- I have cited all data and information obtained within the scope of this study and that I have included these sources in the bibliography,
- This study complies with the similarity criteria determined by the Graduate School of Natural and Applied Sciences of Kocaeli University in terms of the plagiarism software to which Kocaeli University is subscribed,
- I have not done any falsification of the data used,
- I have not submitted any part of this thesis/project as another thesis/project work at this university or another university.

☐ Any stage of this thesis/project work has not been provided any financial/infrastructural support by any institution/organization.

☑ The data and information produced within the scope of this thesis/project work were carried out by the Scientific Research Projects Coordination Unit of Kocaeli University with the financial/infrastructure support within the scope of the project number FYL-2022-3028

I declare that I accept all the moral and legal consequences at any time that may arise regarding my work in the event of situation contrary to this statement.

.....

Abdulrahman Mohammed AL-SANEA

PUBLISHING AND INTELLECTUAL PROPERTY RIGHTS

I declare that I have given Kocaeli University the permission to archive all, or any part of my graduate thesis/project approved by the Graduate School of Natural and Applied Sciences, in printed and electronic format, and make it available for use at the conditions specified as follows. Within this permission, all intellectual property rights except for the usage rights granted by Kocaeli University will remain with me and the usage rights of all or a part of my thesis/project in future studies such as articles, books, communiqués, licenses, patents is my own on condition both that the name of my advisor is reserved and within the knowledge of both parties.

I declare and undertake that the thesis/project is my own original work, that I have not violated the rights of others and that I am the only authorized owner of my thesis/project. I undertake to use the copyrighted texts in my thesis, which must be used with written permission from their owners, with written permission, and to submit copies of them to the University when requested.

Within the scope of the ***"Directive on Collecting, Organizing and Making Access to Graduate Theses in Electronic Environment"*** published by the Council of Higher Education (CoHE), my thesis is made available in the CoHE National Thesis Center / Kocaeli University Libraries Open Access System, except for the conditions stated below.

☐ With the decision of the institute board of directors, the opening of my thesis/project to access has been postponed for 2 years from the date of graduation.

☑ With the reasoned decision of the institute board of directors, the opening of my thesis/project to access has been postponed for 6 months from the date of graduation.

☐ No confidentiality decision has been made regarding my thesis/project.

.....

Abdulrahman Mohammed AL-SANEA

PREFACE AND ACKNOWLEDGEMENT

I am extremely grateful to Allah for granting me the strength and persistence to successfully complete my Master's thesis. The journey of this research project has been both challenging and rewarding, and I owe my success to the unwavering support of numerous individuals.

First and foremost, I would like to express my deepest gratitude to my thesis supervisor, Prof. Dr. Yasin KİŞİOĞLU, whose supervision, guidance, and encouragement have been fundamental in shaping this work. Additionally, I would like to extend my heartfelt thanks to Assoc. Prof. Dr. Talip ÇELIK and Asst. Prof. Dr. Serkan AKTAŞ for their invaluable support throughout the process. Their expertise and assistance have significantly contributed to the success of this research.

I am also thankful to the esteemed faculty and staff of the biomedical engineering department at Kocaeli University for providing an enriching academic environment. Their dedication to teaching and research has been truly inspiring and has left an indelible impact on my academic and personal growth.

My family has been a pillar of support throughout my academic journey. I am immensely grateful to my parents for their unconditional love, encouragement, and sacrifices, which have made it possible for me to pursue my dreams. To my siblings, thank you for your constant belief in me and for always being there when I needed you the most. To my wife, whose support, understanding, and love have been a constant source of inspiration and strength throughout this journey, I am profoundly grateful for your unwavering faith in me.

Lastly, I would like to acknowledge the financial support provided by the Scientific Research Projects Coordination Unit of Kocaeli University with Project Number FYL-2022-3028, Uzunciftlik Nuh Cimento Vocational High School, and the Biomechanics Lab in the Biomedical Engineering Department at Kocaeli University, without which this research would not have been possible.

In conclusion, I dedicate this thesis to all those who have contributed to my growth as a researcher and as a person. Your collective impact has been profound, and I am eternally grateful.

June - 2023 Abdulrahman Mohammed AL-SANEA

CONTENTS

ETHICAL STATEMENT AND RESEARCH FUND SUPPORT i
PUBLISHING AND INTELLECTUAL PROPERTY RIGHTS ii
PREFACE AND ACKNOWLEDGEMENT iii
CONTENTS iv
LIST OF FIGURES vi
LIST OF TABLES ix
INDEX OF SYMBOLS AND ABBREVIATIONS x
ABSTRACT xi
ÖZET xiii
GENIŞLETILMIŞ TÜRKÇE ÖZET xv
1. INTRODUCTION 1
1.1. Problem Statement 1
1.2. Objective 1
1.2.1. General Objective 1
1.2.2. Specific Objectives 2
1.3. Thesis Layout 2
2. LITERATURE REVIEWS 3
2.1. Dental Implant Systems 3
2.1.1. Endosseous Screw-Shaped Implants 3
2.1.1.1. One-piece implants 3
2.1.1.2. Two-piece implants 4
2.2. Screw Loosening 4
2.2.1. Screw Loosening in Implant-Supported Prostheses 5
2.2.2. Screw Loosening: Statistical Insights 5
2.2.3. Factors and Parameters Influencing Abutment Screw Loosening 6
2.2.4. Preventing Screw Loosening Techniques 7
2.2.4.1. Silicone Plug 7
2.3. Surface Roughness 8
2.3.1. Surface Modification Techniques and Screw Loosening 11
2.4. Screw Thread Manufacturing Techniques 12
2.5. Finite Element Method (FEM) 12
3. METHODOLOGY 14
3.1. Computational Study: Finite Element Analysis 14
3.1.1. Research Hypothesis 14
3.1.2. FE Model Generation 15
3.1.3. Static Test 16
3.1.4. Modal Analysis 19
3.1.5. Statistical Analyses 20
3.2. Experimental study: Manufacturing and Testing Methods 20
3.2.1. Research Hypothesis 20
3.2.2. Implant Materials 20
3.2.3. Dental Implant Geometry 21
3.2.4. Dental Implant Manufacturing Procedures 22
3.2.4.1. Abutment Screw Manufacturing Methods 22
3.2.4.1.1. Machining Method 22
3.2.4.1.2. Die Method 25

3.2.4.1.3. Thread Rolling Method 28
3.2.4.2. Screw Head Formation 31
3.2.4.3. Abutment Manufacturing 32
3.2.4.4. Implant Manufacturing 33
3.2.4.4.1. Production of Internal Threads in Implants 33
3.2.5. Assembled Model of Dental Implant 34
3.2.6. Analysis Tests and Measurements 34
3.2.6.1. Surface Roughness Assessment (Contour Measurements) 34
3.2.6.2. Vibration Test and Torque Loss Assessment 36
3.2.6.3. Scanning Electron Microscopy (SEM) Analysis 37
3.2.6.4. Statistical Analyses 38
4. RESULTS AND DISCUSSIONS 39
4.1. Results 39
4.1.1. Computational Study Results 39
4.1.2. Experimental Study Results 44
4.1.2.1. Surface Roughness Assessment Results 44
4.1.2.2. Torque and Vibration Tests Results 49
4.1.2.3. SEM Analysis Results 52
4.1.2.4. Statistical Analysis Results 52
4.2. Discussions 59
4.2.1. Computational Study Discussion 59
4.2.2. Experimental Study Discussion 62
5. CONCLUSIONS AND RECOMMENDATIONS 66
5.1. Conclusions 66
5.2. Recommendations 66
REFERENCES 68
APPENDIXES 77
PUBLICATIONS AND WORKS 84
BIOGRAPHY 85

LIST OF FIGURES

Figure 2.1. One-piece dental implant....3
Figure 2.2. Multi-parts dental implant and its structure....4
Figure 2.3. A, Polyvinyl siloxane, cotton pellet, and composite. B, Temporary composite over head of screw and dimples in angled abutment....7
Figure 2.4. A, Access canal and hex portion of screw head with antirotational grooves, B, Dimples. C, Placement and direction of rotation (arrows) of root canal filler....8
Figure 2.5. Schematic of a surface profile z(x)....10
Figure 3.1. Implant design parameters investigated....15
Figure 3.2. Figure 3.2. Three-dimensional computer-aided design models used with different parameters. A, Abutment screw lengths: 4 mm (L1), 5 mm (L2), and 6 mm (L3). B, Abutment screw head diameters: 2.65 mm (D1), 2.75 mm (D2), and 2.85 mm (D3). C, Abutment implant angles: 30 degrees (θ1), 45 degrees (θ2), and 60 degrees (θ3). D, Assembled model. E, mesh model....15
Figure 3.3. A, Abutment screw design parameters values used. B, Interface between abutment screw and screw channel....17
Figure 3.4. Boundary conditions. A, Screw preload 542 N. B, Load applied to upper surface of abutment 200 N. C, Fixed support (external surface of implant)....18
Figure 3.5. 6-mm metal rods of grade 5 Ti alloy....21
Figure 3.6. Final design of dental implant before being manufactured....21
Figure 3.7. Computer Numerical Control (CNC) machine used....22
Figure 3.8. Process of manufacturing abutment screw using the CNC lathe machine. A, Workpiece setup. B, Screw blank. C, Machined screw....24
Figure 3.9. Group of machined screws (10 samples)....24
Figure 3.10. A die tool used for cutting external threads on a screw blank by forcing it through the die's form....25
Figure 3.11. A screw blank of the desired length and size (M4x12) produced through the machining method....25
Figure 3.12. Aligning the die perpendicular to the workpiece's longitudinal axis for accurate and consistent thread formation....26
Figure 3.13. Illustration of the thread cutting process with clockwise die rotation (yellow arrow)....27
Figure 3.14. Completion of the threading process at desired thread length (L_t=10 mm)....27
Figure 3.15. Group of die screws (10 samples)....28
Figure 3.16. Figure 3.16. Thread rolling machine used. A, Final setup of the thread rolling machine for screw production. B, A pressure gauge, serving as a position switch. C, A screw blank between two flat dies)....29
Figure 3.17. A Group of screw blanks before being threaded using the thread rolling method....30
Figure 3.18. Group of thread rolled screws (10 samples)....30
Figure 3.19. All machined, die, and thread-rolled screws (30 samples) produced....30
Figure 3.20. Milling machine used to produce a specific driver type and

form a screw head.....31
Figure 3.21. A, Manufacturing a specific type of driver using milling machine. B, Final shape of the specific driver.....31
Figure 3.22. Screw head formation using milling machine.....32
Figure 3.23. Two abutment screws showing manufacturing failure at the screw head 32
Figure 3.24. Group of abutments produced using the CNC machine.....32
Figure 3.25. Group of implants produced using the CNC machine.....33
Figure 3.26. Taps used for creating the internal threads of implants. (A) Cutting tap, (B) Rolling tap.....33
Figure 3.27. Different types of implants. A, Machined implants. B, Thread rolled implants.....34
Figure 3.28. The completed assembly of the dental implant model.....34
Figure 3.29. Contour measuring device used to measure surface roughness of dental implant screw.....35
Figure 3.30. The digital torquemeter used for the assessment of torque losses in screw samples.....36
Figure 3.31. A vibrator device used. A, 4 nuts to increase the effect of a force applied. B, Metal circle to increase the effect of vibration. C, Abutment. D, Implant. E, Holder.....37
Figure 3.32. Scanning electron microscope (SEM) used.....38
Figure 3.33. Two screw samples from each group were analyzed using SEM.....38
Figure 4.1. Stress distribution in one model. A, Implant. B, Abutment. C, Abutment screw.....39
Figure 4.2. A-C, Main effect of abutment implant angle (θ), abutment screw head diameter (D), and abutment screw length (L) at each level of maximum stresses of implant components, total deformation, and natural frequency for all models.....42
Figure 4.3. Profilogram of sample M1 (machined screw), showing thread pitch, angle, and depth.....45
Figure 4.4. Profilogram of sample M2 (machined screw), showing thread pitch, angle, and depth. The marked areas (indicated by small black squares) highlight regions of surface texture, indicating the lower surface roughness of this sample compared to samples D1 and D2.....46
Figure 4.5. Profilogram of sample D1 (Die screw), showing thread pitch, angle, and depth.....46
Figure 4.6. Profilogram of sample D2 (die screw), showing thread pitch, angle, and depth. The marked areas (indicated by small black squares) highlight regions of significant surface irregularities, indicative of the higher surface roughness of this screw sample.....47
Figure 4.7. Profilogram of sample TR1 (thread rolled screw), showing thread pitch, angle, and depth.....47
Figure 4.8. Profilogram of sample TR2 (thread rolled screw), showing thread pitch, angle, and depth. The marked areas (indicated by small black squares) show regions with moderate surface irregularities, representing the medium surface roughness of this sample compared to the other samples. The dashed line

represents the mean line, which is used as a reference for surface roughness measurements....48
Figure 4.9. SEM images of machined screw sample M1 at different amplifications (X25, X200, and X1000) 53
Figure 4.10. SEM images of machined screw sample M2 at different amplifications (X10, X25, X 100, X200, and X1000)....54
Figure 4.11. SEM images of two different regions of thread rolled screw sample TR1 at different amplifications (X25, X100, X200, and X1000 X1000)....55
Figure 4.12. SEM images of thread rolled screw sample TR2 at different amplifications (X10, X25, X100, X200, and X1000)....56
Figure 4.13. SEM images of two different regions of die screw sample D1 at different amplifications (X25, X100, X200, X1000, and X5000).....57
Figure 4.14. SEM images of die screw sample D2 at different amplifications (X10, X25, X100, X200, X1000, and X5000)....58
Figure 4.15. Variation in intersection point between screw thread and screw slot at different abutment implant angles. A, 30 degrees. B, 45 degrees. C, 60 degrees....61
Figure 4.16. Surface irregularities and micro-imperfections on the rounded crest of screw M1, Machined screw. TR1, Thread-rolled screw. D1, Die screw....64
Figure 4.17. SEM images revealing different surface irregularities on screw surface. M1, Machined screw. TR1, Thread-rolled screw. D1, Die screw....64

LIST OF TABLES

Table 2.1. Center-Line Average and Roughness Grades.....11
Table 3.1. Combinations of abutment implant angle (θ), abutment screw head diameter (D), abutment screw length (L) with model nodes and elements numbers used in this work.....16
Table 3.2. Measurements and preload value for model.....17
Table 3.3. Material properties used in this analysis.....18
Table 3.4. Materials used for manufacturing dental implants.....21
Table 4.1. Maximum von Mises stress of implant components, total deformation and natural frequency for all models.....40
Table 4.2. K independent Kruskal-Wallis test *P* values (significance level at *P*<.05).....41
Table 4.3. Multiple pairwise comparisons using Dunn test *P* values (significance level at *P*<.05).....41
Table 4.4. Thread characteristics of different abutment screw samples.....44
Table 4.5. Surface roughness parameters for different abutment screw samples.....49
Table 4.6. Torque, detorque, and torque loss measurements before and after vibration test for machined screws paired with machined implants.....49
Table 4.7. Torque, detorque, and torque loss measurements before and after vibration test for machined screws paired with thread-rolled implants.....50
Table 4.8. Torque, detorque, and torque loss measurements before and after vibration test for thread rolled screws paired with machined implants.....51
Table 4.9. Torque, detorque, and torque loss measurements before and after vibration test for thread rolled screws paired with thread-rolled implants.....51
Table 4.10. Torque, detorque, and torque loss measurements before and after vibration test for die screws paired with machined implants.....52
Table 4.11. Torque, detorque, and torque loss measurements before and after vibration test for die screws paired with thread-rolled implants.....52
Table 4.12. Torque loss comparisons using one-way ANOVA and independent samples T-test *P* values (significance level at *P*<.05).....53

INDEX OF SYMBOLS AND ABBREVIATIONS

P	: Thread pitch (mm)
T	: Tightening Torque (Nmm)
θ	: Abutment Implant Angle (deg)
D	: Abutment Screw Head Diameter (mm)
L	: Abutment Screw Length (mm)
L_t	: Thread length (mm)
μ_t	: Coefficient of Friction for the Threads
μ_n	: Coefficient of Friction for the Screw Head
d_2	: Pitch Diameter of the Thread (mm)
d_n	: Major Diameter of the Thread (mm)
β	: Flank Angle (deg)
F	: Screw Preload (N)
μ	: Coefficient of Friction
σ	: Variance
Ra	: Average Roughness (mm)
Rq	: Root Mean Square Roughness (mm)
Rz	: Maximum Height of the Profile (mm)
M1	: Machined Screw Sample 1
M2	: Machined Screw Sample 2
D1	: Die Screw Sample 1
D2	: Die Screw Sample 2
TR1	: Thread-Rolled Screw Sample 1
TR2	: Thread-Rolled Screw Sample 2
M	: Machined Implant
TR	: Thread Rolled Implant
M4	: Metric Four Screw Size

Abbreviations

3D	: Three Dimensions or Three-Dimensional
ANSI	: American National Standards Institute
CAD	: Computer-Aided Design
CNC	: Computer Numerical Control
EB-PVD	: Electron Beam Physical Vapor Deposition
FE	: Finite Element
FEA	: Finite Element Analysis
Hz	: Hertz
ISO	: International Organization for Standardization
PEEK	: Polyetheretherketone
PNT	: Plasma Nitriding Treatment
PTFE	: Polytetrafluoroethylene
SEM	: Scanning Electron Microscopy
TiN	: Titanium Nitride
WC	: Tungsten Carbide

EFFECTS OF INTERNAL CONTACT SURFACES OF DENTAL IMPLANTS AND ABUTMENT SCREW SURFACE ROUGHNESS ON SCREW LOOSENING

ABSTRACT

Dental implants have revolutionized dentistry; however, complications such as screw loosening remain persistent challenges for manufacturers, dentists, and patients. This research aimed to comprehensively investigate the factors affecting screw loosening in dental implants, with a specific focus on the effects of internal contact surfaces and screw surface roughness. To achieve this, a two-pronged approach of computational modeling and experimental analysis was employed.

The computational study utilized 3-dimensional (3D) finite element analysis (FEA) to evaluate and compare the mechanical effects of the abutment implant angle (θ), the abutment screw head diameter (D), and the abutment screw length (L) on screw loosening. A total of 27 models presenting various mechanical scenarios were built by using combinations of three different abutment implant angles (30 degrees, 45 degrees, and 60 degrees), abutment screw head diameters (2.65 mm, 2.75 mm, and 2.85 mm), and abutment screw lengths (4 mm, 5 mm, and 6 mm). In FEA, a static test with a 200-N force inclined 30 degrees in the implant axial direction was applied to the upper surface of the abutment in order to evaluate and compare the maximum von Mises stresses of the implant components and the maximum total deformation in all models. In addition, modal analysis was applied to identify the natural frequencies in all models under free (unforced) vibration, and a Kruskal-Wallis statistical test (α=.05) was performed followed by multiple pairwise comparisons using the Dunn test. The Kruskal-Wallis test demonstrated a significant influence of the abutment implant angle on implant stress, total deformation, and natural frequency (P<.001). For example, increasing the abutment implant angle from 30 degrees to 45 degrees and 60 degrees can considerably reduce the model's natural frequencies to 18% and 26%, respectively. Similarly, the test underscored the significant impact of the abutment screw head diameter on both abutment screw stress and abutment stress (P=.010 and P=.002, respectively). However, the abutment screw length appeared to have no significant effect on any of the dependent variables (P>.05). The 3D FEA study concluded that the abutment implant angle and the abutment screw head diameter significantly influenced the stresses of dental implant components, total deformation, and natural frequency of the model, which may impact the mechanical stability of the screw joint. Nevertheless, the abutment screw length does not appear to significantly affect these values.

Simultaneously, an experimental study was conducted to investigate the effect of dental implant abutment screw surface roughness on screw loosening. A total of 30 M4-sized screws, made of grade 5 titanium alloy (Ti-6Al-4V), were manufactured using machining, thread rolling, and die methods. Additionally, six steel abutments, six steel implants with internal threads created using cutting and thread rolling taps, and an aluminum holder

were fabricated. The surface roughness of six abutment screws, two from each group, was assessed using a contour measuring device and scanning electron microscopy (SEM). Furthermore, the torque losses of each group's samples were evaluated before and after a vibration test by using a digital torque meter. Each group was divided into two subsets: one subset was paired with machined implants, and the other was paired with thread-rolled implants. In this process, a dental implant was secured in a holder, and each abutment screw was tightened to approximately 100 Ncm, and a 24-hour vibration test was conducted at a frequency of 75 Hz. Post-vibration, the implant was detorqued to measure torque loss. A one-way ANOVA and an independent samples t-test (α=.05) were conducted. Machined screws, thread-rolled screws, and die screws exhibited an average total torque loss of 3.51%, 5.12%, and 7.53% when paired with machined implants, and 2.42%, 4.32%, and 6.27% when paired with thread-rolled implants, respectively. Furthermore, detailed SEM images revealed distinct differences in surface roughness among these screws. For example, machined screws exhibited lower surface roughness compared to thread-rolled and die screws. In contrast, die screws demonstrated higher surface roughness, a finding consistent with the profilograms obtained. Statistically, the one-way ANOVA and the independent samples t-test revealed a significant influence of the abutment screw type on the total torque loss (P<.05). Moreover, the implant type had a significant effect on the torque loss values before and after the vibration test (P<.05). In conclusion, a correlation was found between abutment screw surface roughness and screw loosening. Importantly, machined screws demonstrated less loosening compared to thread-rolled screws and die screws, which can be attributed to the lower surface roughness. Moreover, it was found that modifying the internal threading process of the implant and adjusting the surface roughness of the screws could control screw loosening effectively.

Keywords: Dental Implants, Finite Element Analysis, Internal Contact Surfaces, Screw Loosening, Surface Roughness, Thread Rolling.

DIŞ İMPLANTLARIN İÇ TEMAS YÜZEYLERİNİN VE DAYANAK VİDASI YÜZEY PÜRÜZLÜLÜĞÜNÜN VİDA GEVŞEMESİ ÜZERİNDEKİ ETKİLERİ

ÖZET

Diş implantları dişçiliği devrimleştirdi; ancak vida gevşemesi gibi komplikasyonlar üreticiler, dişçiler ve hastalar için sürekli zorluklar oluşturmaya devam etmektedir. Bu araştırma, diş implantlarında vida gevşemesini etkileyen faktörleri kapsamlı bir şekilde incelemeyi amaçlamaktadır, özellikle iç temas yüzeylerinin ve vida yüzey pürüzlülüğünün etkileri üzerine odaklanmaktadır. Bunu başarmak için, hesaplamalı modelleme ve deneysel analiz olmak üzere iki uçlu bir yaklaşım kullanılmıştır.

Bu hesaplamalı çalışma, 3 boyutlu (3D) sonlu eleman analizi (FEA) kullanarak, vidanın gevşemesi üzerindeki mekanik etkileri değerlendirmek ve karşılaştırmak için abutment implant açısı (θ), abutment vida başı çapı (D) ve abutment vida uzunluğu (L)'nun mekanik etkilerini değerlendirdi. Toplamda, üç farklı abutment implant açısı (30 derece, 45 derece ve 60 derece), abutment vida başı çapları (2,65 mm, 2,75 mm ve 2,85 mm) ve abutment vida uzunlukları (4 mm, 5 mm ve 6 mm) kombinasyonları kullanılarak çeşitli mekanik senaryoları sunan 27 model oluşturuldu. FEA'da, tüm modellerde implant bileşenlerinin maksimum von Mises gerilmelerini ve maksimum toplam deformasyonunu değerlendirmek ve karşılaştırmak için abutmentin üst yüzeyine implant aksiyal yönünde 30 derece eğik 200-N kuvveti ile statik bir test uygulandı. Ayrıca, tüm modellerde serbest (zorlamasız) titreşim altındaki doğal frekansları belirlemek için modal analiz uygulandı ve bir Kruskal-Wallis istatistiksel testi (α=.05) gerçekleştirildi, ardından Dunn testi kullanılarak çoklu ikili karşılaştırmalar yapıldı. Kruskal-Wallis testi, abutment implant açısının implant gerilmesi, toplam deformasyon ve doğal frekans üzerinde önemli bir etkiye sahip olduğunu gösterdi (P<.001). Örneğin, abutment implant açısını 30 dereceden 45 dereceye ve 60 dereceye artırma, modelin doğal frekanslarını sırasıyla %18 ve %26 oranında önemli ölçüde azaltabilir. Benzer şekilde, test, abutment vida başı çapının hem abutment vida gerilmesi hem de abutment gerilmesi üzerinde önemli bir etkisi olduğunu vurguladı (sırasıyla P=.010 ve P=.002). Ancak, abutment vida uzunluğunun bağımlı değişkenlerden herhangi biri üzerinde anlamlı bir etkisi görünmemektedir (P>.05). 3D FEA çalışması, abutment implant açısının ve abutment vida başı çapının, diş implant bileşenlerinin gerilmeleri, toplam deformasyon ve modelin doğal frekansı üzerinde önemli bir etkisi olduğunu sonucuna vardı, bu da vida eklemi

Aynı anda, diş implantı abutment vidası yüzey pürüzlülüğünün vidanın gevşemesi üzerindeki etkisini araştırmak için deneysel bir çalışma gerçekleştirildi. grade 5 titanyum alaşımlı (Ti-6Al-4V) 30 adet M4 boyutunda vida, talaş, pafta ve ovalama yöntemleri kullanılarak üretildi. Ayrıca, altı çelik abutment, kesme ve diş açma burguları kullanılarak iç diş oluşturulan altı çelik implant ve bir alüminyum tutucu üretildi. Her gruptan ikişer olan altı abutment vidasının yüzey pürüzlülüğü, bir kontur ölçüm cihazı ve taramalı elektron mikroskobu (SEM) kullanılarak değerlendirildi. Ayrıca, her grubun örneklerinin

tork kayıpları, bir dijital tork metre kullanılarak titreşim testinden önce ve sonra değerlendirildi. Her grup, tornalanmış implantlarla eşleştirilen bir alt gruba ve diş açmalı implantlarla eşleştirilen diğer bir alt gruba ayrıldı. Bu işlemde, bir diş implantı bir tutucuda sabitlendi ve her abutment vidası yaklaşık 100 Ncm'ye sıkıldı ve 75 Hz frekansta 24 saatlik bir titreşim testi yapıldı. Titreşimden sonra, implantın torku gevşetildi. Tek yönlü ANOVA ve bağımsız örnekler t-testi (α=.05) gerçekleştirildi. Tornalanan vidalar, diş açma vidaları ve kalıp vidaları sırasıyla tornalanan implantlarla eşleştirildiğinde ortalama toplam tork kaybı %3.51, %5.12 ve %7.53 ve diş açmalı implantlarla eşleştirildiğinde %2.42, %4.32 ve %6.27 olarak belirlendi. Ayrıca, detaylı SEM görüntüleri, bu vidalar arasında yüzey pürüzlülüğünde belirgin farklar ortaya koydu. Örneğin, tornalanan vidalar, diş açma ve kalıp vidalarına göre daha düşük yüzey pürüzlülüğü sergiledi. Buna karşılık, kalıp vidaları daha yüksek yüzey pürüzlülüğü gösterdi, bu bulgu elde edilen profilogramlarla tutarlıydı. İstatistiksel olarak, tek yönlü ANOVA ve bağımsız örnekler t-testi, abutment vidası tipinin total tork kaybı üzerinde önemli bir etkiye sahip olduğunu ortaya koydu (P<.05). Ayrıca, implant tipinin, titreşim testinden önce ve sonra tork kaybı değerleri üzerinde önemli bir etkisi olduğu bulundu (P<.05). Sonuç olarak, abutment vidası yüzey pürüzlülüğü ile vidanın gevşemesi arasında bir ilişki bulundu. Özellikle, talaşlı vidalar, paftalı ve ovalamalı vidalarına göre daha az gevşeme gösterdi ve bu, daha düşük yüzey pürüzlülüğüne atfedilebilir. Ayrıca, implantın iç dişleme işlemini değiştirerek ve vidaların yüzey pürüzlülüğünü ayarlayarak vidanın gevşemesinin etkili bir şekilde kontrol edilebileceği bulundu.

Anahtar Kelimeler: Dental Implantlar, Iç Temas Yüzeyleri, Ovalama, Sonlu Elemanlar Analizi, Vida Gevşemesi, Yüzey Pürüzlülüğü.

DIŞ İMPLANTLARIN İÇ TEMAS YÜZEYLERİNİN VE DAYANAK VİDASI YÜZEY PÜRÜZLÜLÜĞÜNÜN VİDA GEVŞEMESİ ÜZERİNDEKİ ETKİLERİ

GENIŞLETILMIŞ TÜRKÇE ÖZET

Son birkaç on yılda, dental implantlar, diş kaybına dayanıklı ve estetik olarak hoş bir çözüm sunarak diş hekimliği alanında devrim yaratmıştır. Başarılarına rağmen, dental implant üreticilerinin bugün karşılaştığı yaygın ve karmaşık bir sorun vardır. Bu sorun, zamanla abutment vidasının gevşemesidir, bu da implant protezi başarısızlığına yol açabilir. Çene kemiğindeki implant gövdesi, bir abutment vidası ile proteze bağlanır. İşte bu yüzden, implant protezinin genel başarısı için onun stabilitesi büyük önem taşır.

Dental implantlardaki vida gevşemesi, üreticiler, diş hekimleri ve hastalar için önemli bir zorluk oluşturmaktadır. Abutment vidasının tekrar gevşemesini azaltmaya yönelik yoğun çabalar olmasına rağmen, iç temas yüzeylerinin toplu etkisi (abutment implant açısı (θ), abutment vidanın baş çapı (D) ve abutment vidanın uzunluğu (L)) üzerinde vida gevşemesi henüz araştırılmamıştır. Bu üç parametrenin vida gevşemesini önemli ölçüde etkileyip etkilemediği ve eğer etkiliyorsa, hangisinin en büyük etkiye sahip olduğu hala belirsizdir.

Ayrıca, bazı çalışmalar yüzey pürüzlülüğünün vidası ve karşılık gelen parçası arasındaki mekanik bağlantıyı etkileyebileceğini, bu da vidanın gevşeme olasılığını etkileyebileceğini göstermektedir. Ancak, bu potansiyel korelasyonla ilgili daha sistematik ve doğru bir araştırmaya ihtiyaç vardır. Ayrıca, bugüne kadar yapılan araştırmalar, farklı üretim yöntemlerinden etkilenen abutment vidalarının yüzey pürüzlülüğünün, vida gevşeme olasılığına nasıl etki ettiğini kapsamlı bir şekilde incelememiştir.

Abutment vidasının gevşeme sıklığı, dental implantlar içindeki iç temas yüzey alanındaki değişikliklerle ve abutment vidasının yüzey pürüzlülüğündeki varyasyonlarla önemli ölçüde etkilenebilir. Sonuç olarak, bu araştırma bu faktörleri daha derinlemesine incelemeyi amaçlamaktadır. Öncelikle, dental implantlar içindeki iç temas yüzeylerinin vida gevşemesi üzerindeki potansiyel etkisini araştırmak için hesaplamalı bir çalışma gerçekleştirilecektir. İkincil olarak, abutment vidasının yüzey pürüzlülüğünün gevşeme üzerindeki etkilerini araştırmak için deneysel bir çalışma yürütülecektir. Bu nedenle, bu araştırma, hem hesaplamalı hem de deneysel bir çalışma aracılığıyla konuyu kapsamlı bir şekilde incelemektedir.

Bu tez beş bölümden oluşmaktadır; ilk bölüm konuya genel bir bakış sunar ve çalışmanın amaçlarını sunar. İkinci bölümde literatür taramaları incelenmektedir. Tezin üçüncü bölümünde, dental implantlardaki vida gevşemesine katkıda bulunan faktörlere yönelik hem hesaplamalı hem de deneysel araştırmalar gerçekleştirilmektedir. Bu, iç temas yüzeylerindeki varyasyonların etkilerini incelemek için hesaplamalı modellemeyi ve

farklı üretim yöntemleriyle üretilen vidalardaki yüzey pürüzlülüğünü deneysel olarak analiz etmeyi içerir. Dördüncü bölüm, üçüncü bölümde gerçekleştirilen hesaplamalı ve deneysel çalışmalardan elde edilen sonuçların kapsamlı bir analizini ve tartışmasını sunmaktadır. Son bölüm olan beşinci bölüm, ana bulguları özetleyerek, derinlemesine sonuçlar sunarak ve dental implantlar alanında gelecekteki araştırmalar için önerilerde bulunarak tezi sonlandırır.

Bugün, Sonlu Elemanlar Analizi (FEA) ile hesaplamalı modelleme, biyomedikal mühendislik uygulamalarında önemli bir yöntem olarak kabul edilmekte ve abutment vidasının gevşemesini değerlendirmek için birçok çalışmada kullanılmıştır (Chen ve diğ., 2021; Kitagawa ve diğ., 2005; Pournasrollah ve diğ., 2019).

İç temas yüzeylerinin (θ, D ve L) vida gevşemesi üzerindeki etkileri henüz topluca araştırılmamıştır. Bu nedenle, bu hesaplamalı çalışma, bu üç parametrenin vida gevşemesini etkileyip etkilemediğini ve eğer etkiliyorsa, bu parametrelerden hangisinin implant vidalarının gevşemesi üzerinde daha büyük bir etkiye sahip olduğunu belirlemeyi amaçlamaktadır.

(Chen ve diğ., 2021) bazı FEA çalışmalarının, abutment vidasındaki maksimum von Mises gerilmelerindeki artışı vida gevşemesiyle doğrudan ilişkilendirdiğini belirtti. Bu nedenle, hesaplamalı çalışmada, özellikle abutment vidası ve implant olmak üzere dental implant bileşenlerinin maksimum von Mises gerilmesi ve maksimum toplam deformasyonu, tüm modellerdeki vida gevşemesini değerlendirmek ve karşılaştırmak için bir gösterge olarak kullanıldı. Değerlendirmede kullanılan ikinci yöntem, modal analiz kullanılarak modelin titreşim modlarındaki doğal frekansları kullanmaktı. Bu yaklaşım, bu çalışmada bir dental implant olan bir sistemin dinamik davranışını, çeşitli koşullar altında değerlendirmek için özellikle yararlıdır.

Bu araştırmadaki sıfır hipotezi, abutment implant açısı (θ), abutment vidanın baş çapı (D) ve abutment vidanın uzunluğu (L)'nun dental implant bileşenlerinin gerilmeleri, toplam deformasyon ve dental implant tasarımının doğal frekansı üzerinde anlamlı bir etkisinin olmadığını belirtir. Bu da sırayla vida eklemi ve dental implantlardaki vida gevşemesi olasılığının mekanik kararlılığını etkilemez.

Bu çalışmada, dental implant bileşenlerinin mekanik davranışını kapsamlı bir şekilde değerlendirmek için hem statik hem de modal analizler kullanılmıştır. Statik analiz, belirli bir yük altında (bu çalışmada 200N) gerilme dağılımı ve deformasyona ilişkin içgörü sağlarken, modal analiz bir sistemin (bu durumda bir dental implant) titreşim kuvvetleri altında dinamik tepkisini ve kararlılığını anlamada yardımcı olur (bu çalışmada serbest (zorlanmamış) titreşim kullanılmıştır). Bu iki yaklaşımı birleştirerek, dental implantlardaki vida gevşemesini etkileyen faktörlerin daha kapsamlı bir değerlendirmesi beklenmektedir.

Faktör grupları arasında anlamlı farklılıklar olup olmadığını belirlemek için, bazı verilerin normal dağılım göstermediği Shapiro-Wilk normalite testi ile belirlendiğinden dolayı, parametrik olmayan bir Kruskal-Wallis istatistik testi uygulandı. Kruskal-Wallis testinden sonra, Dunn testi kullanılarak çoklu ikili karşılaştırmalar yapıldı. İstatistiksel analizler, IBM SPSS İstatistik yazılım programı (versiyon 29.0.1.0, IBM Corp., Amerika) kullanılarak gerçekleştirildi ve P-değeri 0,05'in altında olanlar istatistiksel olarak anlamlı kabul edildi.

Bu araştırmada, üç farklı üretim yöntemi kullanılarak üç grup dental implant vidası üretildi. Her yöntem, sınıf 5 titanyum alaşımından (Ti-6Al-4V) yapılmış on adet M4 boyutunda vida üretmek için kullanıldı. Ek olarak, bir grup abutment, implant ve bir tutucu çelik malzeme kullanılarak üretildi. Daha sonra, bazı vida örneklerinin yüzey pürüzlülüğü kontur ölçüm cihazı kullanılarak ölçüldü. Ayrıca, bir dijital tork metre, her grubun örneklerinin titreşim testinden önce ve sonra tork kayıplarını değerlendirmek ve karşılaştırmak için kullanıldı. Son olarak, bir taramalı elektron mikroskobu (SEM) vida profili boyunca yüzey topografisini incelemek için kullanıldı.

Bu araştırmada, ticari abutment vidalarının mekanik özellikleri ve biyouyumluluğu nedeniyle Ti-6Al-4V'den yapıldığı için dental implant vidaları için sınıf 5 titanyum alaşımı seçildi. Ayrıca, implantlar ve abutmentlar için çelik malzeme kullanılırken, tutucu için alüminyum kullanıldı. Bu araştırmada kullanılan tüm malzemeler Tablo 3.4'te listelenmiştir.

M2 boyutunda dental implant vida üretmenin, M2 vida dişlerinin hassas boyutu nedeniyle vida yüzey pürüzlülüğünün ölçülmesini oldukça zorlaştırdığı bulunmuştur. Bu nedenle, bu çalışmada kullanılan tüm abutment vidaları M4 vida boyutunda üretildi. Ek olarak, implant ve abutmentin tüm boyutları ve geometrisi buna göre modifiye edildi. Şekil 3.6, üretilmeden önceki dental implantın son tasarımını ve boyutlarını göstermektedir.

Dental implant üretim yöntemleri yıllar içinde önemli ölçüde gelişti, bu da hastaların sonuçlarını iyileştirdi ve üretim süreçlerini basitleştirdi. Bu araştırmada, dental implant ve bileşenlerini üretmek için üç farklı üretim yöntemi kullanıldı. Kullanılan yöntemler, işleme, döküm ve diş sarma şeklindeydi. Her bileşenin ayrıntılı üretim prosedürleri şu şekildedir:

Bilgisayar destekli tasarım (CAD) SolidWorks yazılım programı dental implant tasarımının 3D modelini oluşturmak için kullanıldı, ardından CNC makinesi için talimatlara (G-kodu) dönüştürüldü. Bilgisayar Destekli İmalat (CAM) Mastercam yazılım programı, CAD dosyasından talimatları takip etmek ve iş parçasından istenen şekli oluşturmak için kesin olarak malzeme çıkarmak üzere programlandı.

Bu yöntemde, Şekil 3.7'de gösterilen bilgisayar nümerik kontrol (CNC) makinesi, iç dişleri olmadan altı adet abutment, altı adet implant, on adet dental implant vidası örneği

üretmek için kullanıldı ve aynı zamanda diş sarma ve kalıp yöntemleri kullanılarak diş açılmadan önce diğer vida örneklerini üretmek için de kullanıldı.

İkinci yöntemde, Şekil 3.10'da gösterilen önceden şekillendirilmiş kalıp, işleme yöntemi kullanılarak ürettikten sonra bir vida boşluğunda dış dişleri oluşturmak için kullanıldı. Bu işleme diş kesme denir ve on adet dental implant vidası örneği üretmek için kullanıldı.

Üçüncü yöntemde, Şekil 3.16'da gösterilen diş sarma makinesi, işleme yöntemi ile önceden hazırlanmış on vida boşluğunda (Şekil 3.17) dış dişleri üretmek için kullanıldı. Diş sarma işlemi, iş parçası malzemesinin plastik deformasyonunu, işleme ve kalıp yöntemlerinin aksine malzeme kesme veya çıkarmak yerine diş oluşturmak için içerir.

Bu çalışmada, Şekil 3.26'da gösterildiği gibi hem kesme hem de sarma musluklar, işleme yöntemi kullanılarak üretilen tüm implantların iç dişlerini üretmek için kullanıldı. İç dişleri kesme musluğu ile oluşturulan implantlar, doğuştan aşınma yaratan bir araç olduğu için, çalışma boyunca işlenmiş implantlar (İmplant Tipi M) olarak anılacaktır (Şekil 3.27A). Tersine, iç dişleri sarma musluğu kullanarak yapılan implantlar, aşınma oluşturmayan bir araç olduğu için, Diş Sarma İmplantları (İmplant Tipi TR) olarak tanımlanacaktır (Şekil 3.27B).

Bu araştırmanın bağlamında, her vida grubunun yüzey pürüzlülüğünü ölçmek, vida gevşemesi üzerindeki abutman vida yüzey pürüzlülüğünün etkisini araştırmak için kritik bir adımdır.

Bu çalışmada, vidaların yüzey pürüzlülüğü profil (kontur) ölçümleri ile ölçüldü. Şekil 3.29'da gösterildiği gibi stilus donanımlı bir kontur ölçme cihazı, pürüzlülüğün nümerik bir temsilini elde etmek için kullanıldı. Bu testte, kontur ölçme cihazının stilusu doğrusal olarak hareket eder, bu da yüzey üzerinde tek bir yol elde etmemizi sağlar. Bu cihaz, her gruptan iki örneğin yüzey pürüzlülüğünü ölçmek için kullanıldı. Her örneğin profilogramları sonuçlar bölümünde gösterilmiştir.

Şekil 3.30'da gösterildiği gibi dijital bir torkmetre, tüm örnekler için tork kayıplarını ölçmek için kullanıldı. Bu süreçte, her vida örneği başlangıçta yaklaşık 100 Ncm tork ile sıkıldı. Ardından, bir vida gevşetildi ve gevşetme için gerekli tork (detork) ölçüldü. Uygulanan (sıkma) tork ile detork arasındaki fark, tork kaybını değerlendirmek için yaygın olarak kullanılır. Her vida örneği, vibrasyon testinin uygulanmasından önce aynı başlangıç torkuna, yaklaşık 100 Ncm'ye tekrar sıkıldı.

Bu çalışmada, Şekil 3.31'de gösterilen bir titreşim cihazı (vibrator) gerçek bir ağız ortamında diş abutman vidalarına maruz kalacakları mekanik stres koşullarını taklit etmek için kullanıldı. Bu cihazı kullanmanın temel amacı, bu simüle edilmiş koşullar altında her grubun örnekleri arasındaki tork kayıplarını değerlendirmek ve karşılaştırmaktı.

Vibratör, Şekil 3.31'de gösterildiği gibi diş implantının dikey ekseniyle göre 30 derecelik bir açıyla sıkıştırma çekme makinesine monte edildi. Bu pozisyon, diş implantlarında yorgunluk testiyle ilgili olan ISO 14801'e uygun olarak seçildi. Uygulanan kuvvetin diş implantı üzerindeki etkisini artırmak için vibratörün çubuğunun ucuna dört somun takıldı. Ayrıca, vibrasyonun etkisini genişletmek için abutman yüzeyi ile temas alanını büyütmek amacıyla çubuğa bir metal daire bağlandı (Şekil 3.31B). Sonunda, vibrasyon cihazı, tüm abutman vidaları için 24 saat boyunca 75 Hz frekansta çalıştırıldı. Bu süre sonunda, diş implantı tekrar detork edilerek sonuçtaki tork kaybı ölçüldü.

Bu araştırmada, Şekil 3.32'de gösterildiği gibi bir Taramalı Elektron Mikroskobu (SEM) kullanıldı. Bu mikroskop, abutman vidasının yüzeyinin çeşitli büyütme oranlarında, özellikle X10, X25, X100, X200, X1000 ve X5000'de detaylı görüntülerini yakalamak için kullanıldı.

SEM analiz prosedürü, her gruptan iki örneğin temizlenmesini ve hazırlanmasını (Şekil 3.33), hazırlanan örneklerin SEM odasına yerleştirilmesini ve ardından örneklerin elektron demetiyle taranmasını içermektedir. Elde edilen görüntüler daha sonra analiz edildi ve sonuçlar bölümünde sunuldu.

Statik testin bulguları, abutman vidası, abutman ve implant için maksimum von Mises eşdeğer gerilme ve tüm modeller için maksimum toplam deformasyon açısından sunulmuştur (Tablo 4.1). Sonlu eleman (FE) modelinin modal analiz simülasyon sonuçları, serbest titreşim altında elde edildi ve tüm modeller için doğal frekans açısından sunuldu, özellikle asimetrik titreşim modunda (mod 1) iken (Tablo 4.1). Şekil 4.1A-C, bir model için implant bileşenlerindeki gerilme dağılımını göstermektedir.

Kruskal Wallis istatistiksel testi, P=0.05 anlamlılık düzeyi ile, bu çalışmada araştırılan üç faktörün abutman vidası, abutman ve implant için maksimum eşdeğer gerilmeler üzerindeki etkisini değerlendirmek için gerçekleştirildi. Ayrıca, test tüm modeller için toplam deformasyon ve doğal frekanslar üzerindeki etkilerini de değerlendirdi. Tablo 4.2'de gösterildiği gibi, Kruskal Wallis testi, abutman implant açısının implant gerilmesi, toplam deformasyon ve doğal frekans üzerinde önemli bir etkisi olduğunu ortaya koydu ($P<0.001$). Ayrıca, bu bulgular Dunn testi kullanılarak çoklu ikili karşılaştırmalarla doğrulandı. Bu test, ölçülen değerler için tüm üç grup çifti (30-45, 30-60 ve 45-60 derece) arasında önemli farklar olduğunu gösterdi. Ancak, 45-60 derece grup çifti arasındaki toplam deformasyonda, istatistiksel olarak anlamlı olmayan bir fark olduğu gözlemlendi ($P=0.272$), bu da Tablo 4.3'te sunuldu.

Abutman vida başı çapıyla ilgili olarak, Kruskal-Wallis testi, hem abutman vida gerilmesi hem de abutman gerilmesi üzerindeki önemli etkisini vurgulamıştır (sırasıyla $P=0.010$ ve $P=0.002$) (Tablo 4.2). Dunn testi kullanılarak yapılan daha ileri araştırmalar, abutman vida gerilmesi için grup çifti (2.65-2.75) mm ve abutman gerilmesi için grup çiftleri (2.65-2.85) mm ve (2.75-2.85) mm arasında önemli farklar olduğunu ortaya koydu (Tablo 4.3).

Ancak, abutman vida uzunluğunun, tümü için P değerlerinin 0.05'ten büyük olduğu bağımlı değişkenler üzerinde anlamlı bir etkisi olmadığı görülm (Tablo 4.2).

Maksimum von Mises eşdeğer gerilmenin ana etkisi, implant geriliminin abutman implant açısı tarafından büyük ölçüde etkilendiğini göstermektedir. Örneğin, abutman implant açısı 30 dereceden 45 dereceye arttığında implant gerilmindeki değişim oranı %76 ve -28% idi ve bu oranlar sırasıyla 60 dereceye çıktığında da devam etti (Şekil 4.2A). Ek olarak, modellerin maksimum toplam deformasyonu, abutman implant açısı 30'dan 45 dereceye değiştiğinde %55 arttı ve açı 30'dan 60 dereceye değiştiğinde daha düşük bir oran olan %17 arttı (Şekil 4.2A). Ayrıca, ana etki grafiği (Şekil 4.2A) abutman implant açısındaki bir artışa karşılık doğal frekansta bir azalmayı ortaya koymaktadır. Özellikle, abutman implantın açısı 30 dereceden 45 dereceye ve 60 dereceye arttığında, modellerin doğal frekansları sırasıyla %18 ve %26 azaldı.

Abutman vidası baş çapının (D) ana etkisini incelediğimizde, çapın 2,65'ten 2,75 mm'ye değiştiğinde abutman vidasının maksimum von Mises gerilmesinin %9 arttığını, çapın 2,65'ten 2,85 mm'ye arttığında ise %3 arttığını bulduk (Şekil 4.2B). Buna karşılık, vida baş çapındaki artış, abutman gerilmesinin sırasıyla 264.15 MPa'dan 252.07 MPa'ya ve 226.16 MPa'ya düşmesine neden oldu (Şekil 4.2B).

Vida uzunluğu söz konusu olduğunda, implantın, abutmanın ve abutman vidasının maksimum von Mises eşdeğer gerilmesi arasında net bir ilişki gözlemlenmedi (Şekil 4.2C). Ek olarak, L değerlerini 4 mm'den 5 mm'ye ve 6 mm'ye artırmanın modelin doğal frekansları üzerinde herhangi belirgin bir etkisi olduğu kanıtlanmadı (Şekil 4.2C). Bu gözlemler, istatistiksel testler tarafından doğrulandı ve vida uzunluğunun bu ölçülen parametreler üzerinde önemli bir etkisi olmadığını gösterdi (Tablo 4.2).

Tüm modeller için maksimum toplam deformasyonun ana etki grafiğine baktığımızda, incelenen faktör grupları içinde net bir doğrudan veya ters ilişki bulunamamıştır. Ancak, toplam deformasyonun en yüksek olduğu gözlendiğinde model parametreleri, bir abutman implant açısı olan 45 derece, vida baş çapı olan 2.75 mm ve vida uzunluğu olan 5 mm'yi içeriyordu (Şekil 4.2A-C).

İki makine ile işlenmiş vida (M1 ve M2), iki kalıp vida (D1 ve D2) ve iki diş açma rulosu vida (TR1 ve TR2) Şekiller 4.3-4.8'de sırasıyla gösterilmektedir. Bu profilogramlar, vida dişlerinin adım, açı ve derinlik gibi önemli özelliklerini gösterir. Bu parametreler, her örneğin profilogramından çıkarılmıştır ve Tablo 4.4'te nümerik olarak sunulmaktadır. Bu profilogramlar, Tablo 4.4'te sıralanan kuantitatif verileri ile birlikte, vida dişlerinin geometrik özelliklerine kapsamlı bir bakış sunar. Bu parametrelerin farklı üretim yöntemleri arasında sistemli bir karşılaştırması, diş özelliklerindeki varyasyonlara değerli içgörüler sağlar ve vida gevşemesi olayının potansiyel etkisini anlamada yardımcı olur. Tablo 4.4'ü inceleyerek, gruplar içinde makul bir tutarlılık olduğu gözlemlenebilir ve aynı zamanda çeşitli üretim yöntemleri arasındaki farkları da ortaya koyar.

İşlenmiş vidalar grubu, her biri beş vida içeren iki alt gruba ayrıldı. İlk alt grup işlenmiş implantlarla (İmplant Tipi M) eşleştirildi, diğeri ise diş açma rulosu implantıyla (İmplant Tipi TR) eşleştirildi. Tablo 4.6 ve 4.7, titreşim testinden önce ve sonra her örnek için uygulanan tork değerlerini, detork değerlerini ve tork kaybındaki değişiklikleri göstermektedir. Tablo 4.6, işlenmiş vidaların işlenmiş implantlarla eşleştirildiğini, Tablo 4.7 ise diş açma rulosu implantlarıyla eşleştirildiğini belirtir. Ortalama toplam tork kaybı değerleri hesaplanırken, verilerde olası bir sapmayı ortadan kaldırmak ve adil bir karşılaştırma sağlamak için son derece yüksek veya negatif toplam tork kaybı (%) değerleri hariç tutulmuştur. Bu anomali değerler, açıklık için tabloda mavi ile işaretlenmiştir.

Tablo 4.8, işlenmiş implantlarla eşleştirilen diş açma rulosu vidaları için titreşim testinden önce ve sonra tork, detork ve tork kaybı ölçümlerini sunmaktadır. Bu diş açma rulosu vidaları, ortalama bir toplam tork kaybı olan %5.12'yi göstermiştir. Bu ortalamanın hesaplanmasında beklenmeyen bir tork kaybı varyasyonunu temsil ettiği için anomali bir negatif değer (-1.05%) dikkate alınmamıştır.

Benzer şekilde, Tablo 4.9, diş açma rulosu implantlarıyla eşleştirilen diş açma rulosu vidaları için ilgili ölçümleri sergilemektedir. Veriler, ortalama bir toplam tork kaybı olan %4.32'yi göstermiştir. Bu hesaplama, titreşim testinden sonra tork kaybında beklenen eğilime aykırı olan negatif bir değeri (-0.81%) ve önemli derecede yüksek bir değeri (19.20%) hariç tutmuştur. Bu tablolar, testin titreşim stresine maruz kalan diş açma rulosu vidalarının, eşleştirildikleri implant türlerinden bağımsız olarak, tork kayıpları yaşadığını vurgulamaktadır. Anomali değerler, açıklık için tabloda mavi ile işaretlenmiştir.

Tablo 4.10, işlenmiş implantlarla eşleştirilen kalıp vidaları için titreşim testinden önce ve sonra tork, detork ve tork kaybı ölçümlerini detaylandırmaktadır. Kalıp vidaları, titreşim testinden sonra tork kaybındaki beklenen artışa aykırı olan bir negatif değeri (-2.61%) hariç tutarak ortalama bir toplam tork kaybı olan %7.53'ü gösterdi. Bu anomali değer, açıklık için tabloda mavi ile işaretlenmiştir.

Benzer şekilde, Tablo 4.11, diş açma rulosu implantlarıyla eşleştirilen kalıp vidaları için ölçümleri belirtir. Bu durumda, ortalama toplam tork kaybı %6.27 olarak hesaplanmıştır. Hesaplamadan, titreşim testinden sonra tork kaybındaki beklenen eğilimden sapma gösteren önemli derecede yüksek bir değer (%21.36) ve bir negatif değer (-3.58%) hariç tutulmuştur. Bu değerler, tabloda mavi ile işaretlenerek belirginleştirilmiştir. Bu sonuçlar, kalıp vidalarının, eşleştirildikleri implant türlerinden bağımsız olarak, titreşim testinden sonraki tork kayıplarını gösterdiğini vurgulamaktadır.

Şekil 4.9-4.14, altı vida örneğinin yüzeylerini göstermektedir: sırasıyla iki işlenmiş vida (M1 ve M2), iki kalıp vida (D1 ve D2) ve iki diş açma rulosu vida (TR1 ve TR2). Detaylı SEM görüntüleri, bu türler arasında yüzey pürüzlülüğünde belirgin farklar olduğunu ortaya koymaktadır. İşlenmiş vidalar, kalıp ve diş açma rulosu vidalara göre daha düşük

yüzey pürüzlülüğüne sahiptir. Diğer yandan, kalıp vidaları daha yüksek yüzey pürüzlülüğü göstermekte, bu bulgu profilometri sonuçlarıyla tutarlıdır.

Bu araştırmanın bulgularıyla ilgili olarak, modelin doğal frekansı, abutment implant açısı arttıkça önemli ölçüde azaldı (Şekil 4.2A), bu da implant bileşenlerinin stabilitesinin azaldığını gösteriyor. Daha yüksek doğal frekansların daha büyük stabiliteyle ilişkilendiği varsayımımıza dayanarak bu sonuca vardık. Bu varsayım, bir modelin rezonansta olduğunda maksimum yer değiştirmeyi sergilediği anlayışından kaynaklanmaktadır, bu da daha yüksek doğal frekanslara sahip modellerin daha stabil olduğu anlamına gelir. Stabilite azalmasının nedeni, abutment implant açısı azaldıkça abutment ile implant arasındaki temas yüzey alanının azalmasına bağlanabilir. Ayrıca, bu çalışmanın bağlamında, bir modelin stabilitesi azaldıkça vida gevşemesi olasılığının arttığı varsayılmaktadır, bu da model stabilitesi ve vida gevşetme arasında değiştirilebilirlik oluşturmaktadır.

Modal analiz sonuçları, serbest titreşimler altında FE modelinde altı tür titreşim modunu içerir. Bu modlar modelin normal titreşim modlarını temsil eder: asimetrik, simetrik, sallama, bükülme, makaslama ve sallanma. Diğer beş modun doğal frekanslarının ana etkisi, mode 1'de olduğu gibi abutment implant açısındaki artışla ters orantılı ve abutment vida baş çapındaki artışla doğru orantılıdır. Bu nedenle, tüm modellerdeki doğal frekanslar, sonuç ve grafiklerin bolluğundan kaçınmak için yalnızca ilk modu kullanarak sunuldu ve karşılaştırıldı.

Bu çalışmada, abutment vida uzunluğu, abutment vidasının gevşemesini açıkça etkilemedi. Bu bulgu, diğer çalışmalarla (Lee & Cha, 2018; Yeo ve diğ., 2014) tutarlıdır, ancak vida tutunmasını artırmak için daha uzun ve daha fazla dişe sahip bir vida öneren başka bir çalışma (Kanneganti ve diğ., 2018) ile çelişmektedir. Çalışmada kullanılan modeller arasındaki tek fark tasarımdır, malzeme özellikleri, yük ve sınır şartları ve temas tanımları aynı kalmıştır. Tablo 4.1'deki sonuçlar, farklı vida uzunlukları arasında elde edilen gerilme değerlerindeki farkın çok küçük ve istatistiksel olarak anlamlı olmadığını gösteriyor, bu da vida uzunluğunun von Mises gerilmesine etkisi olmadığını gösteriyor. Şekil 4.15, abutment implant açısı değiştirildiğinde vida dişi ve diş yuvası arasındaki kesişme noktasının değiştiğini göstermektedir. Bu kesişme noktası kritiktir çünkü abutment vidasının maksimum gerilmesi bu bölgede bulunmaktadır, Şekil 4.2C'de gösterildiği gibi. Genel olarak, bu ilişkinin olmaması, vida dişi ile diş yuvası arasındaki kesişme noktasının konumuna bağlanabilir.

Kontur ölçüm cihazının stili, yüzey boyunca tek bir yolu ölçmek için kullanıldı. Bu yüzeyin pürüzlülüğü, Şekil 4.3-4.8'de gösterildiği gibi profilogramlar aracılığıyla değerlendirilebilir. Şekil 4.5 ve 4.6, işaretli bölgelerde gözlemlenebilir şekilde ölçü vidasının daha yüksek yüzey pürüzlülüğüne sahip olduğunu belirtmektedir. Aksine, Şekil 4.3 ve 4.4'te gösterilen işlenmiş vidalar, daha az yüzey pürüzlülüğü göstermektedir. Dişli vidalar, diğer iki yönteme kıyasla ara yüzey pürüzlülüğü sergilemektedir.

Tablo 4.6 ve 4.7'den, işlenmiş vidaların, işlenmiş veya dişli implantlarla eşleştirilip eşleştirilmediğine bakılmaksızın, titreşim testinden önce ve sonra tork kayıplarına sahip olduğu görülebilir. Ancak, işlenmiş vidaların işlenmiş implantlarla eşleştirilmesi (3,51%) ile dişli implantlarla eşleştirilmesine (2,42%) kıyasla ortalama toplam tork kaybı biraz daha yüksektir. Toplam tork kaybı, vida gevşemesinin önemli bir ölçüsüdür; bu nedenle, bu gözlemlere dayanarak, işlenmiş vidaların işlenmiş implantlarla eşleştirilmesinin, işlenmiş vidaların dişli implantlarla eşleştirilmesine kıyasla vida gevşemesi için daha yüksek bir eğilimle sonuçlanabileceği çıkarılabilir.

Benzer şekilde, Tablo 4.10 ve 4.11'de sunulan sonuçlara dayanarak, işlenmiş implantlarla eşleştirilen ölçü vidaları, dişli implantlarla eşleştirilenlere kıyasla %7,53 daha yüksek ortalama toplam tork kaybına sahipken, dişli implantlarla eşleştirilenlerin ortalama toplam tork kaybı %6,27 idi. Bu, ölçü vidalarının işlenmiş implantlarla eşleştirildiğinde vida gevşemesi için daha yüksek bir eğilim gösterdiğini önermektedir. Bu bulgular, işlenmiş vidaların işlenmiş implantlarla eşleştirildiğinde dişli implantlarla eşleştirildiğindeki gibi daha yüksek vida gevşemesine yatkın olduğunu doğrulayan daha önceki gözlemleri desteklemektedir.

Bu ortalama değerler hesaplanırken, son derece yüksek veya negatif toplam tork kaybı (%) değerleri adil bir karşılaştırma sağlamak ve verilerdeki olası sapmayı ortadan kaldırmak için dışlandı. Bu aykırı değerler, tork uygulama veya ölçüm sürecinin önemli ölçüde değişebileceği durumları belirtebilir ve bu nedenle, dışlamaları tipik koşullar altında tork kaybı davranışının daha temsilci bir değerlendirmesini sunmaya yardımcı olur.

Bu kombinasyonlu 3D Sonlu Eleman Analizi (FEA) ve deneysel çalışmadan elde edilen bulgulara dayanarak aşağıdaki sonuçlara ulaşılmıştır:

Çalışma sonuçları, abutment implant açısı ve abutment vidanın baş çapı için boş hipotezi reddetti, bu da bu parametrelerin diş implantı bileşenlerinin gerilmesini, toplam deformasyonu ve diş implantının doğal frekansını önemli ölçüde etkilediğini gösterdi. Bu, sırayla, vida bağlantısının mekanik stabilitesini ve diş implantlarında vida gevşemesi olasılığını potansiyel olarak etkileyebilir.

Ancak, abutment vida uzunluğu için boş hipotez reddedilemedi, bu da bağımlı değişkenlerin üzerinde önemli bir etkisi olmadığını gösterdi. Abutment vida uzunluğunun diş implantlarının mekanik stabilitesindeki rolünü tam olarak anlamak için daha fazla araştırmaya ihtiyaç duyulabilir.

Deneysel çalışmamız birçok önemli bulguya yol açtı. Yüzey pürüzlülüğü ölçümleri, tork ve titreşim testleri ve SEM görüntüleme sonuçları analiz edildiğinde, bu çalışmada kullanılan her üretim yönteminin benzersiz bir yüzey pürüzlülüğü ürettiği açıktır. Yüzey pürüzlülüğündeki bu değişiklik, vida gevşemesi derecesini buna göre etkiler. Bu nedenle,

vida gevşemesi ve vida yüzey pürüzlülüğü arasında önemli bir korelasyon olduğu sonucuna varılabilir.

İşlenmiş vidalar, hem dişli vidalara hem de ölçü vidalarına kıyasla daha az gevşeme gösterdi. Bu, işlenmiş vidaların diğer türlere kıyasla daha düşük yüzey pürüzlülüğüne sahip olmasına bağlanabilir.

Vida gevşemesi, vidaların yüzey pürüzlülüğünü ayarlayarak ve/veya implantın iç dişli işleme sürecini değiştirerek kontrol edilebilir. Bu çalışmada, dişli implantlar işlenmiş implantlara kıyasla daha az vida gevşemesi ile sonuçlandı, bu da bu yöntemin potansiyel faydasını göstermektedir.

Bu çalışma esas olarak vida gevşemesi üzerindeki yüzey pürüzlülüğünün etkisine odaklanırken, vida gevşemesine katkıda bulunan diğer faktörlere, malzeme özelliklerinin etkisi, implant veya vidanın tasarımı ve biyolojik faktörlerin etkisi gibi, daha fazla araştırma yapılması önerilmektedir.

Bu çalışma, farklı üretim yöntemlerinin, vida gevşemesini etkileyen farklı yüzey pürüzlülük seviyeleri ile sonuçlandığını bulmuştur. Yüzey pürüzlülüğü ve vida gevşemesi üzerindeki etkileriyle ek üretim süreçlerini keşfetmek önerilmektedir.

Bu çalışmada kullanılan vidalar metrik 4 boyutundadır, bu da diş implantlarında tipik olarak kullanılan boyutlardan farklıdır. Bununla birlikte, üretim süreci, yüzey pürüzlülüğü ve vida gevşemesi arasındaki korelasyon hakkındaki bulgular temelde değerlidir. Bu bulguları doğrudan klinik pratiğe uygulanabilir kılmak için, diş implantlarında tipik olarak kullanılan vidaların boyutları kullanılarak benzer çalışmalar yapılmalıdır. Bu nedenle, bu çalışmanın bulgularının uygulanabilirliğini doğrulamak ve genişletmek için diş implantlarında yaygın olarak kullanılan vida boyutları aralığında bu deneyleri tekrarlamak önerilmektedir.

Çeşitli kaplama ve yüzey işlem süreçlerinin yüzey pürüzlülüğü ve vida gevşemesi üzerindeki etkisi araştırılabilir. Bu, yüzey özelliklerini değiştirerek vida gevşemesini azaltmak için potansiyel çözümler sunabilir.

1. INTRODUCTION

Over the past few decades, dental implants have revolutionized the field of dentistry by providing a durable and aesthetically pleasing solution to tooth loss. Despite their success, there is still a common, complicated issue encounters dental implant manufacturers today. This issue is the loosening of the abutment screw over time, which can lead to implant prosthesis failure. The implant body in the jawbone is connected to the prosthesis by an abutment screw. That is why its stability is significant for the overall success of the implant prosthesis.

1.1. Problem Statement

Screw loosening in dental implants presents a significant challenge for manufacturers, dentists, and patients alike. Despite rigorous efforts to reduce the recurrence of abutment screw loosening, the collective effect of the internal contact surfaces (the abutment implant angle (θ), the abutment screw head diameter (D), and the abutment screw length (L)) on screw loosening has yet to be investigated. Whether these three parameters significantly influence screw loosening remains unclear, and if so, which has the most substantial impact.

Moreover, some studies indicate that surface roughness may affect the mechanical connection between the screw and its corresponding part, which may affect the probability of the screw loosening. However, a more methodical and accurate investigation into this potential correlation is required. Furthermore, no research to date has comprehensively examined how the surface roughness of abutment screws, influenced by different manufacturing methods, impacts the likelihood of screw loosening.

1.2. Objective

1.2.1. General Objective

To comprehensively investigate the factors affecting screw loosening in dental implants, with a specific focus on the effects of internal contact surfaces and screw surface roughness.

1.2.2. Specific Objectives

The specific objectives are to:

1. Use computational modelling to evaluate and compare the mechanical effects of the abutment implant angle (θ), the abutment screw head diameter (D), and the abutment screw length (L) on screw loosening.
2. Conduct experimental studies to characterize the surface roughness of dental implant abutment screws manufactured by different methods, including machining, thread rolling, and die.
3. Determine the correlation between surface roughness and screw loosening and understand the impact of manufacturing methods on this relationship.
4. Evaluate the torque loss of these screws under applied vibration to simulate a clinical scenario.
5. Analyze the microscopic variations among the screws using Scanning Electron Microscopy (SEM), and associate these observations with screw loosening.

1.3. Thesis Layout

This thesis consists of five chapters, the first chapter provides an overview of the topic and presents the objectives of the study. Literature reviews are explored in chapter two. In the third chapter of the thesis, both computational and experimental investigations into the factors contributing to screw loosening in dental implants are carried out. This includes computational modeling to study the effects of variations in internal contact surfaces within a dental implant and an experimental analysis of surface roughness across screws produced by different manufacturing methods. The fourth chapter presents a comprehensive analysis and discussion of the results derived from the computational and experimental studies conducted in chapter three. The final chapter, chapter five, concludes the thesis by summarizing the main findings, offering insightful conclusions, and providing recommendations for future research in the field of dental implants.

2. LITERATURE REVIEWS

2.1. Dental Implant Systems

A dental implant is an artificial device, placed in contact with oral connective and bone tissues, which has the function to replace the natural tooth root (Boemio et al., 2011). Dental implants can reach the clinical success if they are not toxic to the cells in the surrounding tissues, or undergo dissolution and cause systemic damage to the patient, and they must be able to form a stable bone-implant interface that is capable of carrying occlusal loads, and transferring or distributing stresses to the adjacent bone so that bone vitality is maintained over long periods (Hench & Wilson, 1993).

2.1.1. Endosseous Screw-Shaped Implants

Today, endosseous titanium implants are widely used in restorative dentistry to restore missing teeth. There are two types of dental implants, one-piece (monoblock) and two-piece (multi-parts), depending on the area to be applied in the mouth (Resnik, 2020).

2.1.1.1. One-Piece Implants

As shown in Figure 2.1, these types of implants, in which the abutment and the implant body consist of one piece, are applied in a one-stage surgery. They are generally used in cases of narrowing of the mesiodistal space due to congenital tooth defects, in cases where the natural teeth root distance is less than 3 mm and as orthodontic anchorage devices (Resnik, 2020).



Figure 2.1. One-piece dental implant (Resnik, 2020).

2.1.1.2. Two-Piece Implants

Multi-parts implant consists of implant, abutment and abutment screw. It is applied to patients undergoing two-stage surgery. In first stage, it is placed into the jawbone under the soft tissue for approximately 2-5 months according to the patient's bone structure and other factors for the osseointegration process. After the osseointegration process is complete, the abutment is connected to the implant with a screw and a crown then can be placed on the abutment (the second stage). These types of implants are widely used today as they allow more compatible restorations in the preparation of the prosthetic superstructure. As shown in Figure 2.2, the abutment is attached to the implant with a screw. A conical central surface is used for precise contact and maximum contact resistance against the forces coming to the implant. Thanks to the internal hexagonal connection, the implant system resists the torsional forces during tightening the abutment screw and against the torsional forces of the implant upper group. After a hole is drilled in the bone with a self-tapping screw, the implant can be screwed directly into the bone without guiding need.

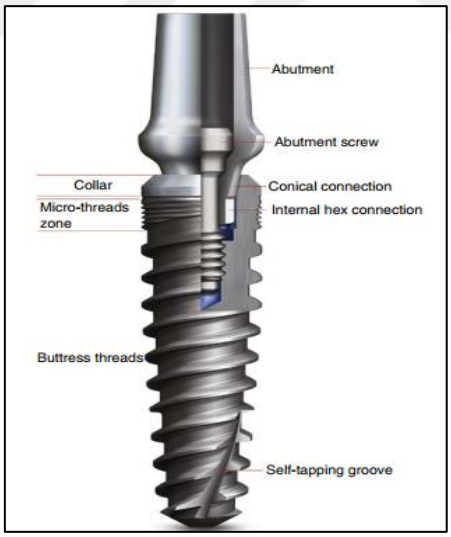


Figure 2.2. Multi-parts dental implant and its structure (Resnik, 2020).

2.2. Screw Loosening

Micromovements of the retaining screws, caused by the occlusal forces acting on the prosthesis, can lead to their eventual loosening (von Krammer, 1999). Implant manufacturers have tried to address this issue by integrating design features that prevent

rotation in their systems (Dixon et al., 1995). Research has indicated that the incidence of instability in abutment screws ranges from 12.7% to 43% (Jung et al., 2008; Jemt, 1990). Another study found that approximately 26% of abutment screws required retightening after being in use for a year (Jemt et al., 1991).

In restorations that attach directly to the implant, the implant and abutment are connected through the preload achieved by the tightening torque applied to the prosthetic screw (Armentia et al., 2021; Patterson & Johns, 1992), providing the essential structural integrity to the restoration (Barbosa et al., 2011; Stüker et al., 2008; Lang et al., 2003). The recommended torque value is provided by manufacturers based on various factors related to the design of the implant (Dixon et al., 1995).

2.2.1. Screw Loosening in Implant-Supported Prostheses

Dental implant prostheses can be fixed either with cement or screws. The majority of previous research has shown that cement can cause peri-implantitis (Quaranta et al., 2017; Staubli et al., 2017). Lack of cement and good retrievability are considered advantages of a screw-retained implant prosthesis compared to a cement-retained implant prosthesis which offers superior esthetics (Ma & Fenton, 2015). Accordingly, screw-retained implant prostheses are preferred over permanent cement-retained implant prostheses (Ma & Fenton, 2015). However, screw loosening is considered one of the most common complications in both screw-retained and cement-retained implant prostheses (Cho et al., 2004; Lee et al., 2020), but it was reported to be more common in screw-retained implant prostheses (Lee et al., 2020). In contrast, (Assenza et al., 2005) conducted an experimental study in six adult male Beagles to evaluate the frequency of the screw loosening between screwed and cemented abutments. Twelve months later, the screwed abutments had eight (27%) loose screws, whereas the cemented abutments exhibited no loosening.

2.2.2. Screw Loosening: Statistical Insights

In a long-term study, (Kreissl et al., 2007) evaluated the incidence of the most common issues such as screw fracture, screw loosening, veneer porcelain fracturing and structural fracture in implant-supported fixed partial dentures. As a result, abutment screw loosening was reported to be the most common issue, with a cumulative incidence of 6.7% in six single crowns and two cantilever bridges (Kreissl et al., 2007). In addition,

many short- and long-term studies reported the incidence of screw loosening in 7.2% of 1928 implants placed in 837 patients,6 in 27.3% of 107 single-implant restorations placed in 92 patients (Jemt et al., 1991), in 6.7% of 205 fixed-implant restorations placed in 76 patients (Kreissl et al., 2007), in 10.3% of 39 single implants and 12.1% of 174 multiple implants placed in 106 patients (Cho et al., 2004), in 6.8% of all implants (Brägger et al., 2001), and in 5.8% as a cumulative incidence (Pjetursson et al., 2004). (Goodacre et al., 2003) indicated that abutment screw fracture occurred in 2% of 13160 implants and abutment screw loosening occurred in 6% of 6256 implants and can reach up to 45% in implant single crowns. Consequently, loosening the dental implant-abutment screw is one of the most common and complicated issues encountered by dental implant manufacturers.

2.2.3. Factors and Parameters Influencing Abutment Screw Loosening

Factors and parameters that influence abutment screw loosening were investigated and reported in many studies, as follows: screw length (Kanneganti et al., 2018; Lee & Cha, 2018; Yeo et al., 2014), angulation-correcting implants (Hotinski & Dudley, 2019), external hex abutments (Ha et al., 2011), implant diameter (Londhe et al., 2020), contamination by blood and saliva during the implant treatment process (Koosha et al., 2020), lubricant use (Wu et al., 2017), coating screws with gold (Bulaqi et al., 2019), adding a conical spring washer to a gold screw (Korioth et al., 1999), coating screws with a diamond-like layer (de Moura et al., 2017), microleakage (Sahin & Ayyildiz, 2014), abutment collar length (Siadat et al., 2015), abutment screw retightening (Bulaqi et al., 2015; Farina et al., 2014), using anti-rotation resistance features, such as notches or micro-stops (Aboyoussef et al., 2000; Kofron et al., 2019), abutment screw head shape (Arnetzl et al., 2016; Coppedê et al., 2013), implant-abutment connection designs (Sammour et al., 2019; Siadat et al., 2018), lateral forces (Londhe et al., 2020; Khraisat et al., 2004), frequent reuse or replacement the retained abutment screw (Butkevica et al., 2018; Weiss et al., 2000; Arshad et al., 2018; Guzaitis et al., 2011; Xiao et al., 2017), interchangeable abutments (Park et al., 2017; Alonso-Pérez et al., 2018; Kim et al., 2012), torque values (Siamos et al., 2002; Lee et al., 2002; Kim & Lim, 2020), preload values (Guda et al., 2008), and abutment screw material (Farina et al., 2012). In addition, (Lee et al., 2020) came to the conclusion that screw loosening is affected by implant position,

implant type and manufacturer, implant diameter, implant-abutment connection type, implant prosthesis retention type, and type of implant prosthesis. (Duncan et al., 2003) reported that screw loosening in males (9.4%) was much higher than in females (3.1%), while it was unaffected by the sex factor (Lee et al., 2020). While these studies have highlighted some aspects of screw loosening, a significant knowledge gap remains. Specifically, the internal contact surfaces of dental implants, a potentially crucial factor in screw loosening, have been largely overlooked.

2.2.4. Preventing Screw Loosening Techniques

There are a lot of research have been done to prevent screw loosening. The used methods were gold screws, silicone plug, different implant-abutment joint design, and screw cement (Cavazos Jr & Bell, 1996). Although the efforts of the researchers to prevent the screw loosening, it still a common problem.

2.2.4.1 Silicone Plug

(Cavazos Jr & Bell, 1996) have proposed a new technique for preventing abutment screw loosening by using internal dimples on the internal surface of abutment screw cylinder above the screw and filling the cylinder with elastomeric impression material such as polyvinyl siloxane which is used indirectly in prosthodontics and restorative dentistry. A Cotton pellet was placed above the polyvinyl siloxane material and condensed using an amalgam condenser. Finally, a temporary composite (Fermit) was used to seal the opening (Figure 2.3A). Their method can also be used for angled abutments (Figure 2.3B).

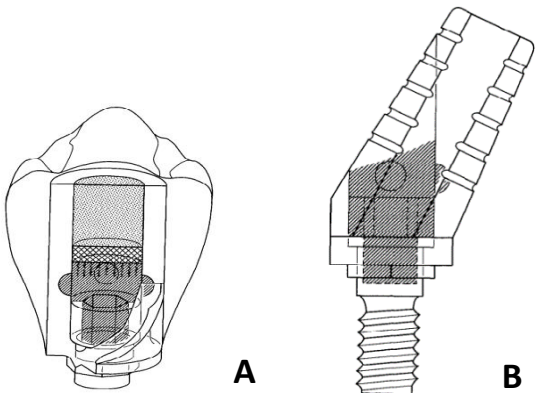


Figure 2.3. A, Polyvinyl siloxane, cotton pellet, and composite. B, Temporary composite over head of screw and dimples in angled abutment.

This technique is unwieldy because it requires two synchronous syringes to ensure that the access canal to screw is filled correctly with a silicone. Therefore, this technique has been modified by Roberto. There were two modifications added to Cavazos's technique, the first is using a root canal filler instead of the syringes to pack a material into abutment screw cylinder and using acrylic resin instead of a composite (von Krammer, 1997). However, Roberto did another study to simplify the obturation process of the abutment screw cylinder and prevent the screw loosening because in his first study there wasn't a guide for replacing the silicone plug to its correct place after inspection for any reason Figure 2.4A (von Krammer, 1999).

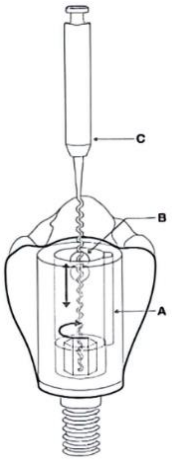


Figure 2.4. A, Access canal and hex portion of screw head with antirotational grooves, B, Dimples. C, Placement and direction of rotation (arrows) of root canal filler.

2.3. Surface Roughness

During the chip removal process in machining, surface flaws occur on the machined surface due to the influence of physical, chemical, temperature, and mechanical movements between the tool and the workpiece, depending on the machining operation, type of cutting tool, and machining conditions. The irregular deviations that occur in the nominal surface line in the upward and downward direction are called "surface roughness". There are many factors affecting surface roughness. These include the way the workpiece is attached, the axis and business gaps of the bench, structural defects due to the machined material, irregular chip flow during machining of brittle materials, cutting speed, feed speed, chip depth, cooling and lubrication conditions of the cutting tool, chemical and metallurgical structure of the workpiece, cutting tool geometry, type of

machine on which machining is performed, machining conditions, and rigidity status. Theoretically, the value of surface roughness is mainly affected by two parameters during cutting. These are the feed speed of the cutting tool and the tip radius. The surface roughness value can be calculated according to Equation (1.1), depending on these two parameters. In the given equation, Rt represents the maximum surface roughness value, fn represents the feed speed (mm/rev), and r represents the cutting tip radius (mm) (Bhushan, 2000).

$$R_t = \frac{{f_n}^2}{8 \cdot r} \tag{2.1}$$

Surface roughness most commonly refers to the variations in the height of the surface relative to a reference plane. It is measured either along a single line profile or along a set of parallel line profiles (surface maps). It is usually characterized by one of the two statistical height descriptors advocated by the American National Standards Institute (ANSI) and the International Standardization Organization (ISO). These are (1) Ra, CLA (center-line average), or AA (arithmetic average) and (2) the standard deviation or variance (σ), Rq or root mean square (RMS). Two other statistical height descriptors are skewness (Sk) and kurtosis (K); these are rarely used. Another measure of surface roughness is an extreme-value height descriptor Rt (or Ry, Rmax, or maximum peak-to-valley height or simply P–V distance). Four other extreme-value height descriptors in limited use, are: Rp (maximum peak height, maximum peak-to-mean height or simply P–M distance), Rv (maximum valley depth or mean-to-lowest valley height), Rz (average peak-to-valley height), and Rpm (average peak-to-mean height) (Bhushan, 2000).

A profile, z(x), in which profile heights are measured from a reference line Figure 2.5. A center line or mean line such that the area between the profile and the mean line above the line is equal to that below the mean line. Ra, CLA, or AA is the arithmetic mean of the absolute values of vertical deviation from the mean line through the profile. The standard deviation σ is the square root of the arithmetic mean of the square of the vertical deviation from the mean line (Bhushan, 2000).

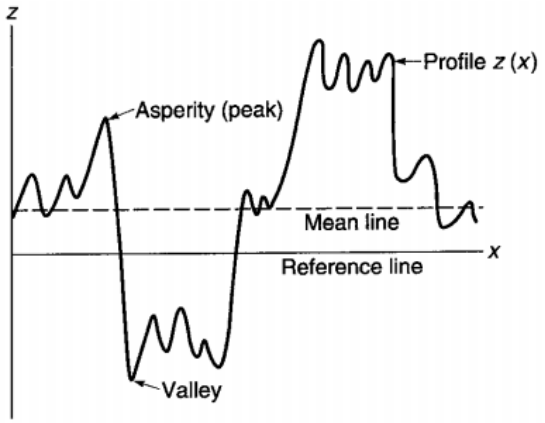


Figure 2.5. Schematic of a surface profile z(x) (Bhushan, 2000).

In mathematical form, it can be written

$$R_a = CLA = AA = \frac{1}{L}\int_0^L |z - m \,|\, dx \tag{2.2}$$

and

$$m = \frac{1}{L}\int_0^L z\, dx \tag{2.3}$$

Where L is the sampling length of the profile (profile length).

The variance is given as

$$\sigma^2 = \frac{1}{L}\int_0^L (z-m)^2 dx \tag{2.4}$$

$$= {R_q}^2 - m^2 \tag{2.5}$$

Where, σ is the standard deviation and Rq is the square root of the arithmetic mean of the square of the vertical deviation from a reference line, or

$${R_q}^2 = RMS^2 = \frac{1}{L}\int_0^L (z^2) dx \tag{2.6}$$

For the special case where *m* is equal to zero,

$$R_q = \sigma \tag{2.7}$$

In many cases, the Ra and σ are interchangeable, and for Gaussian surfaces,

$$\sigma \sim \sqrt{\frac{\pi}{2}}\, R_a \sim 1.25\, R_a \tag{2.8}$$

The value of Ra is an official standard in most industrialized countries. Table 2.1 gives internationally adopted Ra values together with the alternative roughness grade number. The σ is most commonly used in statistical analyses.

Table 2.1. Center-line average and roughness grades (Bhushan, 2000).

Ra Values up to a Value in µm	Roughness Grade Number
0.025	N1
0.05	N2
0.1	N3
0.2	N4
0.4	N5
0.8	N6
1.6	N7
3.2	N8
6.3	N9
12.5	N10
25.0	N11
F(N)	542

2.3.1. Surface Modification Techniques and Screw Loosening

The incidence of abutment screw loosening can be significantly influenced by modifications to the surface roughness of abutment screw. Various methods have been explored to modify the surface roughness of abutment screws to reduce screw loosening. For instance, (Jeong et al., 2014) used electron beam physical vapor deposition (EB-PVD) to deposit films of titanium nitride (TiN) and tungsten carbide (WC) onto abutment screw surface. In another study, (Elias et al., 2006) compared the opening torque of abutment screws coated with four different materials (TiN, titanium carbonitride (TiCN), teflon, and parylene). Furthermore, (Chen et al., 2020) utilized thermal spraying to prepare Polyetheretherketone (PEEK) and Polytetrafluoroethylene (PTFE) coatings on the abutment screw surface, noting an improvement in immediate fastening and long-term anti-loosening performance. Moreover, plasma nitriding treatment (PNT) is a recent

surface modification technique developed to address the problem of screw loosening (Sun et al., 2020). In this context, (Sun et al., 2020) investigated the impact of PNT on dental implant abutment screw joint. Their results showed that PNT not only reduced friction and increased preload force, but also enhanced the anti-loosening performance of the screws under dynamic load.

(Dixon et al., 1995) investigated and compared the amount of torque required to loosen the abutment screws for three implant designs from different manufacturers. The researchers did not measure the surface roughness of the implant screws; instead, they relied solely on mean torque results to compare the implant designs. In another study, (Armentia et al., 2021) examined the impact of dental implant prosthetic screws on fatigue performance. The authors produced screws with both rolled and cut threads and identified the surface roughness parameters of these screws. However, they did not examine how these parameters could be influence screw loosening. To address this gap, this study conducted an experimental investigation to examine both the surface roughness and torque loss (before and after a vibration test) required to loosen abutment screws produced by machining, thread rolling, and die methods.

2.4. Screw Thread Manufacturing Techniques

Screw thread manufacturing in the industry primarily relies on two processes: machining (cutting) and thread rolling (Armentia et al., 2021). In machining, equipment like the CNC lathe precisely remove material from the workpiece to create the desired thread shape. Conversely, in thread rolling, specialized dies with the desired thread profile and pitch engraved on their surfaces form threads on the workpiece through plastic deformation rather than cutting or removing material (Aktas & Kisioglu, 2020; Domblesky & Feng, 2002).

2.5. Finite Element Method (FEM)

FEA has been widely adopted in biomedical engineering applications and has been used in many studies to evaluate abutment screw loosening (Chen et al., 2021; Pournasrollah et al., 2019; Bulaqi et al., 2019a, 2015b; Kanneganti et al., 2018; Wu et al., 2017; Jörn et al., 2014; Kitagawa et al., 2005).

(Chen et al., 2021) indicated that some FEA studies directly linked the increase in maximum von Mises stresses in the abutment screw with screw loosening. Therefore, in the present study, the maximum von Mises stress and the maximum total deformation of dental implant components, particularly the abutment screw and implant, were used to evaluate and compare screw loosening in all models. Additionally, the natural frequencies of the vibrational modes of the model were assessed using modal analysis, an approach that is particularly useful for assessing the dynamic behavior of a system (Chen et al., 2020).

3. METHODOLOGY

This research addresses the influence of internal contact surface area modifications within dental implants and variations in abutment screw surface roughness on screw loosening. Firstly, a computational study was performed to explore the potential impact of internal contact surfaces within dental implants, specifically the abutment implant angle (θ), the abutment screw head diameter (D), and the abutment screw length (L), on screw loosening. Finite element analysis (FEA) and various statistical tests were conducted to determine the interplay between these parameters and their collective influence on the mechanical stability of the screw joint. Secondly, an experimental study was conducted to investigate the influence of different manufacturing methods, specifically machining, thread rolling, and die, on the surface roughness of dental implant abutment screws and their subsequent impact on screw loosening. Additionally, this research aimed to determine whether modifying the internal threading process of the implant would affect the torque loss of abutment screws. Therefore, this research presented a comprehensive investigation of the issue through both a computational and an experimental study.

3.1. Computational Study: Finite Element Analysis

Both static and modal analyses were used to evaluate and compare the stability of 27 models through the evolution of the maximum von Mises stresses for the implant components, maximum total deformation, and natural frequencies. Static analysis provided insight into the stress distribution and deformation under a 200-N load, whereas modal analysis helped in understanding the dynamic response and stability of the dental implant system under unforced vibration. Combining these two approaches provided a more thorough evaluation of the factors affecting screw loosening in dental implants.

3.1.1. Research Hypothesis

The null hypotheses were that the abutment implant angle (θ), the abutment screw head diameter (D), and the abutment screw length (L) would not have a significant effect on the stresses of dental implant components, total deformation, or natural frequency of dental implant design and that they would not influence the mechanical stability of the screw joint and the probability of screw loosening in dental implants.

3.1.2. FE Model Generation

The implant, the abutment, and the abutment screw were analyzed with the parameters illustrated in Figure 3.1. Three abutment screw lengths (4 mm, 5 mm, and 6 mm), three abutment screw head diameters (2.65 mm, 2.75 mm, and 2.85 mm), and three abutment implant angles (30 degrees, 45 degrees, and 60 degrees) were evaluated, with a total of 27 combinations (Figure 3.2, Table 3.1).

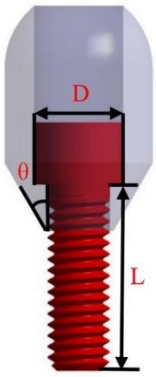


Figure 3.1. Implant design parameters investigated.

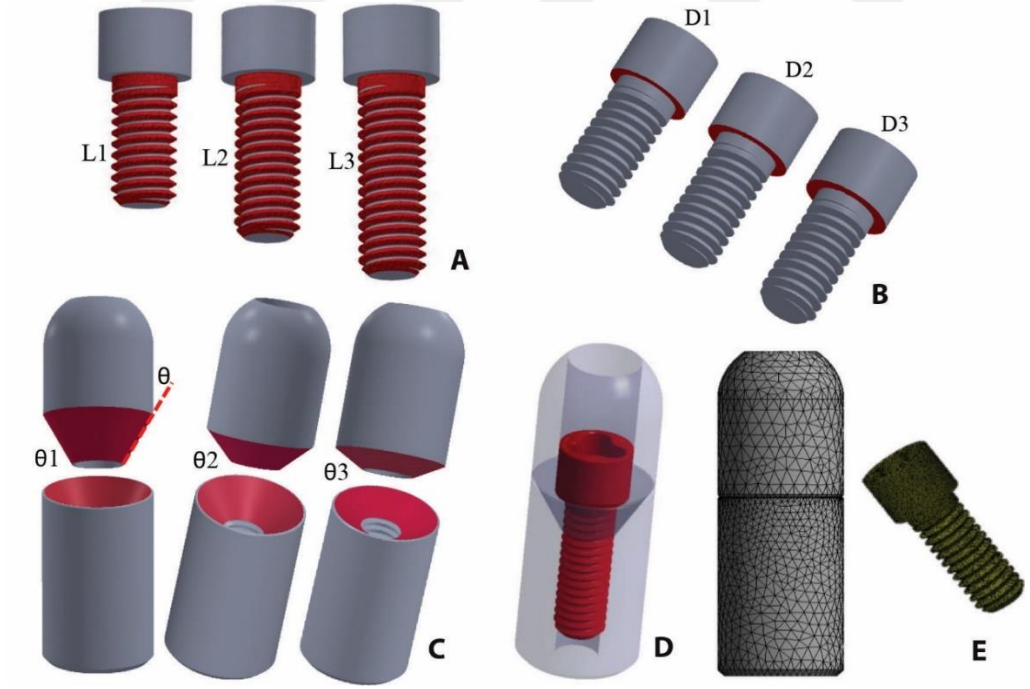


Figure 3.2. Three-dimensional computer-aided design models used with different parameters. A, Abutment screw lengths: 4 mm (L1), 5 mm (L2), and 6 mm (L3). B, Abutment screw head diameters: 2.65 mm (D1), 2.75 mm (D2), and 2.85 mm (D3). C, Abutment implant angles: 30 degrees (θ1), 45 degrees (θ2), and 60 degrees (θ3). D, Assembled model. E, mesh model.

Solid components of the 27 implants were constructed and assembled using a 3-dimensional (3D) computer-aided design (CAD) software program (SolidWorks version 2020; Dassault Systèmes SolidWorks Corp) and exported into a CAD modeling software program (ANSYS version 21; ANSYS, Inc.) for analysis (Figure 3.2). According to the mesh convergence, the screw element size was selected as 0.1 mm, and the element size of other components was 0.25 mm. The mesh of the total model is shown in Figure 3.2E. After the 27 finite element (FE) mesh models had been developed, friction was assumed between all implant components, with a friction coefficient of 0.2 (Jeng et al., 2020).

Table 3.1. Combinations of abutment implant angle (θ), abutment screw head diameter (D), abutment screw length (L) with model nodes and element numbers used.

Abutment Implant Angle (θ) [degrees]	Screw Head Diameter (D) [mm]	Screw Length (L) [mm]	Node Number	Element Number
30	2.65	4	253255	170557
		5	291182	196586
		6	327407	221391
	2.75	4	264181	178301
		5	301131	203631
		6	338699	229433
	2.85	4	274004	185560
		5	311451	211289
		6	348092	236376
45	2.65	4	253963	171066
		5	291401	196781
		6	327816	221694
	2.75	4	264489	178585
		5	301616	204059
		6	338834	229561
	2.85	4	274593	186039
		5	311626	211438
		6	348388	236586
60	2.65	4	254049	171158
		5	291375	196767
		6	304511	207918
	2.75	4	268980	181205
		5	301196	203740
		6	338507	229342
	2.85	4	274370	185926
		5	311683	211525
		6	347807	236199

3.1.3. Static Test

A tightening torque of 25 Ncm was applied to the screw to simulate preload, calculated by substituting the values of the abutment screw design parameters (Table 3.2, Figure

3.3A) in the torque equation (1). A torque of 25 Ncm with a coefficient of friction of 0.2 assumed for all screw threads and screw head resulted in a preload of 542 N, which was transformed along the interface between the surface of the threads of the abutment screw and the surface of the internal threads of the screw channel (Figure 3.4A).

Figure 3.3B illustrates the interface between the screw and the screw channel in the implant design. The screw channel was a threaded, cylindrical hole within the implant body, while the abutment screw had a matching threaded outer surface. The threads on the abutment screw and the screw channel are complementary in terms of their shape, size, and pitch. As the abutment screw is tightened into the screw channel, the threads engage and create friction, which helps to keep the screw in place and prevent loosening. This well-designed interface ensures a strong and secure connection between the abutment and the implant, while also allowing for ease of installation and removal if needed.

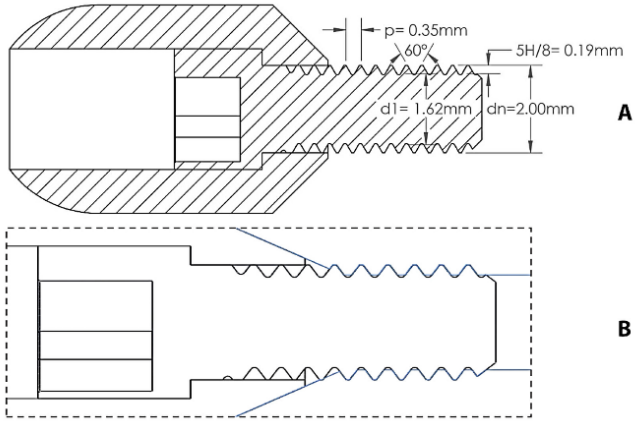


Figure 3.3. A, Abutment screw design parameters values used. B, Interface between abutment screw and screw channel.

Table 3.2. Measurements and preload value for model.

Parameters	Value
T (Nmm)	250
P (mm)	0.35
μ_t	0.2
μ_n	0.2
d_2 (mm)	1.78
d_n (mm)	2
β (deg)	30
F(N)	542

A 200-N force inclined 30 degrees in the axial direction was applied to the upper surface of the abutment (Figure 3.4B) to simulate the maximum masticatory load in the posterior area (Jeng et al., 2020; Yao et al., 2018). All sides of the external surface of the implant were fixed as boundary conditions before the simulation was carried out (Figure 3.4C). The mechanical properties of the materials, including the Poisson ratio and elastic modulus, were standardized, and all materials were assumed to be isotropic, homogeneous, and linearly elastic (Table 3.3) (Jeng et al., 2020; Eraslan & İnan, 2010; Noureddine et al., 2017; Yodrux et al., 2019).

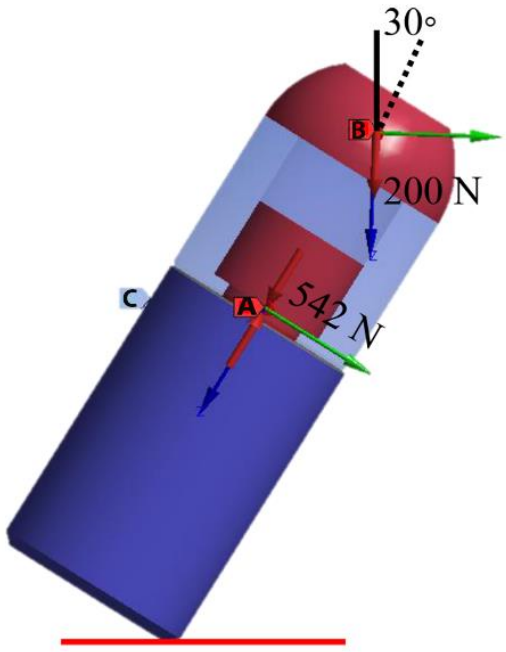


Figure 3.4. Boundary conditions used. A, Screw preload 542 N. B, Load applied to upper surface of abutment 200 N. C, Fixed support (external surface of implant).

Table 3.3. Material properties used in this analysis.

Components	Material	Elastic Modulus E [GPa]	Poisson Ratio υ	Yield Strength σ [MPa]
Abutment Screw, Abutment, Implant	Titanium Alloy (Ti-6Al-4V)	110	0.35	860

Torque calculations

By using the torque equation to calculate screw preload applied in all models:

$$T = \frac{F}{2}\left[\frac{p}{\pi} + \frac{\mu_t d_2}{\cos\beta} + d_n \mu_n\right] \quad (3.1)$$

By solving for F

$$F = \frac{2T}{\left[\frac{p}{\pi} + \frac{\mu_t d_2}{\cos\beta} + d_n \mu_n\right]} \quad (3.2)$$

Where;

T (Nmm)=tightening torque

P (mm)=thread pitch

μt=coefficient of friction for the threads

μn=coefficient of friction for the screw head

d2 (mm)=the effective diameter of thread contact (pitch diameter of the thread)

dn (mm)=the effective diameter of contact between the implant and the joint (major diameter of the thread)

β (deg)=half of thread angle (flank angle)

F (N)=screw preload

By substituting the values of the abutment screw design parameters from Table 3.2 in equation (3.2)

$$F = \frac{2 * 250}{\left[\frac{0.35}{\pi} + \frac{0.2 * 1.78}{\cos 30} + 2 * 0.2\right]} \cong 542 \text{ N}$$

3.1.4. Modal Analysis

The natural frequencies of the 27 models were identified under free vibration by using modal analysis in the ANSYS software program. Free vibration referred to the oscillatory motion of the dental implant in the absence of external forces. All internal contact surfaces in all models were assumed to have a coefficient of friction of 0.2, and the external surface of the implant was fixed from all sides.

3.1.5. Statistical Analyses

To determine whether there were significant differences between factor groups, a nonparametric Kruskal-Wallis statistical test was used because of the nonnormal distribution of some of the data, as determined by the Shapiro-Wilk normality test. Following the Kruskal-Wallis test, multiple pairwise comparisons were conducted using the Dunn test. Statistical analyses were performed using a statistical software program (IBM SPSS Statistics, v29.0.1.0; IBM Corp) (α=.05).

3.2. Experimental Study: Manufacturing and Testing Methods

A total of 30 M4-sized screws were manufactured using machining, thread rolling, and die methods. Each method was used to produce 10 screws made from 6-mm-diameter rods of grade 5 titanium alloy (Ti-6Al-4V) (Figure 3.5). Six steel abutments, six steel implants with internal threads created using cutting and thread rolling taps, and an aluminum holder were fabricated for the purpose of the research. Afterwards, the surface roughness of two screws from each group was measured using a contour measuring device. Furthermore, a digital torque meter was used to evaluate and compare the torque losses of each group before and after a vibration test. Finally, a scanning electron microscope (SEM) was employed to examine the surface topography along the thread profile.

3.2.1. Research Hypothesis

This research hypothesizes that torque loss values, both before and after the vibration test, as well as the total torque loss, would remain consistent across various categories of abutment screws and implants manufactured using different methods when subjected to identical vibration test conditions.

3.2.2. Implant Materials

A grade 5 titanium alloy (Ti-6Al-4V) was selected for the dental implant screws to simulate commercial abutment screws, which are made of Ti-6Al-4V due to its mechanical properties, biocompatibility, and status as the gold standard for dental implants and prosthetic screws (Al-Sanea et al., 2023; Osman & Swain, 2015; Faria et

al., 2012; Wang & Fenton, 1996). In addition, steel material was used for the implants and the abutments, while aluminum was used for the holder. All materials used are listed in Table 3.4.

Table 3.4. Materials used for manufacturing dental implants.

Components	Material
Abutment Screw	Titanium Alloy (Ti-6Al-4V)
Abutment	Steel
Implant	Steel
Holder	Aluminum

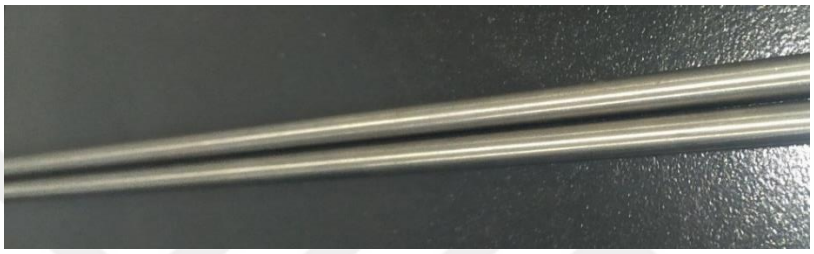


Figure 3.5. 6-mm metal rods of grade 5 Ti alloy.

3.2.3. Dental Implant Geometry

It was found that manufacturing the dental implant screws with M2-size will make the process of measurement of screw surface roughness very challenging due to the precise size of M2 screw threads. Therefore, all abutment screws in this study were manufactured with screw size M4. In addition, all dimensions and geometry of implant and abutment were modified accordingly. Figure 3.6 shows the final design of the dental implant before being manufactured.

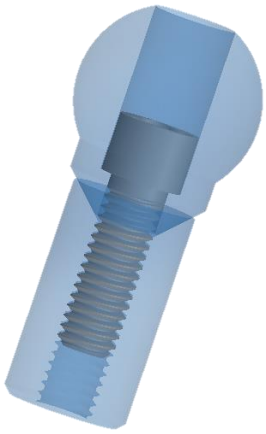


Figure 3.6 Final design of dental implant before being manufactured.

3.2.4. Dental Implant Manufacturing Procedures

Dental implant manufacturing methods have significantly advanced over the years, leading to improved patient outcomes and simplified production processes. In this research, three different manufacturing methods were used for manufacturing dental implant and its components. The methods used are machining, die, and thread rolling. Detailed manufacturing procedures of each component are shown as follows:

3.2.4.1. Abutment Screw Manufacturing Methods

Abutment screws were manufactured using three methods are described in details as follows:

3.2.4.1.1. Machining Method

Computer-aided design (CAD) SolidWorks software program was used to create a 3D model of the dental implant design, then it was converted into instructions (G-code) for the CNC machine using Computer Aided Manufacturing (CAM) Mastercam software program, which was programmed to follow the instructions from the CAD file and precisely remove material from the workpiece to create the desired shape.

In this method, the computer numerical control (CNC) machine shown in Figure 3.7 was used to produce six samples of abutments, six samples of implants without the internal threads, ten samples of dental implant screws, and it was also used to produce other screw samples before being threaded using die and thread rolling methods.



Figure 3.7. Computer Numerical Control (CNC) machine used.

The process of manufacturing abutment screws using the CNC lathe machine involved several steps, from preparing the raw material to cutting the threads and finishing the screw. The steps of this method were as follows:

1. Material preparation:

A 6-mm metal rod of a grade 5 titanium alloy was cut to the desired length for the screw.

2. Workpiece setup:

The cut material was securely set on the CNC lathe chuck using a collet with an M8 size (Figure 3.8A).

3. Facing and turning:

The CNC lathe machine was programmed to perform facing and turning operations to create the desired diameter and length of the screw blank (Figure 3.8B). Facing removes material from the end of the workpiece to create a flat surface, while turning reduces the diameter to the desired size (in this study M4).

The CNC lathe machine is used to rotate the workpiece while a cutting tool removes material along the screw's length, creating its cylindrical shape and smooth surface finish.

4. Thread cutting:

Once the screw blank is prepared, the CNC lathe was programmed to cut the threads. The cutting speed of 100 m/min and the feed rate of 0.7 mm/r were set according to the desired thread pitch and profile. The cutting tool, a single-point threading tool, moves along the axis of rotation at a specific angle to create a helical groove corresponding to the screw's thread profile. The CNC lathe precisely controls the cutting tool's movement and spindle speed, ensuring accurate and consistent thread dimensions (Figure 3.8C).

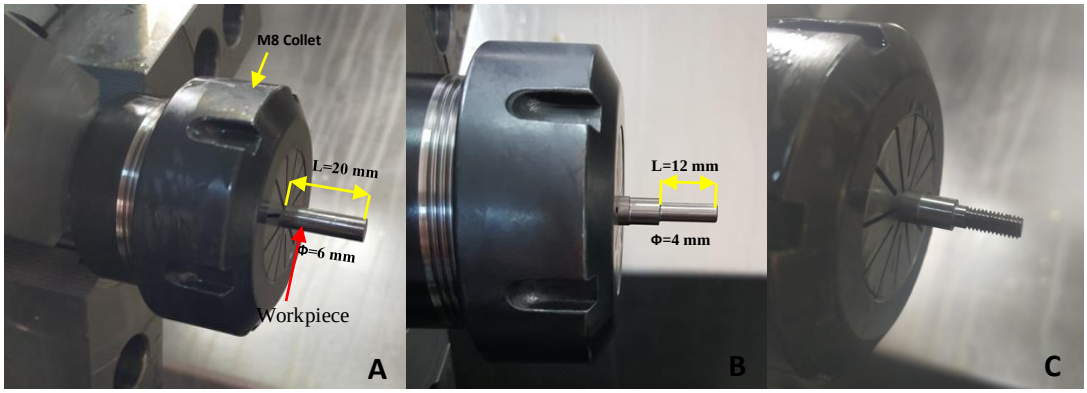


Figure 3.8. Process of manufacturing abutment screw using the CNC lathe machine. A, Workpiece setup. B, Screw blank. C, Machined screw.

5. Parting off:

After completing the turning and thread cutting operations, the finished screw is separated from the remaining stock by parting off. This involves moving a narrow cutting tool perpendicular to the workpiece's axis of rotation, cutting through the material until the screw is released.

6. Secondary operations and finishing:

Additional operations, such as grinding and drilling were necessary to complete the screw. For example, a hole was drilled through the screw head for a specific driver type.

The previous machining operations were repeated to produce 10 samples of machined screws. The machined screws group are shown in Figure 3.9.



Figure 3.9. Group of machined screws (10 samples).

3.2.4.1.2. Die Method

In this method, the preformed die shown in Figure 3.10 was used to create the external threads on a screw blank after it was produced using the machining method. This process is called thread cutting and it was used to produce ten samples of dental implant screws.

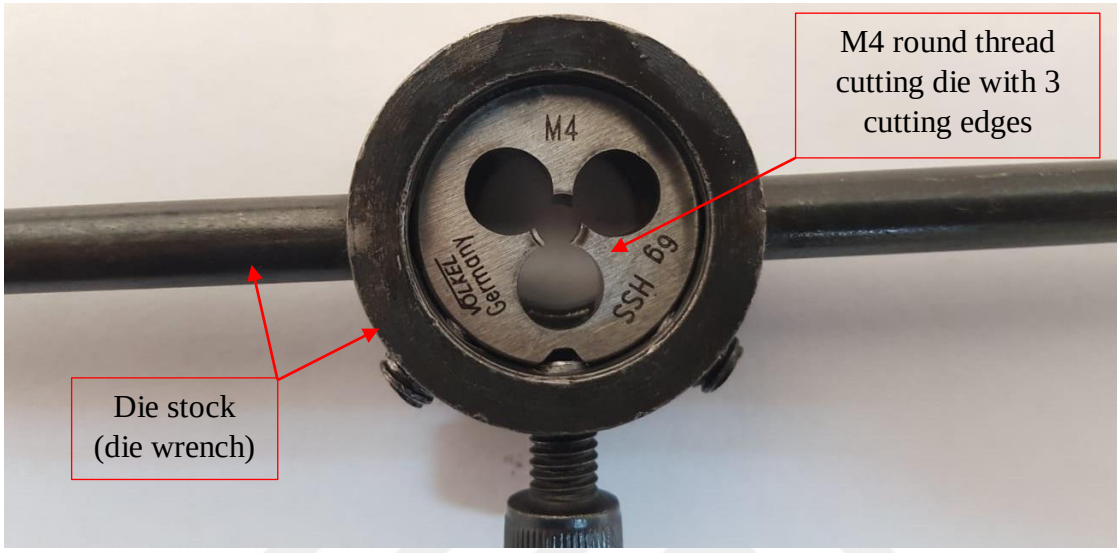


Figure 3.10. A die tool used for cutting external threads on a screw blank by forcing it through the die's form.

The general process for manufacturing threaded screws using the die method in this study is outlined as follows:

1- Production of a screw blank with the desired length and size, as shown in Figure 3.11, by repeating the first three steps of the machining method.



Figure 3.11. A screw blank of the desired length and size (M4x12) produced through the machining method.

2- Thread cutting with a die:

An M4 round thread cutting die with three cutting edges as shown in Figure 3.10, matching the desired thread profile and pitch for the screw, was employed. The die was secured in a die stock (die wrench) for holding and rotating the die.

3- Lubricate:

A cutting oil or lubricant was applied to the workpiece (the screw blank) and the die to reduce friction, heat, and tool wear during the threading process.

4- Align and start threading:

The die was carefully aligned with the workpiece, ensuring that it was perpendicular to the longitudinal axis of the workpiece as shown in Figure 3.12. Additionally, steady pressure was applied to the die while turning it clockwise to engage the cutting edges with the workpiece. Subsequently, the die began cutting threads into the workpiece as it was turned.

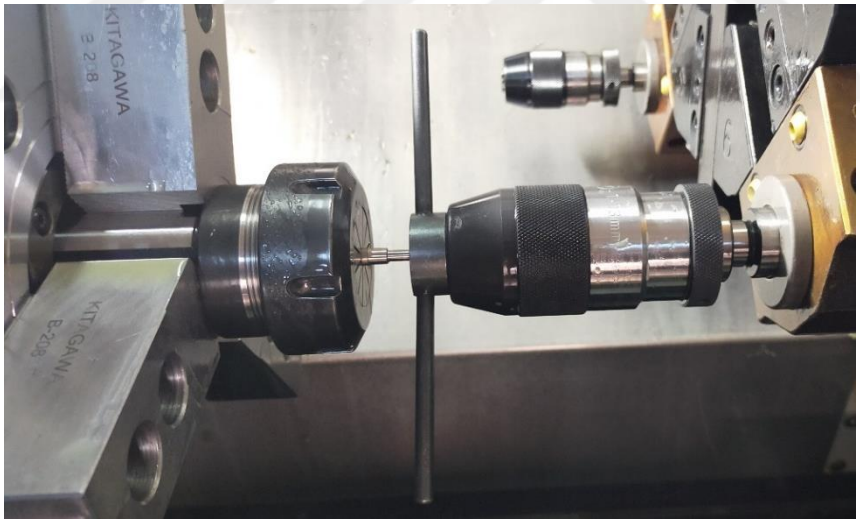


Figure 3.12. Aligning the die perpendicular to the workpiece's longitudinal axis for accurate and consistent thread formation.

5- Cutting the threads:

The die was consistently rotated clockwise, as illustrated in Figure 3.13, under steady applied pressure. After completing each half or full rotation, a slight counter-clockwise turn of the die was carried out to dislodge and clear away any material fragments. This

step is crucial to prevent the obstruction of the die and to facilitate a smoother thread cutting process.

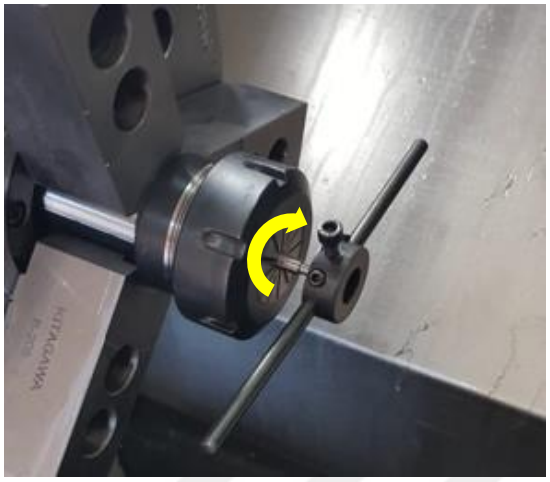


Figure 3.13. Illustration of the thread cutting process with clockwise die rotation (yellow arrow).

6- Finish threading:

The threading process was continued until the desired thread length was achieved (Figure 3.14).

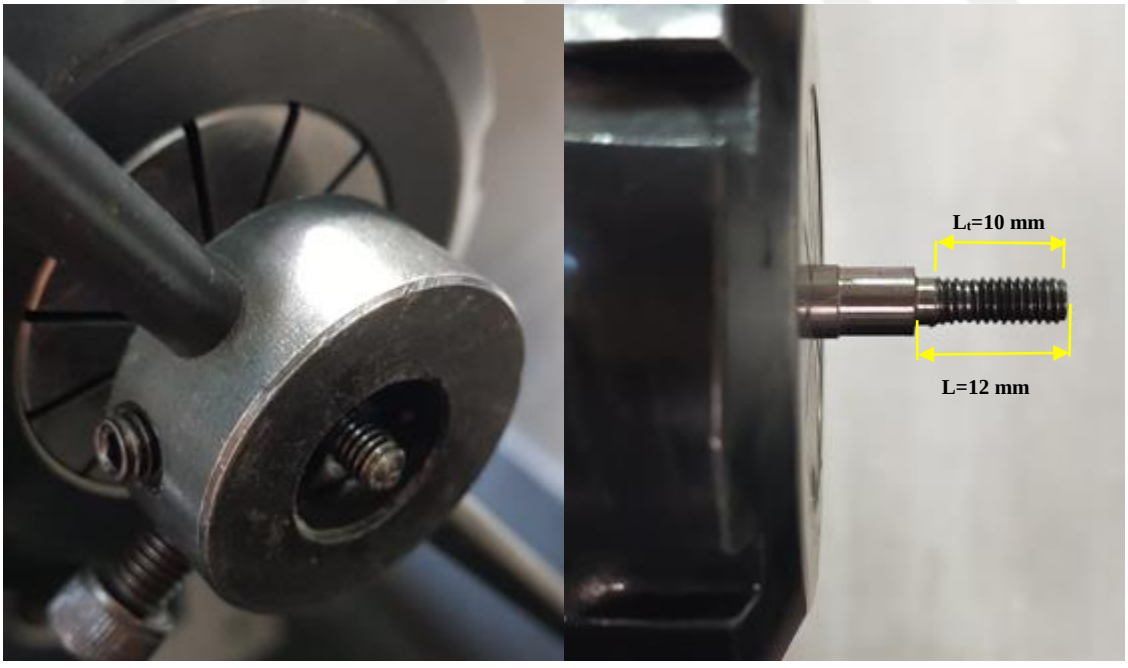


Figure 3.14. Completion of the threading process at desired thread length (L_t=10 mm).

7- Cleaning:

The die was removed from the workpiece, and any remaining cutting oil, chips, or debris were cleaned from the screw threads.

8- Finishing operation:

The finishing process was subsequently carried out using the CNC lathe machine. All screws produced using the die method are shown in Figure 3.15.



Figure 3.15. Group of die screws (10 samples).

3.2.4.1.3. Thread Rolling Method

The thread rolling machine shown in Figure 3.16 was utilized to produce external threads on ten screw blanks (Figure 3.17), which were preprepared using the machining method. The thread rolling process involves plastic deformation of the workpiece material to form threads rather than cutting or removing material, in contrast to the machining and die methods.

The process of producing threaded screws using thread rolling can be described in the following steps:

1- Producing a screw blank with the desired length and size, as shown in Figure 3.16, by repeating the first three steps of the machining method.

2- Setup of the thread rolling machine:

A thread rolling machine was set up with the appropriate thread rolling dies, which were flat dies with the desired thread profile and pitch engraved on their surfaces. The dies were aligned and adjusted in the machine according to the specifications of the screw being produced.

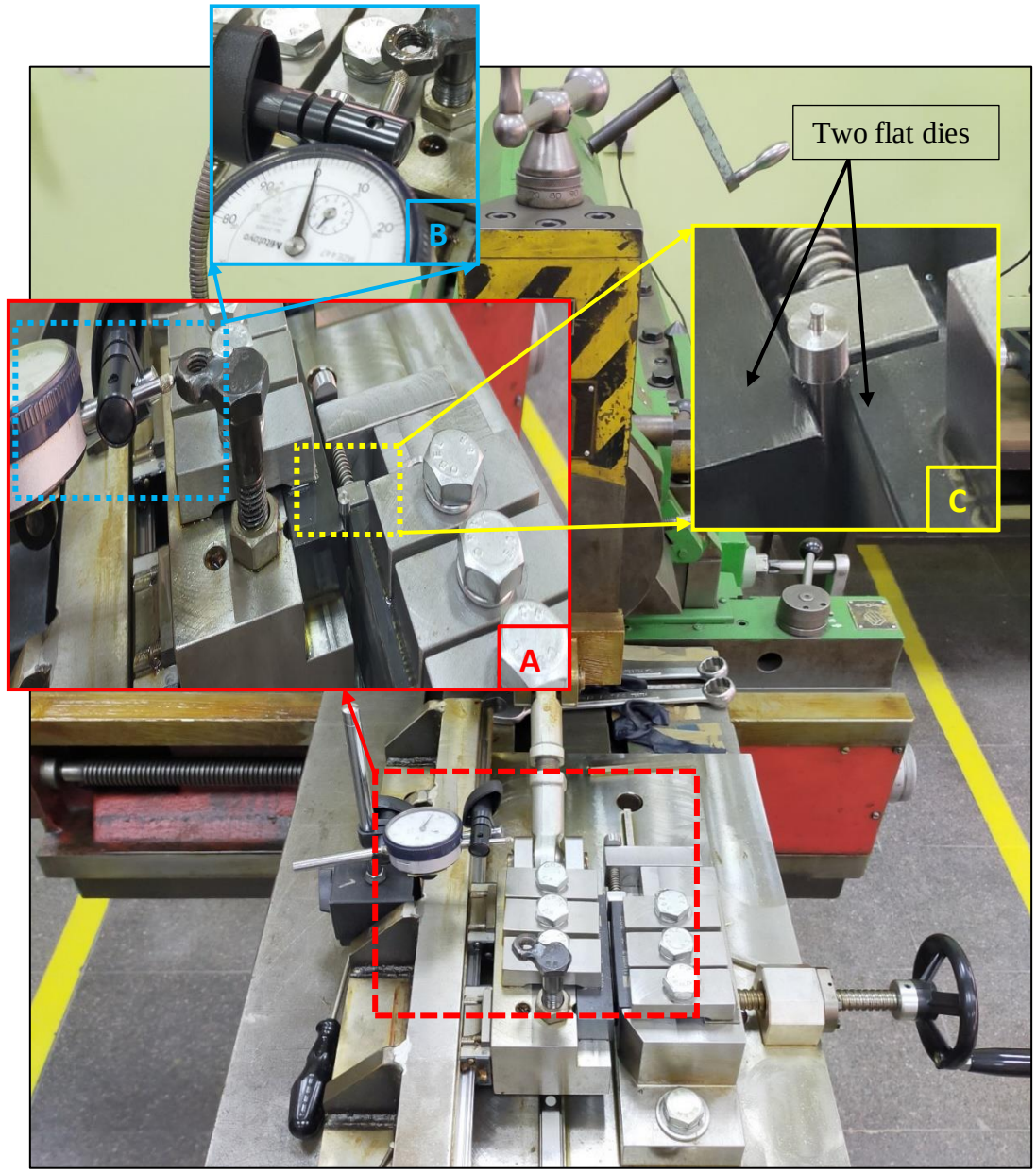


Figure 3.16. Thread rolling machine used. A, Final setup of the thread rolling machine for screw production. B, A pressure gauge, serving as a position switch C, A screw blank between two flat dies.

A pressure gauge, serving as a position switch, was employed to commence a new production cycle. The cycle initiation is triggered when the gauge's indicator comes into contact with the vertical bolt, as shown in Figure 3.16B, and resets to zero.



Figure 3.17. A group of screw blanks before being threaded using the thread rolling method.



Figure 3.18. Group of thread rolled screws (10 samples).

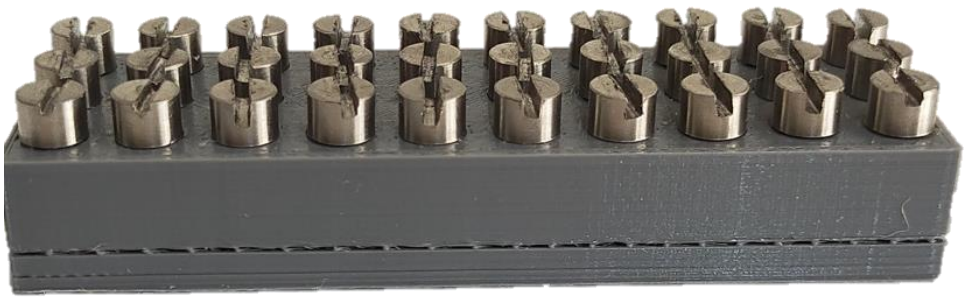


Figure 3.19. All machined, die, and thread-rolled screws (30 samples) produced.

3.2.4.2. Screw Head Formation

Mailing machine, shown in Figure 3.20, was used for manufacturing a specific driver type, shown in Figure 3.21A, based on the design of the screw head. Figure 3.21B shows the final shape of the specific driver. In addition, it was used for the screw head formation as shown in Figure 3.22. However, the process failed due to the small size of screw head (Figure 3.23). To address this issue, a hand saw was subsequently employed to form the screw head.



Figure 3.20. Milling machine used to produce a specific driver type and form a screw head.

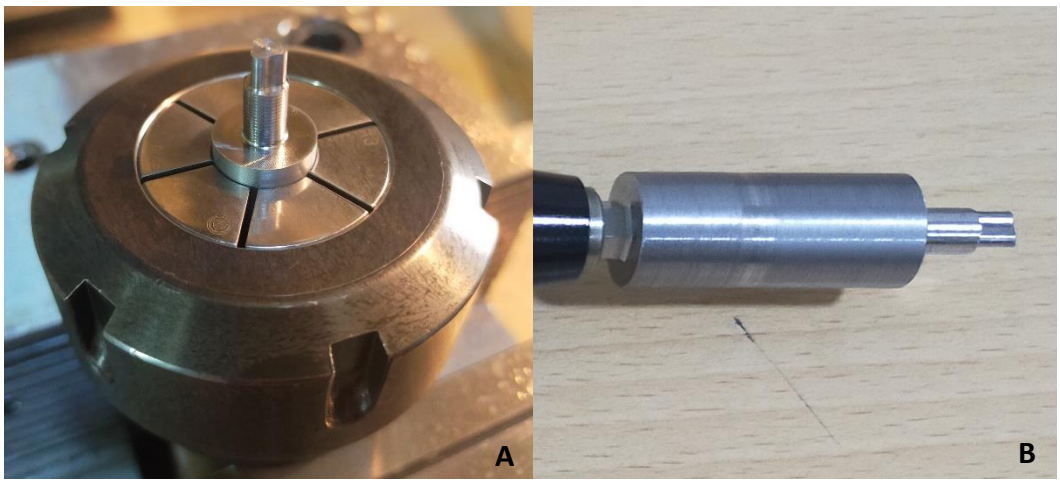


Figure 3.21. A, Manufacturing a specific type of driver using milling machine. B, Final shape of the specific driver.

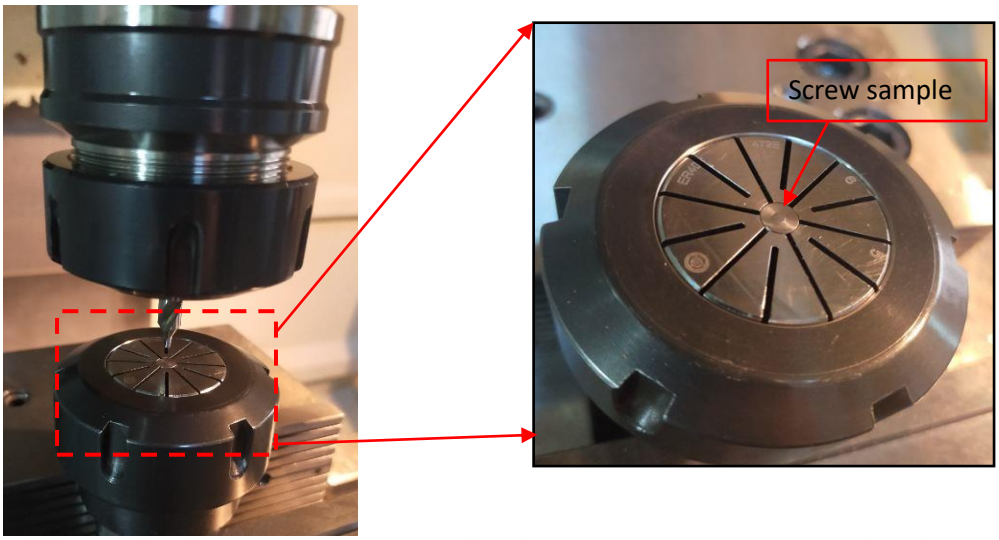


Figure 3.22. Screw head formation using milling machine.



Figure 3.23. Two abutment screws showing manufacturing failure at the screw head.

3.2.4.3. Abutment Manufacturing

Six steel abutments, as shown in Figure 3.24, were manufactured using the CNC machine.



Figure 3.24. Group of abutments produced using the CNC machine.

3.2.4.4. Implant Manufacturing

Six steel implants, as shown in Figure 3.24, were manufactured using the CNC machine.



Figure 3.25. Group of implants produced using the CNC machine.

3.2.4.4.1. Production of Internal Threads in Implants

In this study, both cutting and rolling taps, as shown in Figure 3.26, were utilized to produce the internal threads of the implants, all of which were manufactured using the machining method. Implants whose internal threads were generated with the cutting tap, a tool that inherently creates wear, will henceforth be referred to as machined implants (Implant Type M) throughout the study (Figure 3.27A). Conversely, implants with internal threads made using the rolling tap, a tool that does not induce wear, will be identified as Thread Rolled Implants (Implant Type TR) (Figure 3.27B).

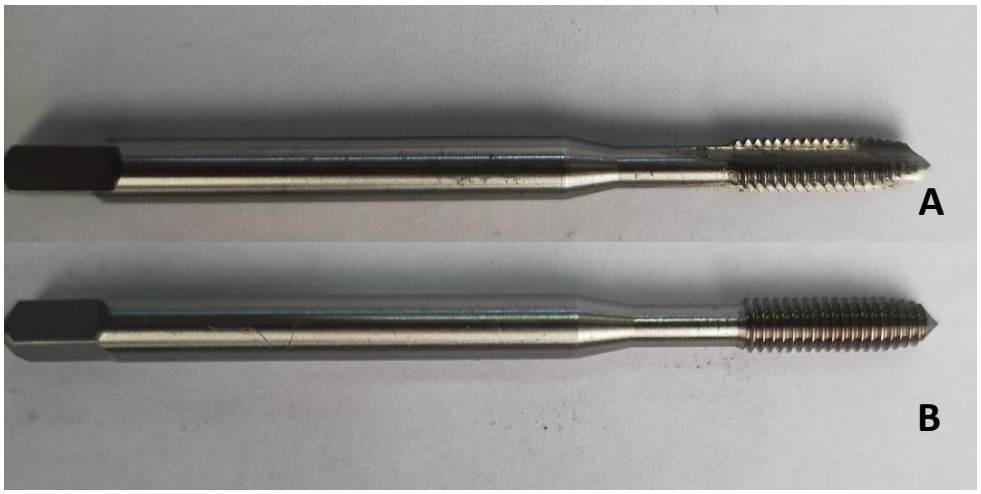


Figure 3.26. Taps used for creating the internal threads of implants. (A) Cutting tap, (B) Rolling tap.

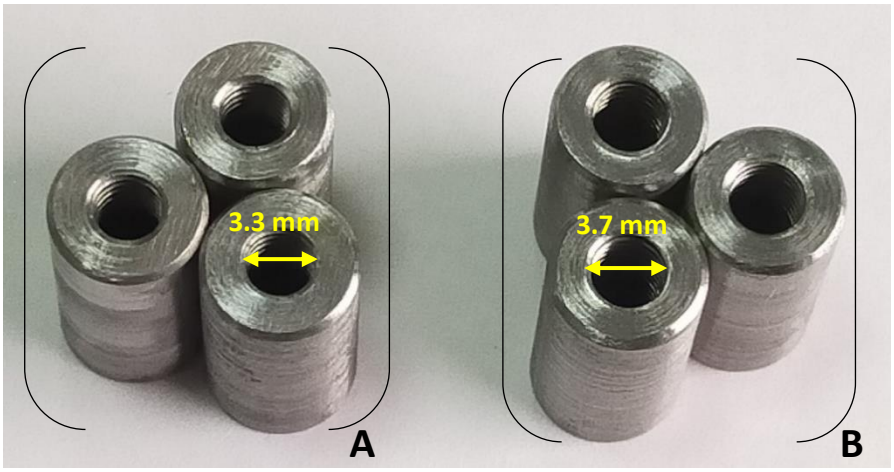


Figure 3.27. Different types of implants. A, Machined implants. B, Thread rolled implants.

3.2.5. Assembled Model of Dental Implant



Figure 3.28. The completed assembly of the dental implant model.

3.2.6. Analysis Tests and Measurements

3.2.6.1. Surface Roughness Assessment (Contour Measurements)

In the context of this research, measuring the surface roughness of each screw group is a critical step to investigate of the effect of abutment screw surface roughness on screw loosening.

In this study, the surface roughness of the screws was measured through profile (contour) measurements. A stylus-equipped contour measuring device, as shown in Figure 3.29, was employed to obtain a numerical representation of the roughness. In this test, the stylus of the contour measuring device moves linearly, allowing us to obtain a single path across

the surface. This device was utilized to measure the surface roughness of two samples from each group. Profilograms of each sample are shown in the results section.

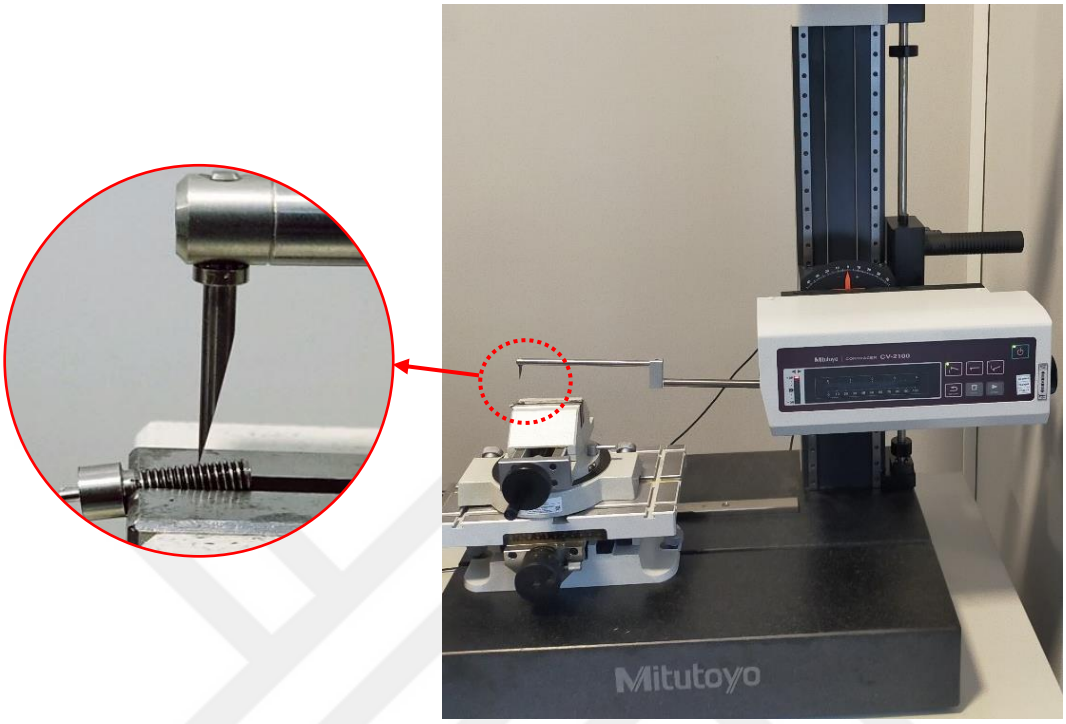


Figure 3.29. Contour measuring device used to measure surface roughness of dental implant screw.

The procedures followed of measuring surface roughness of screws using contour measuring device were as follows:

The abutment screw samples were first cleaned and prepared. Once prepared, each sample was carefully placed on the stage of the contour measuring device. The device's stylus was then delicately lowered onto the surface of the screw at a predetermined starting point. The device was then set to scan a single, linear path along the surface of the screw thread. During this process, the stylus traced the surface contour of the screw, recording the vertical deviations which are indicative of surface roughness. Following this, the recorded data was analyzed to obtain surface roughness parameters Ra (average roughness), Rq (root mean square roughness), and Rz (average maximum height of the roughness profile). These values were obtained for each screw sample and presented in the results section.

3.2.6.2. Vibration Test and Torque Loss Assessment

A digital torquemeter, as shown in Figure 3.30, was utilized to measure torque losses for all samples. In this process, each screw sample was initially tightened to a torque of approximately 100 Ncm. Then, a screw was loosened, and the torque necessary for loosening (detorque) was measured. The difference between applied (tightening) torque and detorque is commonly used to assess torque loss.



Figure 3.30. The digital torquemeter used for the assessment of torque losses in screw samples.

Each screw sample was subsequently retightened to the same initial torque of approximately 100 Ncm before the application of the vibration test.

In this study, a vibration device (vibrator) shown in Figure 3.31 was utilized to simulate the conditions of mechanical stress that dental abutment screws would be subjected to in a real-life oral environment. The primary objective of using this device was to evaluate and compare the torque losses between the samples of each group under these simulated conditions.

Vibration test settings:

The vibrator was installed on the compression tensile machine at an angle of 30 degrees relative to the vertical axis of a dental implant as illustrated in Figure 3.31. This position was chosen in accordance with ISO 14801, which pertains to fatigue testing in dental implants (Aktas et al., 2022). To augment the impact of the applied force on the dental implant, a set of four nuts was affixed to the end of the vibrator's bar. Additionally, a metal circle was attached to the bar to enlarge the contact area with the abutment surface, thereby expanding the effect of vibration (Figure 3.31B). Ultimately, the vibration device was set to operate for 24 hours at a frequency of 75 Hz for all abutment screws. After this period, the dental implant was detorqued again to measure the resulting torque loss.

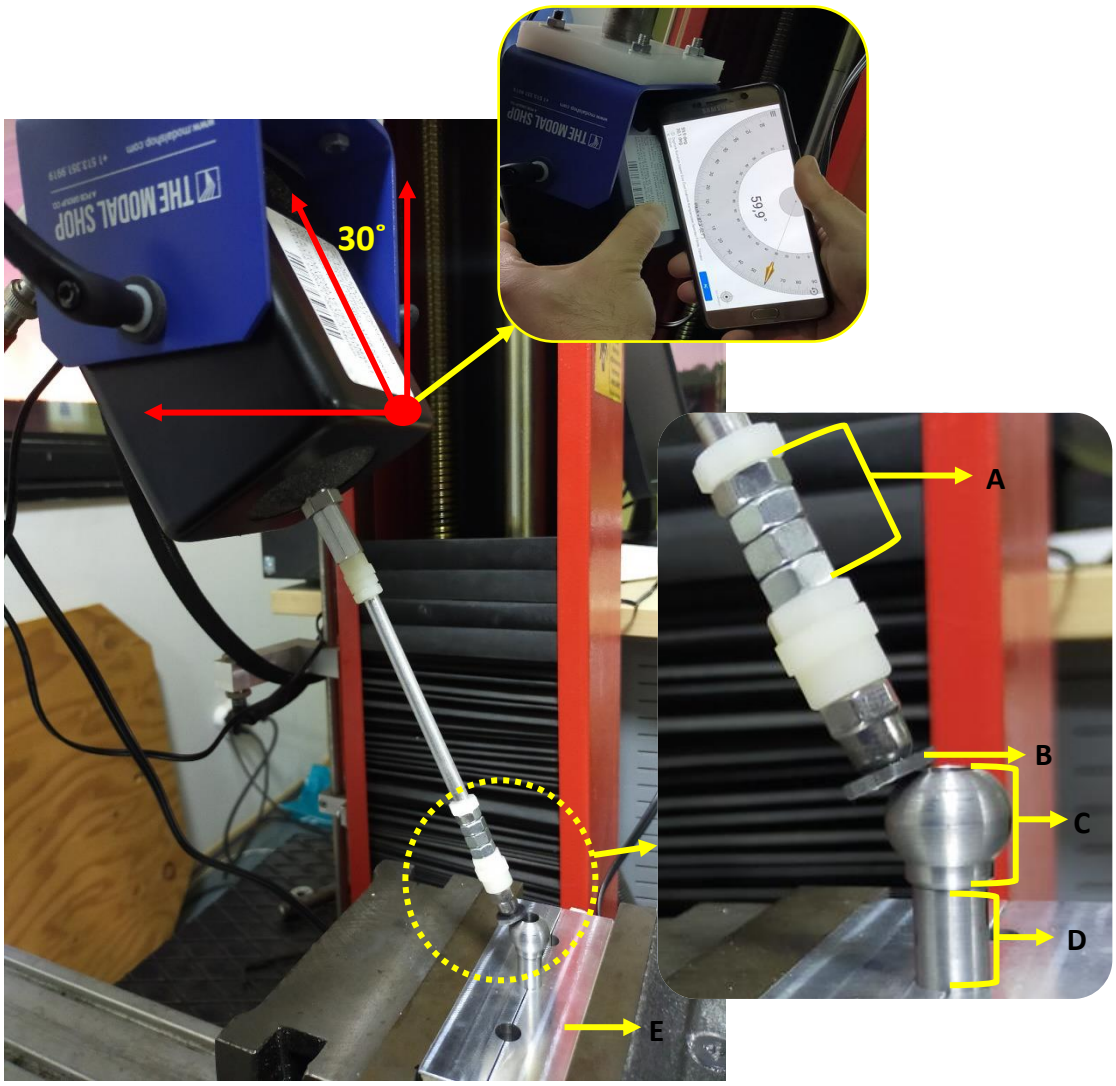


Figure 3.31. A vibrator device used. A, 4 nuts to increase the effect of a force applied. B, Metal circle to increase the effect of vibration. C, Abutment. D, Implant. E, Holder.

3.2.6.3. Scanning Electron Microscopy (SEM) Analysis

In this research, a Scanning Electron Microscope (SEM) as illustrated in Figure 3.32, was employed to capture detailed images of the abutment screw's surface at various magnifications, specifically at X10, X25, X100, X200, X1000 and X5000.

The SEM analysis procedure involved cleaning and preparing two samples from each group (Figure 3.33), positioning the prepared samples within the SEM chamber, and then scanning the samples with the electron beam. The resulting images were then analyzed and presented in the results section.



Figure 3.32. Scanning electron microscope (SEM) used.

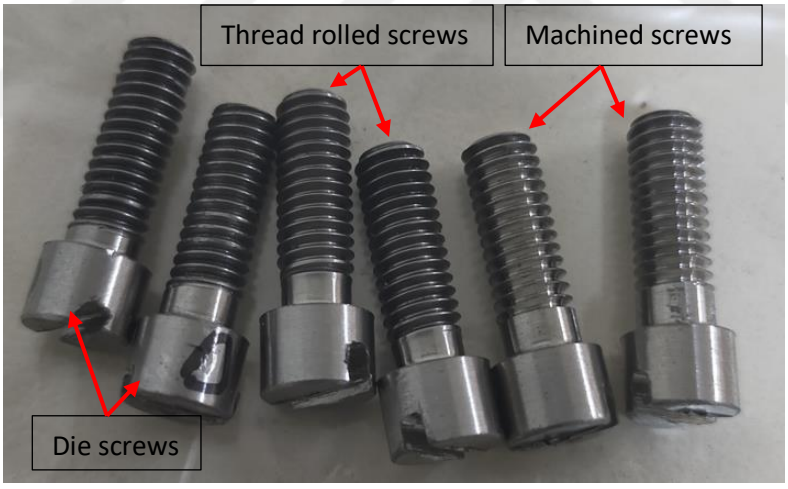


Figure 3.33. Two screw samples from each group were analyzed using SEM.

3.2.6.4 Statistical Analyses

Since the data was found to be normally distributed (as determined by the Shapiro-Wilk normality test), parametric tests were used. The one-way analysis of variance (ANOVA) and the independent samples t-test were used to investigate whether there were significant differences between the factor groups. Statistical analyses were conducted using a statistical software program (IBM SPSS Statistics, v26; IBM Corp) (α=.05).

4. RESULTS AND DISCUSSIONS

4.1. Results

4.1.1. Computational Study Results

The findings of the static test and modal analysis are presented in Table 4.1. Figure 4.1 illustrates stress distribution in implant components for one model. As shown in Table 4.2, the Kruskal-Wallis test revealed a significant influence of the abutment implant angle on implant stress, total deformation, and natural frequency (P<.001). Furthermore, the Dunn test showed significant differences (P<.05) among all three group pairs (30-45, 30-60, and 45-60 degrees) for the same measured values, except for total deformation between the 45-60-degree group pair (P=.272) (Table 4.3).

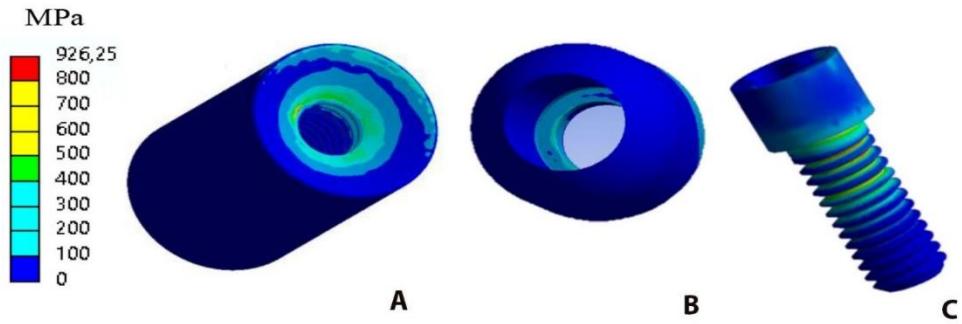


Figure 4.1. Stress distribution in one model. A, Implant. B, Abutment. C, Abutment screw.

The abutment screw head diameter significantly affected both abutment screw stress and abutment stress, (*P*=.010 and *P*=.002, respectively) (Table 4.2). The Dunn test revealed significant differences in abutment screw stress between the group pair (2.65-2.75) mm and in abutment stress between the group pairs (2.65-2.85) mm and (2.75-2.85) mm (Table 4.3). However, abutment screw length had no significant effect on any of the dependent variables (*P*>.05) (Table 4.2).

The main effect of the maximum von Mises equivalent stress indicated that the implant stress was influenced by the abutment implant angle. For example, the rate of change in implant stress was 76% and -28% when the abutment implant angle increased from 30 degrees to 45 degrees and 60 degrees, respectively (Figure 4.2A). Additionally, the maximum total deformation of the models significantly increased to 55% when the abutment implant angle changed from 30 to 45 degrees (*P*<.001) and increased, but at a

Table 4.1. Maximum von Mises stress of implant components, total deformation and natural frequency for all models.

Abutment Angle (θ) [deg]	Screw Head Diameter (D) [mm]	Screw Length (L) [mm]	Maximum von Mises Stress of Abutment Screw (MPa)	Maximum von Mises Stress of Abutment (MPa)	Maximum von Mises Stress of Implant (MPa)	Maximum Total Deformation of Model (mm)	Natural Frequency of Model (Mode 1) (Hz)
30	2.65	4	666.64	261.16	738.10	0.0075079	92098
30	2.65	5	697.32	259.64	711.80	0.0075121	92136
30	2.65	6	689.02	261.00	729.58	0.0075484	92085
30	2.75	4	693.21	240.12	566.33	0.0077083	92753
30	2.75	5	716.85	239.98	580.10	0.0076633	92772
30	2.75	6	721.58	239.64	728.03	0.0076963	92722
30	2.85	4	721.66	354.50	237.43	0.0085641	93138
30	2.85	5	680.09	197.50	605.19	0.0078479	93445
30	2.85	6	695.73	197.83	721.06	0.0078792	93401
45	2.65	4	703.45	264.28	1036.5	0.0089318	75180
45	2.65	5	675.11	263.13	956.87	0.0088812	75186
45	2.65	6	671.84	263.92	663.42	0.0089596	75418
45	2.75	4	702.49	243.25	1035.3	0.0091241	75864
45	2.75	5	926.25	284.46	823.28	0.0353830	75871
45	2.75	6	733.63	242.72	1584.9	0.0091323	75808
45	2.85	4	737.75	216.06	1280.1	0.0092667	76715
45	2.85	5	661.6	215.13	898.50	0.0091817	76727
45	2.85	6	712.38	215.37	1588.8	0.0093205	76662
60	2.65	4	660.99	267.31	482.28	0.0085860	67679
60	2.65	5	674.54	266.40	475.94	0.0086431	67709
60	2.65	6	707.54	270.53	443.77	0.0112000	65672
60	2.75	4	747.46	299.99	313.91	0.0092026	68463
60	2.75	5	691.57	239.66	476.16	0.0088097	68433
60	2.75	6	738.27	238.81	417.76	0.0087534	68417
60	2.85	4	724.89	213.18	470.46	0.0089609	69199
60	2.85	5	675.78	212.98	507.32	0.0090377	69218
60	2.85	6	722.25	212.90	471.25	0.0089451	69210

Table 4.2. K independent Kruskal-Wallis test *P* values (significance level at *P*<.05).

	Abutment Screw Stress	Abutment Stress	Implant Stress	Total Deformation	Natural Frequency
Abutment Implant Angle	.799	.852	<.001	<.001	<.001
Abutment Screw Head Diameter	.010	.002	.952	.336	.276
Abutment Screw Length	.291	.291	.934	.917	.934

Table 4.3. Multiple pairwise comparisons using Dunn test *P* values (significance level at *P*<.05).

	Pairwise Comparisons	Abutment Screw Stress	Abutment Stress	Implant Stress	Total Deformation	Natural Frequency
Abutment Implant Angle [degrees]	Group 30-45			.018	<.001	.016
	Group 30-60			.043	.002	<.001
	Group 45-60			<.001	.272	.016
Abutment Screw Head Diameter[mm]	Group 2.65-2.75	.003	.181			
	Group 2.65-2.85	.070	<.001			
	Group 2.75-2.85	.235	.033			

lesser rate of 17%, when the angle changed from 30 to 60 degrees (*P*=.002) (Table 4.3, Figure 4.2A). Furthermore, the main effect plot (Figure 4.2A) reveals a decrease in natural frequency corresponding to an increase in the abutment implant angle. Specifically, when the angle of the abutment implant increased from 30 degrees to 45 degrees and 60 degrees, the natural frequencies of the models decreased to 18% and 26%, respectively.

For the main effect of abutment screw head diameter (D), the maximum von Mises stress of the abutment screw increased to 9% when the diameter changed from 2.65 to 2.75 mm (*P*<.05) and increased to 3% when the diameter increased from 2.65 to 2.85 mm (Table 4.3, Figure 4.2B). In contrast, the increase in screw head diameter resulted in a decrease in the abutment stress from 264.15 MPa to 252.07 MPa and 226.16 MPa, respectively (Figure 4.2B).

For screw length, no clear relationship was observed between the maximum von Mises equivalent stress of the implant, the abutment, and the abutment screw (Figure 4.2C). Additionally, it was not evident that increasing L values from 4 mm to 5 mm and 6 mm had any distinct effect on the natural frequencies of the model (Figure 4.2C). These observations were corroborated by statistical tests, which demonstrated that screw length had no significant impact on these measured parameters (*P*>.05) (Table 4.2).

When looking at the main effect plot for maximum total deformation across all models, no clear direct or inverse relationship was found within the investigated factor groups. However, the total deformation was observed to be at its highest when the model parameters included an abutment implant angle of 45 degrees, a screw head diameter of 2.75 mm, and a screw length of 5 mm (Figure 4.2A-C).



Figure 4.2. A-C, Main effect of abutment implant angle (θ), abutment screw head diameter (D), and abutment screw length (L) at each level of maximum stresses of implant components, total deformation, and natural frequency for all models.

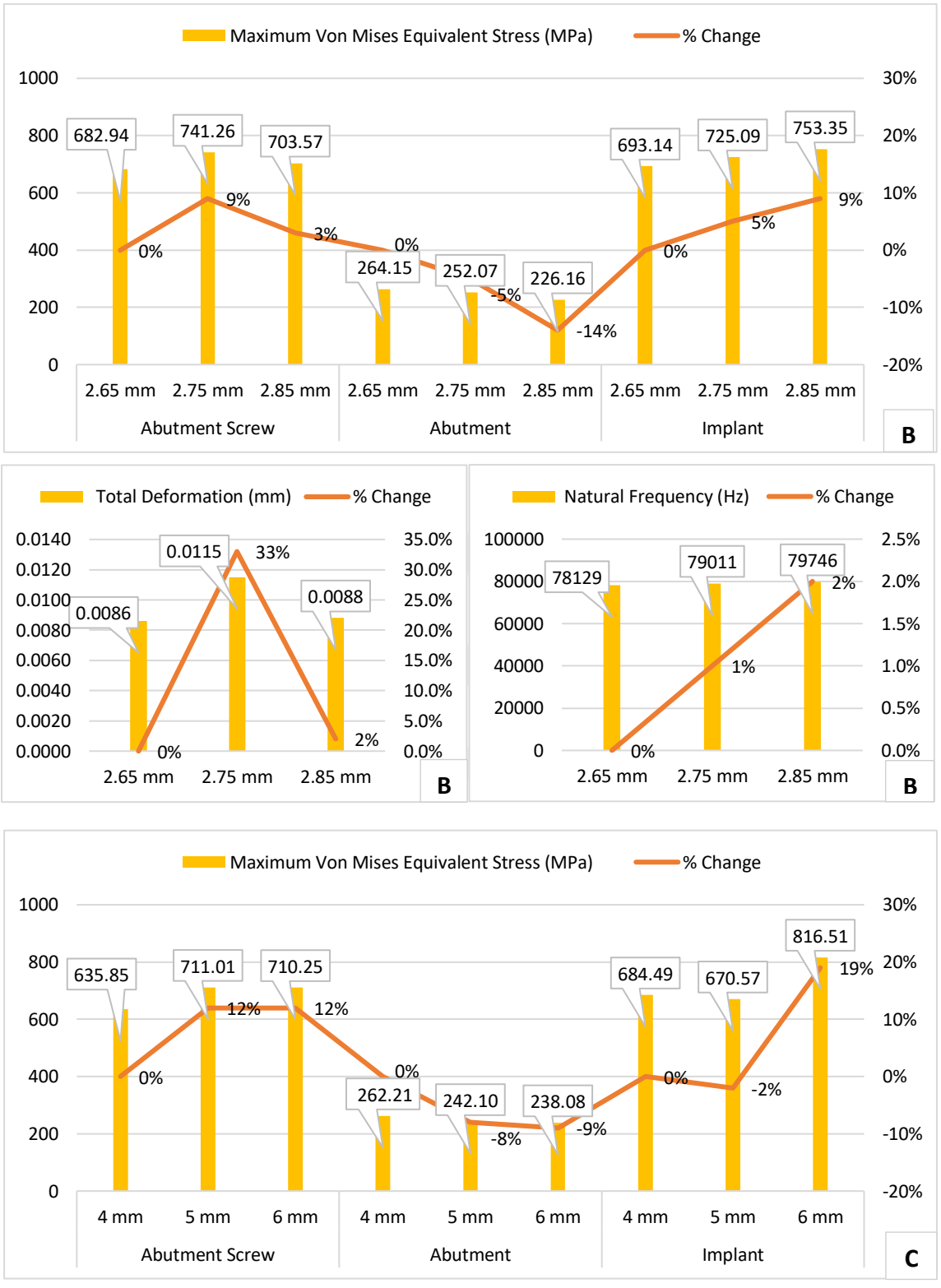


Figure 4.2. (Continued) A-C, Main effect of abutment implant angle (θ), abutment screw head diameter (D), and abutment screw length (L) at each level of maximum stresses of implant components, total deformation, and natural frequency for all models.

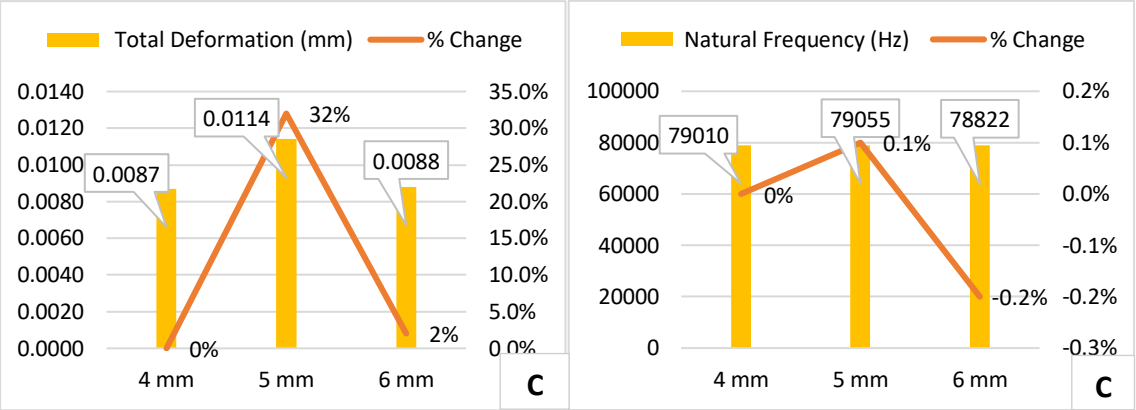


Figure 4.2. (Continued) A-C, Main effect of abutment implant angle (θ), abutment screw head diameter (D), and abutment screw length (L) at each level of maximum stresses of implant components, total deformation, and natural frequency for all models.

4.1.2. Experimental Study Results

4.1.2.1. Surface Roughness Assessment Results

Profilograms of two machined screws (M1 and M2), two die screws (D1 and D2), and two thread-rolled screws (TR1 and TR2) are illustrated in Figures 4.3-4.8, respectively. These profilograms illustrate important characteristics of the screw threads, such as their pitch, angle, and depth. These parameters, extracted from each sample's profilogram, are numerically presented in Table 4.4. These profilograms, along with their respective quantitative data tabulated in Table 4.4, provide a comprehensive view of the geometric characteristics of the screw threads. A systematic comparison of these parameters across different manufacturing methods provides valuable insights into the variations in thread characteristics and helps in understanding their potential influence on the incidence of screw loosening.

Table 4.4. Thread characteristics of different abutment screw samples.

Sample No	Thread Pitch (mm)	Thread depth (mm)	Thread Angle (deg)
M1	0.6989	0.4804	60.7367
M2	0.6924	0.4847	61.0205
D1	0.7238	0.4011	62.1458
D2	0.6896	0.4268	64.8838
TR1	0.7059	0.4644	58.8929
TR2	0.6988	0.4611	58.8585

By examining Table 4.4, it can be observed that there is a reasonable consistency within the groups for both machined screws (M1 and M2) and thread-rolled screws (TR1 and TR2) across all thread parameters (pitch, depth, and angle). However, the die screws (D1 and D2) show noticeable differences across all thread parameters. Overall, Table 2 reveals differences between the various manufacturing methods.

In addition, these profilograms provide visual representations of surface roughness. Significantly, the die screws (D1 and D2) exhibited higher surface roughness, as can be observed in the marked areas. Conversely, the machined screws (M1 and M2) demonstrated lesser surface roughness, while the surface roughness of the thread-rolled screws was between the two other methods (Figure 4.3-Figure 4.8).

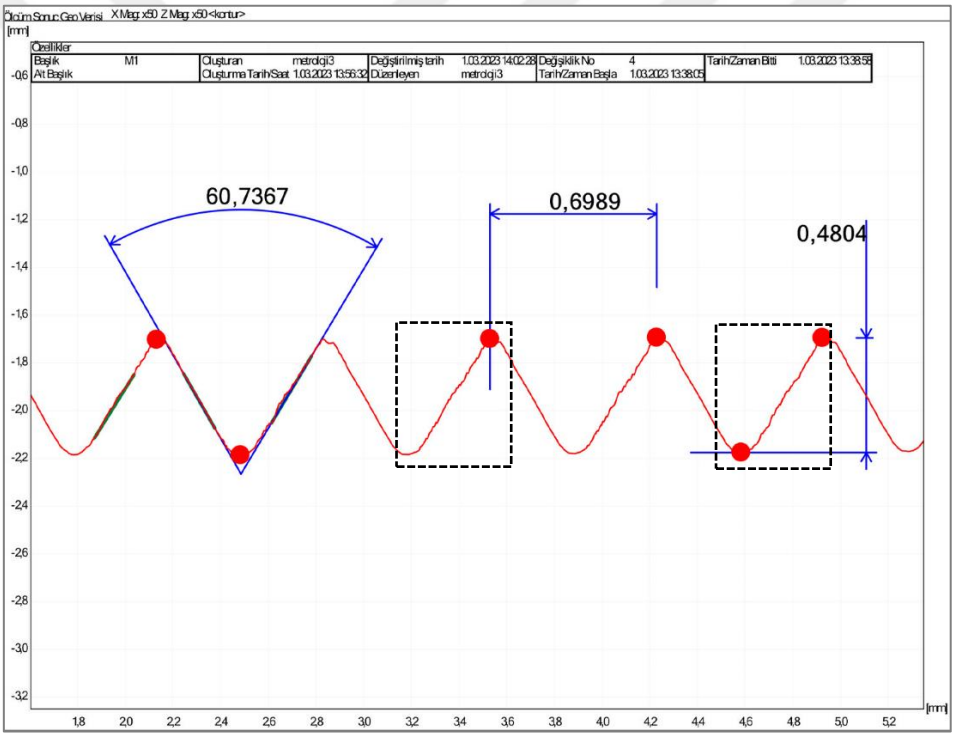


Figure 4.3. Profilogram of sample M1 (machined screw), showing thread pitch, angle, and depth.

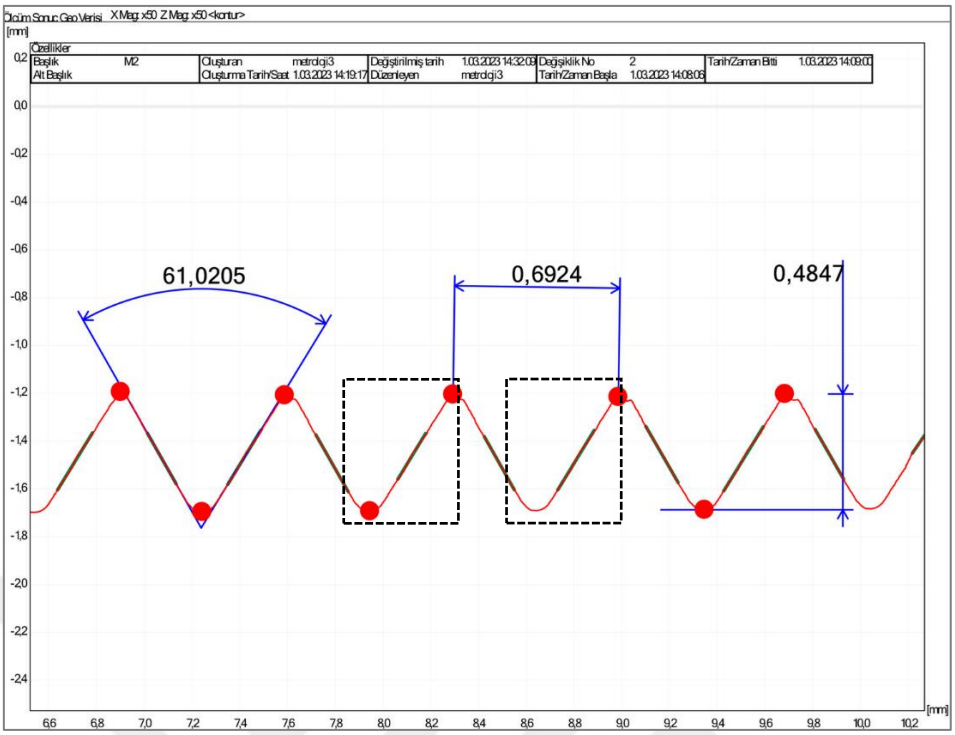


Figure 4.4. Profilogram of sample M2 (machined screw), showing thread pitch, angle, and depth. The marked areas (indicated by small black squares) highlight regions of surface texture, indicating the lower surface roughness of this sample compared to samples D1 and D2.

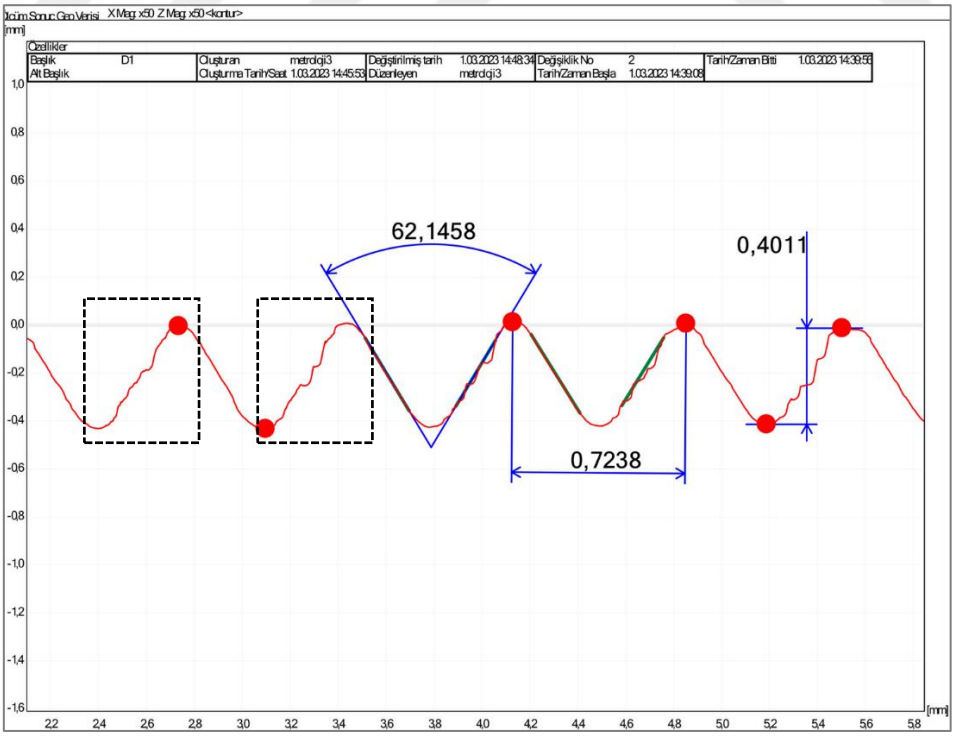


Figure 4.5. Profilogram of sample D1 (die screw), showing thread pitch, angle, and depth.

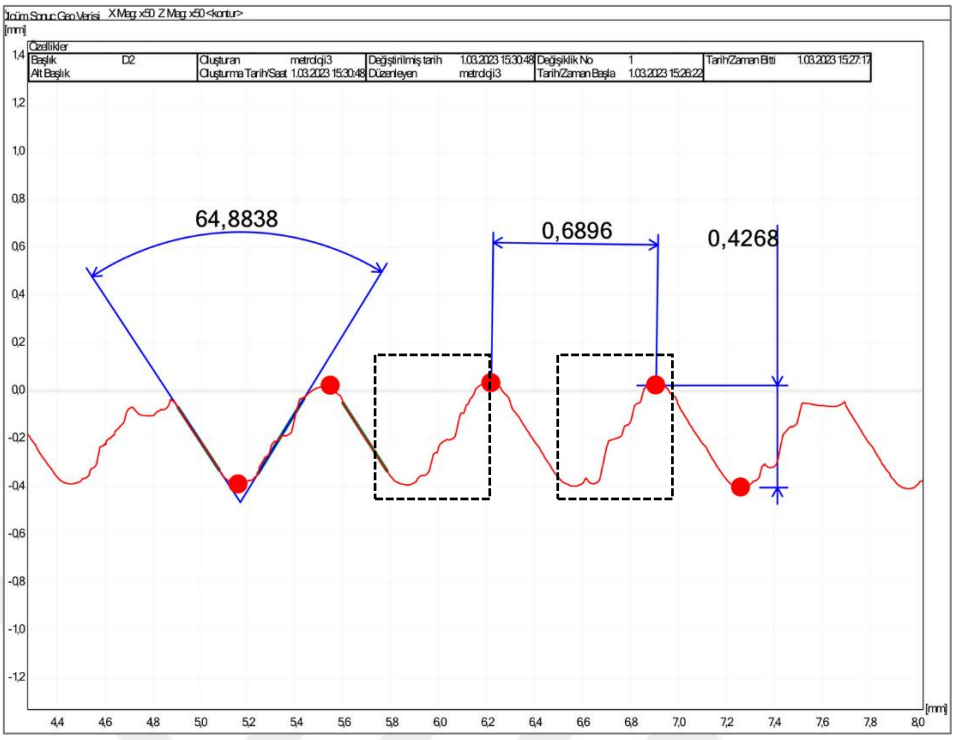


Figure 4.6. Profilogram of sample D2 (die screw), showing thread pitch, angle, and depth. The marked areas (indicated by small black squares) highlight regions of significant surface irregularities, indicative of the higher surface roughness of this screw sample.

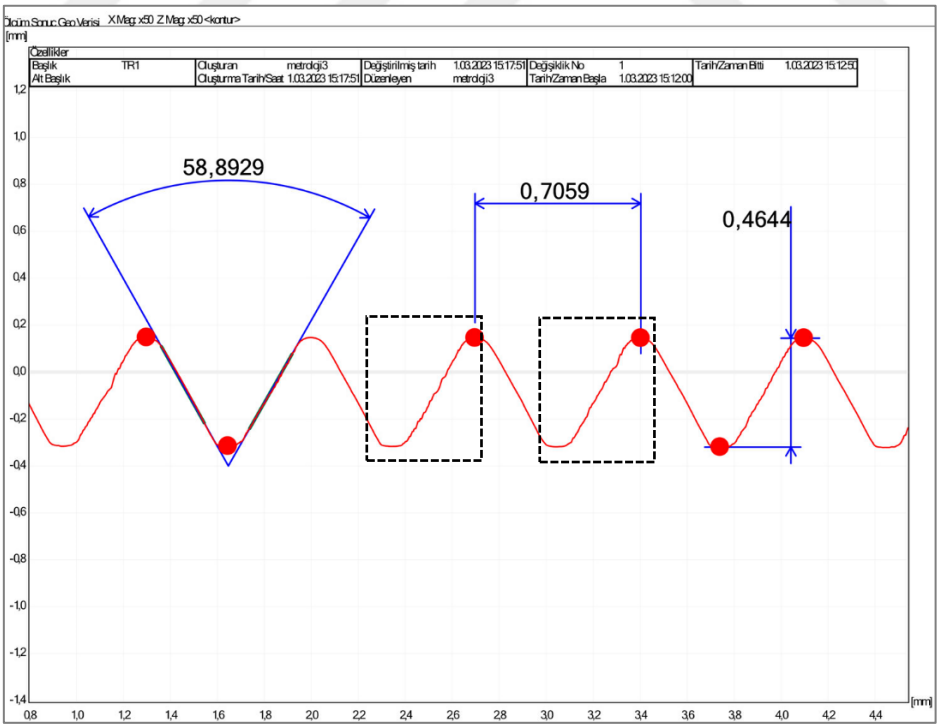


Figure 4.7. Profilogram of sample TR1 (thread rolled screw), showing thread pitch, angle, and depth.

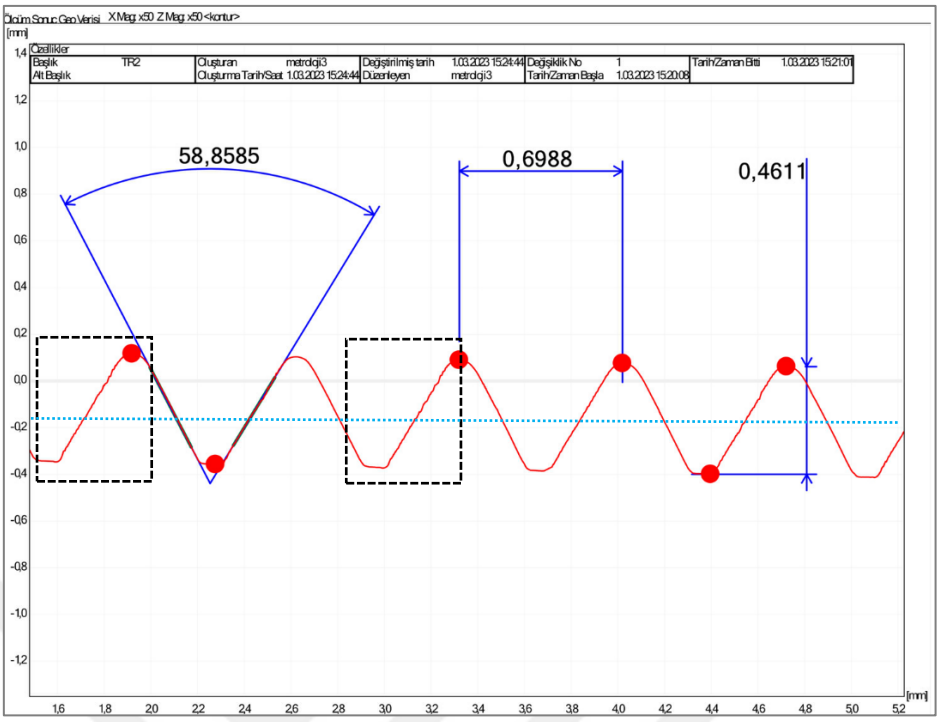


Figure 4.8. Profilogram of sample TR2 (thread rolled screw), showing thread pitch, angle, and depth. The marked areas (indicated by small black squares) show regions with moderate surface irregularities, representing the medium surface roughness of this sample compared to the other samples. The dashed line represents the mean line, which is used as a reference for surface roughness measurements.

In this research, the surface roughness for the aforementioned screw samples was quantified using three parameters: Ra (average roughness), Rq (root mean square roughness), and Rz (maximum height of the profile). The gathered data is listed in Table 4.5. Ra represents the average of the absolute values of the profile height deviations from the mean line, which is shown as a dashed line in Figure 4.8, within the evaluation length. The dashed line is a conceptual representation for understanding; the actual surface roughness measurements were obtained using the contour measuring device.

Lower Ra values suggest a smoother surface, while higher Ra values indicate a rougher surface. Rq, while similar to Ra, incorporates the squaring of deviations prior to averaging and then involves the extraction of the square root of the average. Consequently, Rq is more sensitive to extreme values, whether peaks or valleys, compared to Ra as observable in Table 4.5. Rz, on the other hand, is the average of the absolute values of the five highest peaks and the five lowest valleys over the evaluation length.

Table 4.5. Surface roughness parameters for different abutment screw samples.

Sample No	Ra (mm)	Rq (mm)	Rz (mm)
M1	1.9455	1.9519	0.4941
M2	1.4627	1.4712	0.5021
D1	0.2151	0.2587	0.4449
D2	0.2002	0.2405	0.4361
TR1	0.1516	0.1799	0.4677
TR2	0.1854	0.2266	0.5296

Looking at data in Table 4.5, it can be observed that samples M1 and M2 have significantly higher Ra and Rq values, indicating a rougher surface compared to D1, D2, TR1, and TR2 samples.

4.1.2.2. Torque and Vibration Tests Results

1. Machined Screws

The group of machined screws was divided into two subsets, each consisting of five screws. The first subset was paired with machined implants (Implant Type M), and the other was paired with thread rolled implant (Implant Type TR). Tables 4.6 and 4.7 show the applied torque values, detorque values, and changes in torque loss for each sample both before and after the vibration test. Table 4.6 relates to the machined screws paired with machined implants, and Table 4.7 to those paired with thread-rolled implants.

Table 4.6. Torque, detorque, and torque loss measurements before and after vibration test for machined screws paired with machined implants.

Sample No	Implant Type	Before Vibration Test			After Vibration Test 75 Hz / 24h			Total Torque Loss (%)
		Torque (Ncm)	Detorque (Ncm)	Torque Loss (%)	Retorque (Ncm)	Detorque (Ncm)	Torque Loss (%)	
1	M	99.8	81.4	18.44	100.1	75.6	24.48	6.04
2	M	100.3	77.1	23.13	99.8	75	24.85	1.72
3	M	100.6	78.3	22.17	100.4	73.1	27.19	5.02
4	M	100.2	86.9	13.27	100	67.9	32.10	18.83
5	M	101.3	81.4	19.64	101	79.9	20.89	1.25
Average	-	-	-	-	-	-	-	3.51%

Table 4.7. Torque, detorque, and torque loss measurements before and after vibration test for machined screws paired with thread-rolled implants.

Sample No	Implant Type	Before Vibration Test			After Vibration Test 75 Hz / 24 H			Total Torque Loss (%)
		Torque (Ncm)	Detorque (Ncm)	Torque Loss (%)	Retorque (Ncm)	Detorque (Ncm)	Torque Loss (%)	
1	TR	100.5	83.6	16.82	100	79.8	20.20	3.38
2	TR	100.8	87.2	13.49	99.7	83.4	16.35	2.86
3	TR	100.2	83.1	17.07	101.7	83.3	18.09	1.03
4	TR	101.7	88.2	13.27	102.6	81.4	20.66	7.39
5	TR	100.1	79.5	20.58	100.4	80.4	19.92	-0.66
Average	-	-	-	-	-	-	-	2.42%

When calculating the average of the total torque loss values, any extremely high or negative total torque loss (%) values were excluded to ensure a fair comparison and to eliminate any potential deviation in the data. These values outside the expected range are marked in blue in the table for clarity. This includes notably high values such as 18.83% in Table 4.6, 7.39%, and a negative value -0.66% in Table 4.7.

2. Thread Rolled Screws

Table 4.8 presents the torque, detorque, and torque loss measurements before and after the vibration test for thread-rolled screws paired with machined implants. These thread-rolled screws exhibited an average total torque loss of 5.12%. A negative value (-1.05%) was disregarded in the computation of this average, as it represented an unexpected variation in the total torque loss.

Similarly, Table 4.9 showcases the corresponding measurements for thread-rolled screws coupled with thread-rolled implants. The data indicated an average total torque loss of 4.32%. This computation excluded a negative value (-0.81%) and a significantly high value (19.20%), both contradicting the expected trend in torque loss after the vibration test. These tables underscore that thread-rolled screws, irrespective of the implant types they were paired with, experienced torque losses after being subjected to the vibrational stress of the test. Values outside the expected range were marked in blue in the table for clarity.

Table 4.8. Torque, detorque, and torque loss measurements before and after vibration test for thread rolled screws paired with machined implants.

Sample No	Implant Type	Before Vibration Test			After Vibration Test 75 Hz / 24 H			Total Torque Loss (%)
		Torque (Ncm)	Detorque (Ncm)	Torque Loss (%)	Retorque (Ncm)	Detorque (Ncm)	Torque Loss (%)	
1	M	99.9	72.3	27.63	100.1	70.1	29.97	2.34
2	M	100	83.4	16.60	100	76.2	23.80	7.20
3	M	101.2	81.1	19.86	100.2	74.1	26.05	6.19
4	M	99.2	77.2	22.18	98	77.3	21.12	-1.05
5	M	99.9	79.9	20.02	101	76	24.75	4.73
Average	-	-	-	-	-	-	-	5.12%

Table 4.9. Torque, detorque, and torque loss measurements before and after vibration test for thread rolled screws paired with thread-rolled implants.

Sample No	Implant Type	Before Vibration Test			After Vibration Test 75 Hz / 24 H			Total Torque Loss (%)
		Torque (Ncm)	Detorque (Ncm)	Torque Loss (%)	Retorque (Ncm)	Detorque (Ncm)	Torque Loss (%)	
1	TR	100	85.7	14.30	100.9	67.1	33.50	19.20
2	TR	101.2	77.6	23.32	100.4	77.8	22.51	-0.81
3	TR	100	84.6	15.40	100.7	81.7	18.87	3.47
4	TR	100.3	81.6	18.64	102.9	77.6	24.59	5.94
5	TR	100.7	77.3	23.24	100.8	73.8	26.79	3.55
Average	-	-	-	-	-	-	-	4.32%

3. Die Screws

Table 4.10 delineates the torque, detorque, and torque loss measurements for die screws paired with machined implants before and after the vibration test. The die screws indicated an average total torque loss of 7.53%, following the exclusion of a negative value (-2.61%), which contradicted the expected increase in the total torque loss. This value was marked in blue in the table for clarity.

Similarly, Table 4.11 outlines the measurements for die screws coupled with thread-rolled implants. The average total torque loss in this case was calculated to be 6.27%, with a significantly high value (21.36%) and a negative value (-3.58%) being excluded from the computation. These values, which deviated from the anticipated trend of the total torque loss, were highlighted in blue in the table. These results collectively highlight that die screws, regardless of the type of implants they were paired with, demonstrated torque losses post-vibration testing.

Table 4.10. Torque, detorque, and torque loss measurements before and after vibration test for die screws paired with machined implants.

Sample No	Implant Type	Before Vibration Test			After Vibration Test 75 Hz / 24 H			Total Torque Loss (%)
		Torque (Ncm)	Detorque (Ncm)	Torque Loss (%)	Retorque (Ncm)	Detorque (Ncm)	Torque Loss (%)	
1	M	101.2	72.2	28.66	100.2	74.1	26.05	-2.61
2	M	100.3	73.3	26.92	100.6	70.4	30.02	3.10
3	M	102.4	70.2	31.45	100.5	60.2	40.10	8.65
4	M	100.2	80.8	19.36	100	68.6	31.40	12.04
5	M	102.3	77.7	24.05	98.4	68.5	30.39	6.34
Average	-	-	-	-	-	-	-	7.53%

Table 4.11. Torque, detorque, and torque loss measurements before and after vibration test for die screws paired with thread-rolled implants.

Sample No	Implant Type	Before Vibration Test			After Vibration Test 75 Hz / 24 H			Total Torque Loss (%)
		Torque (Ncm)	Detorque (Ncm)	Torque Loss (%)	Retorque (Ncm)	Detorque (Ncm)	Torque Loss (%)	
1	TR	99.5	70.5	29.15	97.8	72.8	25.56	-3.58
2	TR	100.8	83.1	17.56	101.1	77.5	23.34	5.78
3	TR	101	81.1	19.70	101.6	78.3	22.93	3.23
4	TR	100.6	83.1	17.40	101.4	62.1	38.76	21.36
5	TR	103.3	90.5	12.39	101	78.6	22.18	9.79
Average	-	-	-	-	-	-	-	6.27%

4.1.2.3. SEM Analysis Results

Figures 4.9–4.14 display the surfaces of six screw samples: two machined screws (M1 and M2), two thread rolled screws (TR1 and TR2), and two die screws (D1 and D2), respectively. Detailed SEM images revealed distinct differences in surface roughness among these types. For example, machined screws exhibited lower surface roughness compared to thread-rolled and die screws. In contrast, die screws demonstrated higher surface roughness, a finding consistent with the profilograms obtained (Figures 4.3–4.8).

4.1.2.4. Statistical Analysis Results

The one-way ANOVA and independent samples t-test revealed a significant influence of the abutment screw type on the total torque loss ($P<.05$). Moreover, the implant type had a significant effect on the torque loss values before and after the vibration test ($P<.05$); however, it had not significantly affected the total torque loss ($P>.05$) (Table 4.12).

Table 4.12. Torque loss comparisons using one-way ANOVA and independent samples T-test *P* values (significance level at *P*<.05).

	Torque loss before the vibration test	Torque loss after the vibration test	Total torque loss
Abutment Screw Type	.524	.045	.025
Implant Type	.007	.004	.418

1. Machined screws

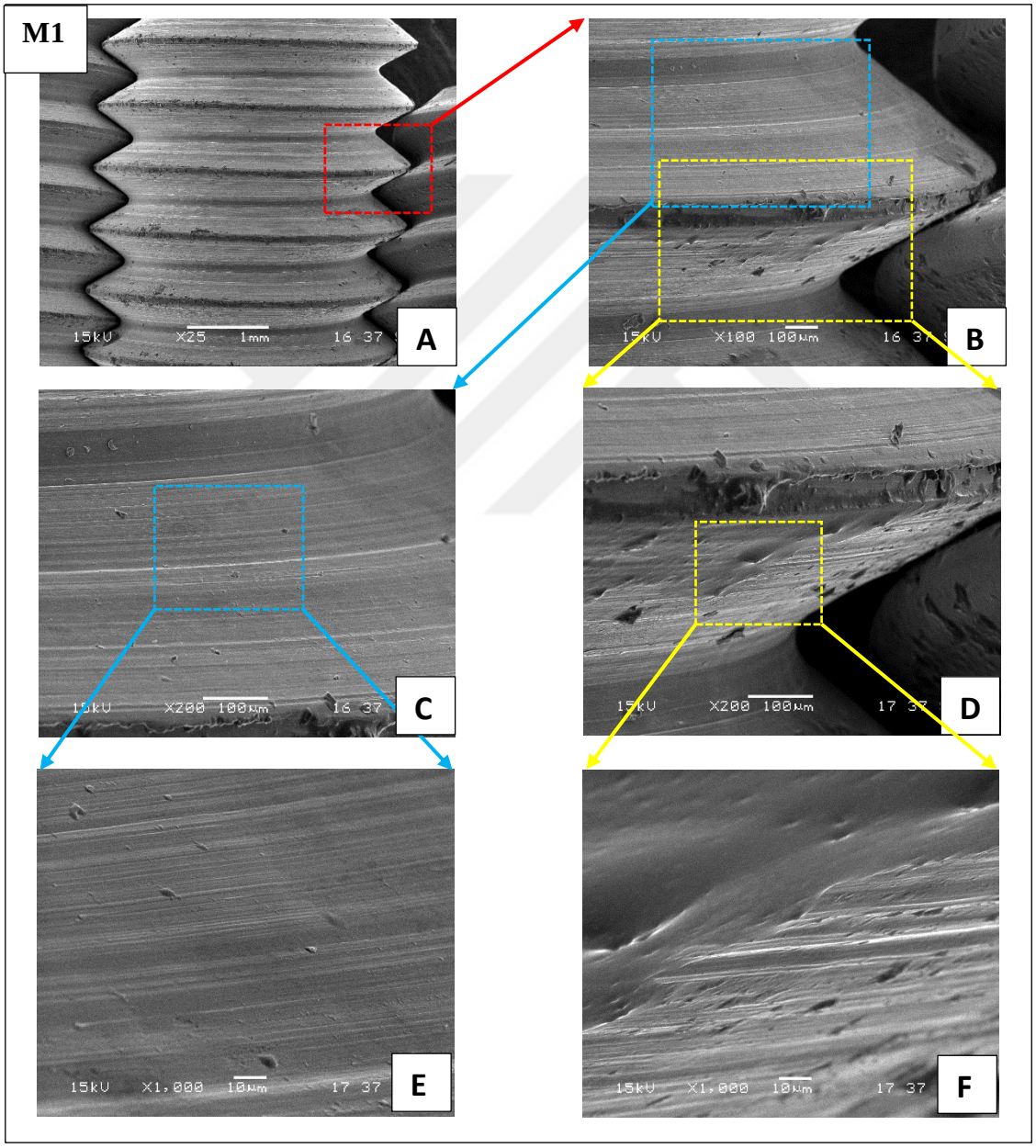


Figure 4.9. SEM images of machined screw sample M1 at different amplifications (X25, X200, and X1000).

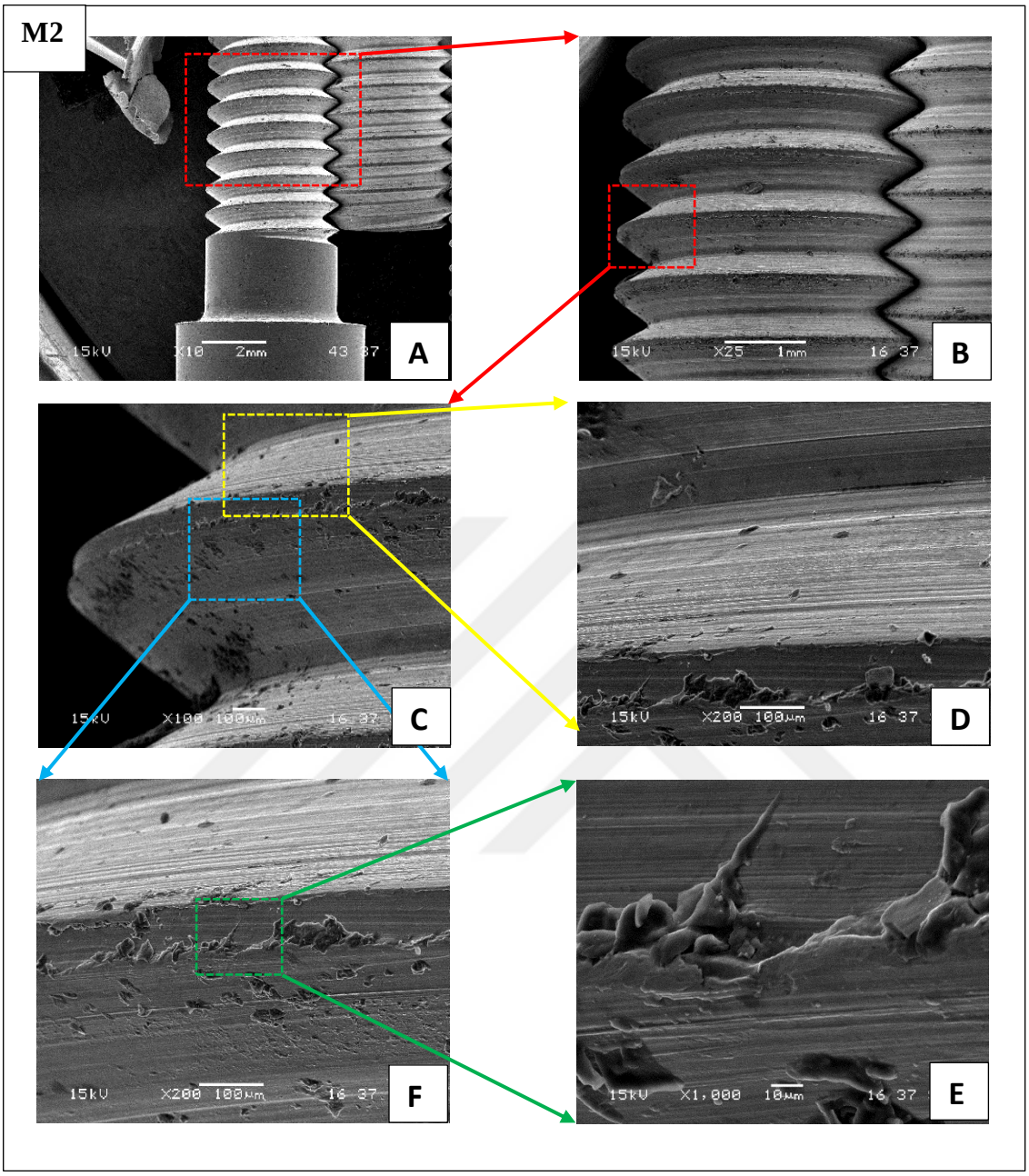


Figure 4.10. SEM images of machined screw sample M2 at different amplifications (X10, X25, X100, X200, and X1000).

2. Thread rolling screws

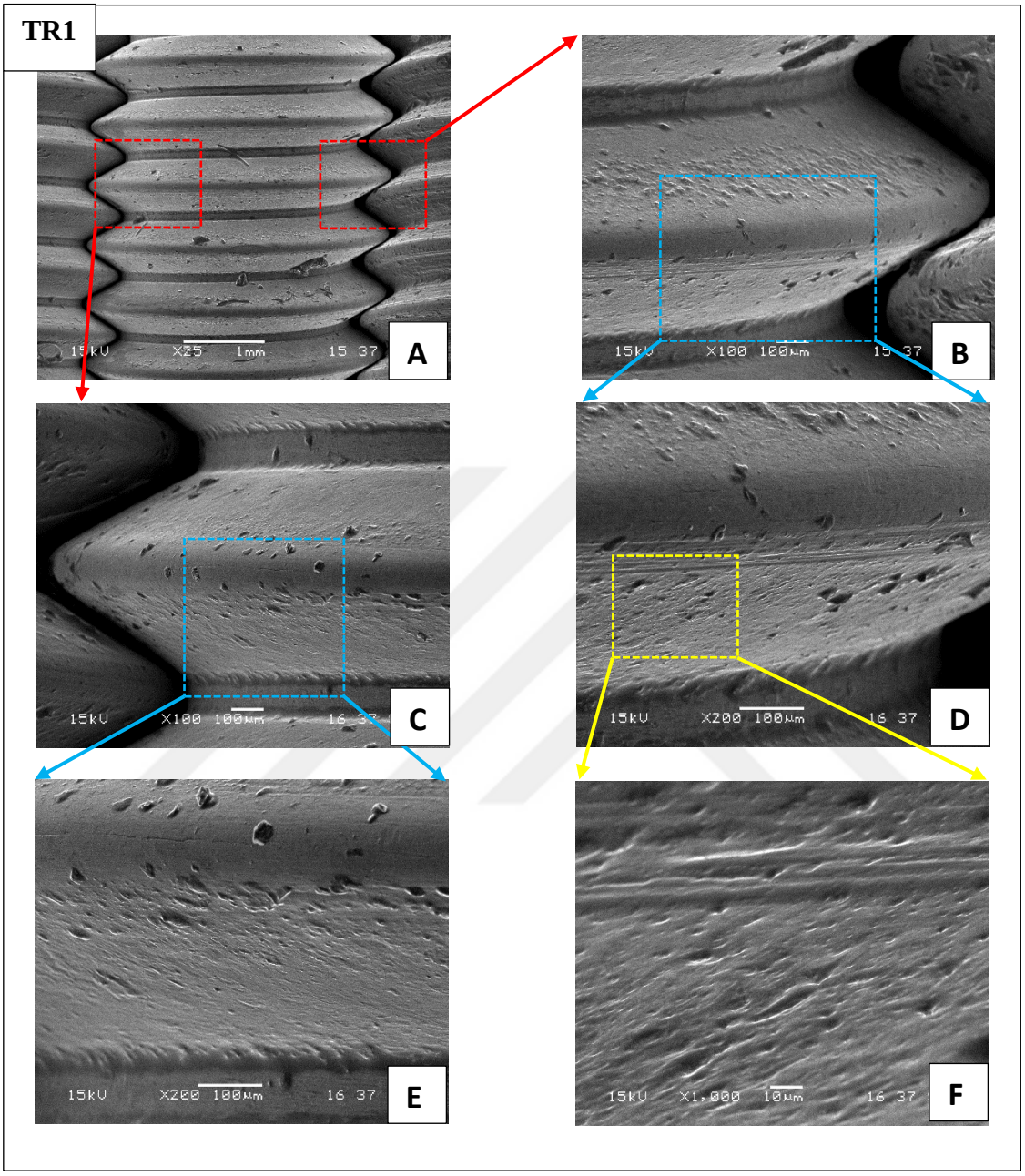


Figure 4.11. SEM images of two different regions of thread rolled screw sample TR1 at different amplifications (X25, X100, X200, and X1000).

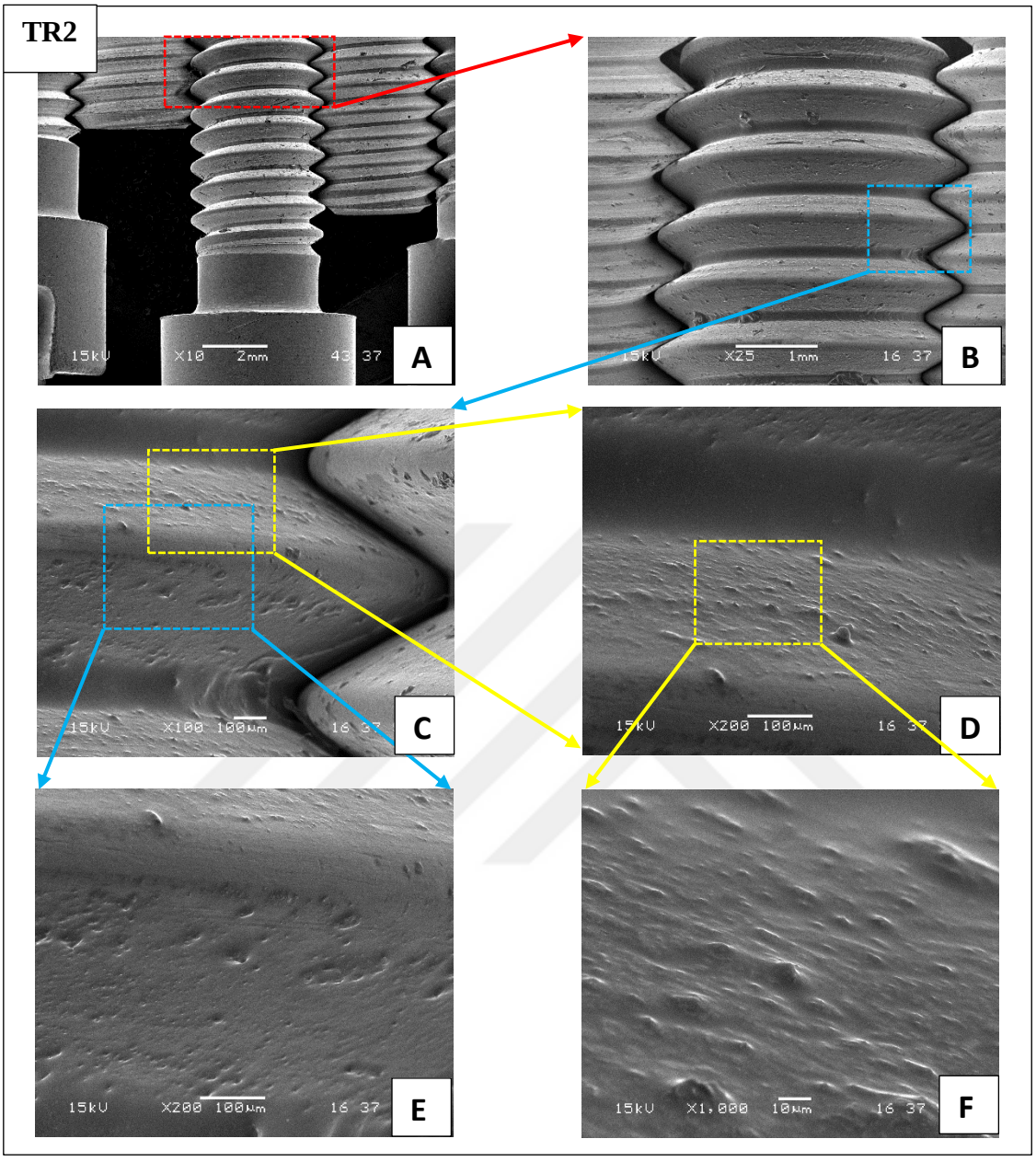


Figure 4.12. SEM images of thread rolled screw sample TR2 at different amplifications (X10, X25, X100, X200, and X1000).

3. Die screws

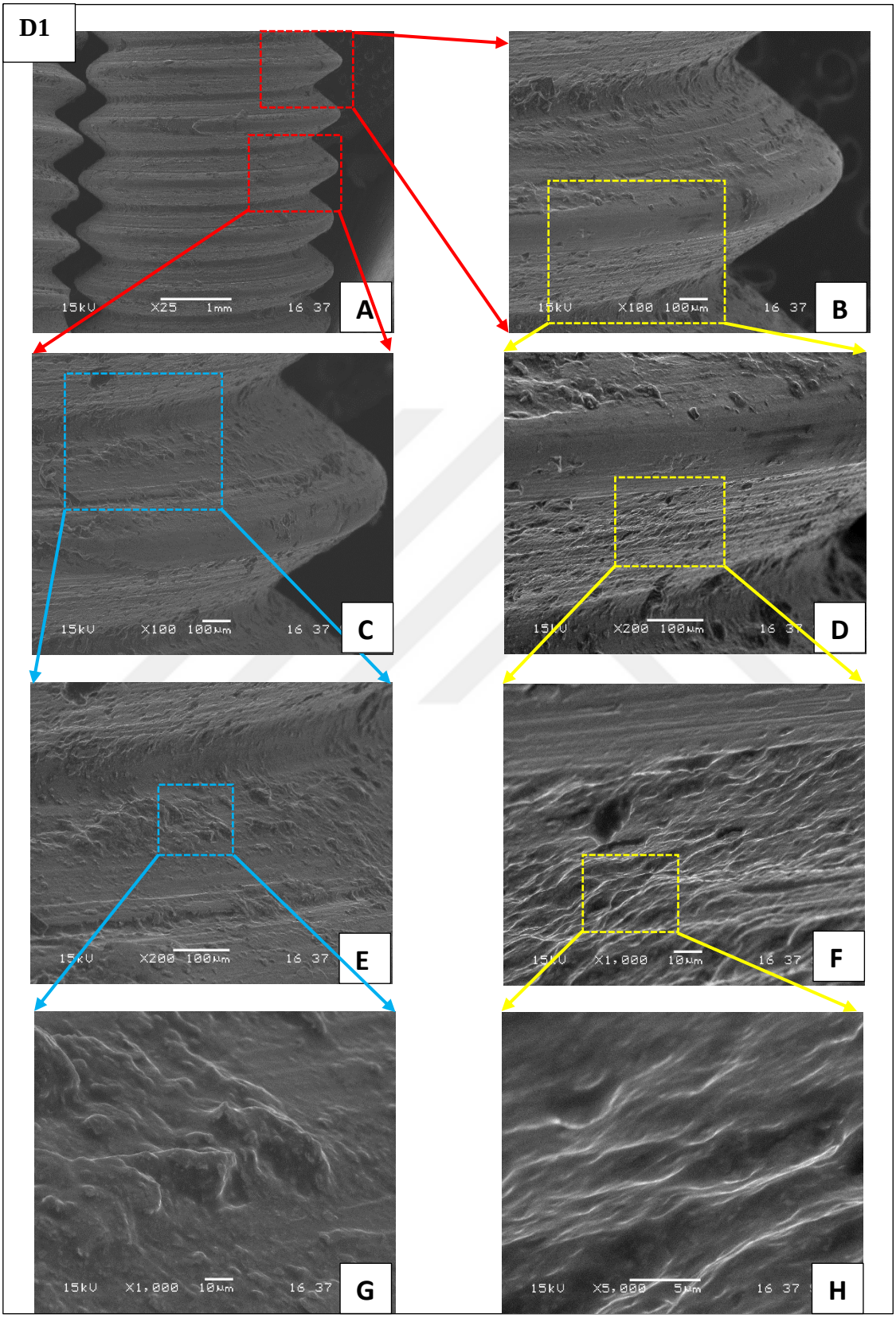


Figure 4.13. SEM images of two different regions of die screw sample D1 at different amplifications (X25, X100, X200, X1000, and X5000).

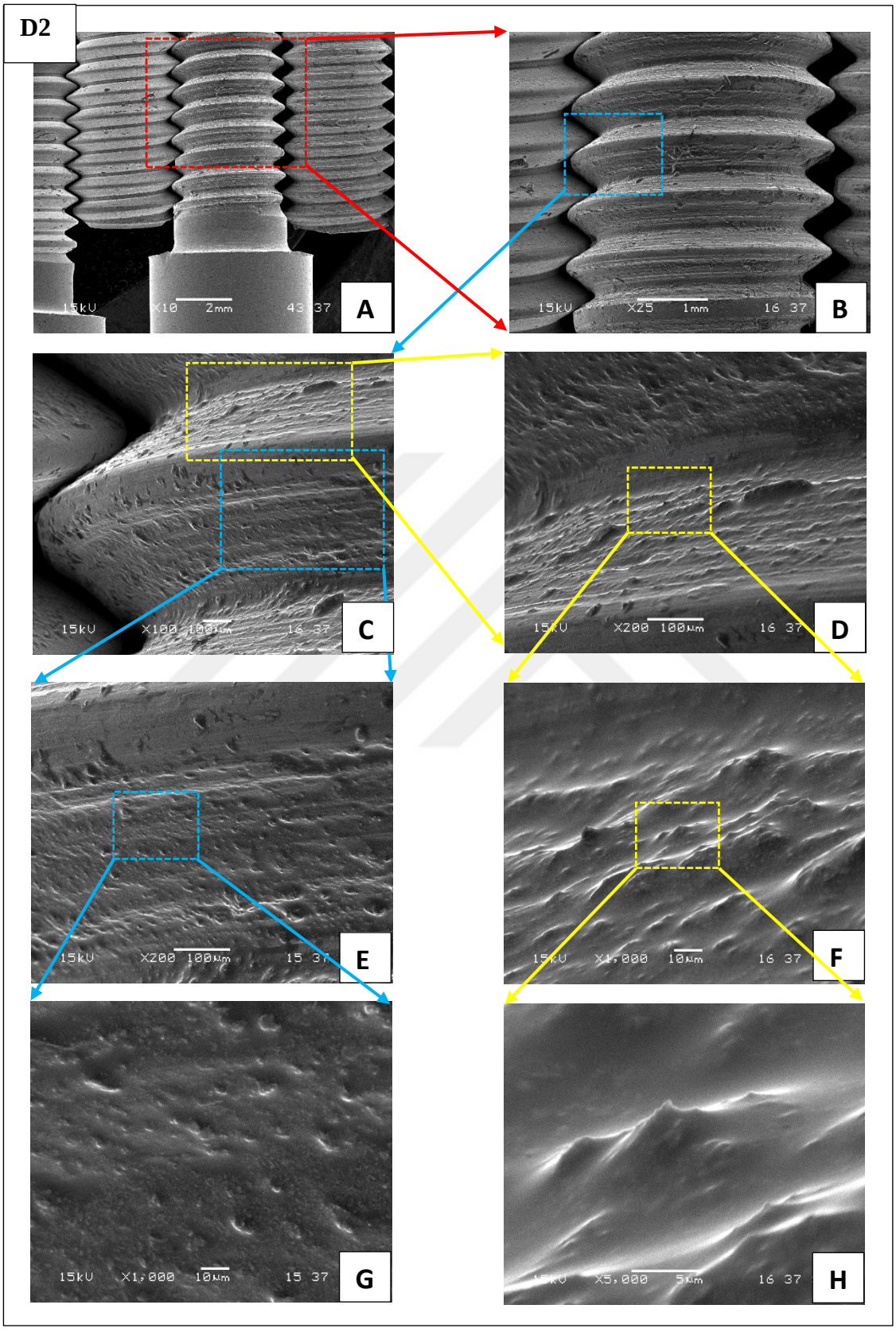


Figure 4.14. SEM images of die screw sample D2 at different amplifications (X10, X25, X100, X200, X1000, and X5000).

4.2. Discussions

4.2.1. Computational Study Discussion

The Kruskal-Wallis analysis test partially supported rejection of the null hypothesis. The abutment implant angle (θ) significantly affected implant stress, total deformation, and natural frequency (P<.001), while no significant impact was detected on abutment screw stress (P=.799) or abutment stress (P=.852). Additionally, the abutment screw head diameter (D) significantly influenced abutment screw stress (P=.010) and abutment stress (P=.002) but had no significant effect on implant stress (P=.952), total deformation (P=.336), or natural frequency (P=.276). Lastly, the findings indicated that abutment screw length (L) had no significant effect on any of the measured variables (P>.05). Furthermore, the Dunn test results in Table 4.3, which provide pairwise comparisons, further supported the partial rejection of the null hypothesis for specific groups and variables.

The purpose of this study was to evaluate and compare the mechanical effects of the internal contact surfaces of a simple multi-part dental implant system on screw loosening by comparing the maximum von Mises equivalent stress of the dental implant components, the maximum total deformation and the natural frequencies for all models. The factors selected in this investigation were the abutment implant angle (θ), the abutment screw head diameter (D), and the abutment screw length (L).

Neither experimental methods nor clinical observations can contribute to identifying the detailed mechanical responses and interactions associated with the structure design parameter variations (Jeng et al., 2020), such as the abutment implant angle, abutment screw head diameter, and abutment screw length examined in this study. To comprehend the biomechanical effect of abutment implant angle with a multi-part internal connection implant, abutment screw head diameter, and abutment screw length on the screw joint stability, a FEA with sensible boundary conditions and internal contact surfaces that simulate real conditions within the implant system was used.

Optimum preload force should generate stresses in the range of 60% and 75% of the yield strength of the abutment screw material (Guda et al., 2008). These stresses can be controlled by either increasing the coefficient of friction or decreasing the tightening

torque to keep the stresses within the optimal range, which in this study should be between 516 MPa and 645 MPa. As shown in the results section, the maximum von Mises stress in all implant components was mostly below the yield strength of the implant material, except for implant stress in some models which exceeded the yield strength of the implant material when the abutment implant angle was 45 degrees, causing plastic deformation. The abutment screw stress in all models exceeded the range of stress caused by optimum preload; however, the stresses were still below the yield strength. However, whether the preload was optimum or not, was not important in this study because the aim was to evaluate and compare between models numerically based on the existing results. In addition, the stress distributed within the implant components must be as convenient as possible because excess stress may result in poor stability between implant components, leading to loosening the screw.

In relation to the findings of this research, the natural frequency of the model decreased significantly as the abutment implant angle increased (Figure 4.2A), indicating a decrease in the stability of implant components based on the assumption that higher natural frequencies would correlate with greater stability. This assumption stems from the understanding that when a model is at resonance, it exhibits maximum displacement, implying that models with higher natural frequencies are more stable. The decrease in stability could be attributed to the reduced contact surface area between the abutment and the implant as the abutment implant angle decreased. Additionally, it was assumed that as the stability of a model decreases, the likelihood of screw loosening increases, leading to the interchangeability of model stability and screw loosening.

Modal analysis results include six types of vibrational modes in the FE model under free vibrations. These modes represent the normal modes of vibration for the model: asymmetric, symmetric, wagging, twisting, scissoring, and rocking. The main effect of the natural frequencies of the other five modes was inversely proportional to the increase in the abutment implant angle and directly proportional to the increase in the abutment screw head diameter, as in mode 1. Therefore, the natural frequencies in all models were presented and compared by using the first mode only to avoid excessive results and plots.

The abutment screw length had no clear effect on the loosening of the abutment screw, consistent with other studies (Yeo et al., 2014; Lee & Cha, 2018), but not with a study

(Kanneganti et al., 2018) that recommended a long screw with more threads to increase screw retention. The only difference between the models used was the design, while the material properties, load and boundary conditions, and contact definitions were the same. Table 4.1 shows that the difference in obtained stress values between the different screw lengths was small and not statistically significant, indicating that screw length has minimal effect on von Mises stress. Figure 4.15 demonstrates that the intersection point between screw thread and thread slot varied when the abutment implant angle was changed. This intersection point is crucial because the maximum stress of the abutment screw is located in this region, as shown in Figure 4.2C. Overall, the absence of this relationship can be attributed to the location of the intersection point between the screw thread and the thread slot.

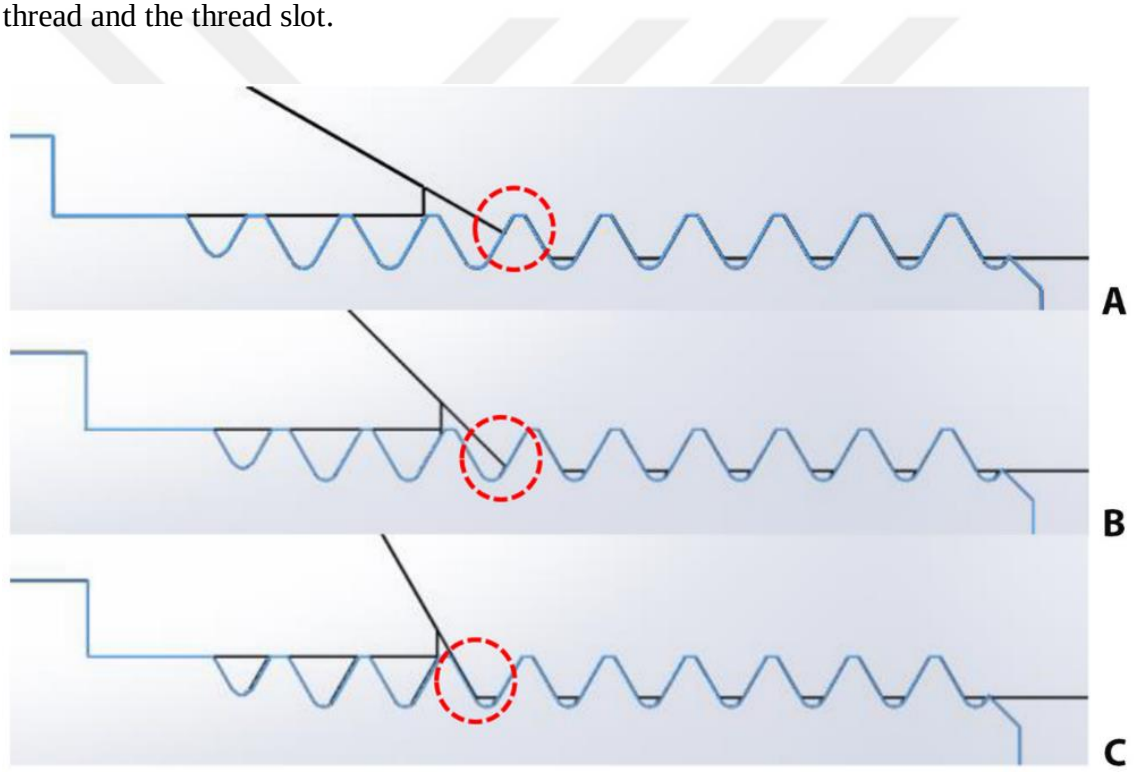


Figure 4.15. Variation in intersection point between screw thread and screw slot at different abutment implant angles. A, 30 degrees. B, 45 degrees. C, 60 degrees.

Although the statistical analyses did not reveal a significant effect of the abutment screw head diameter on implant stress or the natural frequency of the models, the main effect suggests a potential relationship. When the diameter changed from 2.65 to 2.75 mm, there was an observed increase in stress and the natural frequency. Moreover, this trend continued to increase when the diameter increased further to 2.85 mm (Fig. 4.2B). These findings, while not statistically significant in our study, suggest that the abutment screw

head diameter might influence these parameters. This provides a potential direction for future research, which could further investigate this trend using larger sample sizes or different methodologies.

Limitations of this study included simplifications such as modeling the implant without external threads and not considering the simulation of cortical and cancellous bones around the implant in the FE model. However, these simplifications should not impact the comparative results of the investigated parameters. It was assumed that the implant's external threads had no effect on screw loosening, and, while bone may absorb stresses transferred from the implant, affecting the stress values of dental implant components, this aspect was not within the scope of this study. Despite these simplifications, the abutment screw was modeled to accurately represent its real-life counterpart. Therefore, the virtual representation of the abutment screw used in the study considered the physical properties (elastic modulus, yield strength, and Poisson ratio) and geometries (shape, size, and dimensions) of the screw's threads, allowing for a more realistic simulation of the behavior and performance of the actual abutment screw. Further research might be required to fully understand the role of the abutment screw length in the mechanical stability of dental implants.

4.2.2. Experimental Study Discussion

The statistical analysis results partially reject the research hypothesis. The abutment screw type had a significant effect on the measured values of the torque loss after the vibration test (P=.045) and the total torque loss (P=.025). The torque loss before the vibration test, however, had not exhibited significant differences across various abutment screw types (P>.05). This highlights the sensitivity of certain abutment screw types to vibration-induced changes, emphasizing the importance of the vibration test in revealing these distinctions. Moreover, modifying the internal threading process of the implant had a significant effect on the torque loss values before and after the vibration test (P<.05).

The inconsistencies in the thread characteristics of die screws (as presented in Table 4.4) can be traced back to the manual manufacturing process of these screws. This process often lacks precision due to factors such as human error, wear and tear of the die tool, and variability in applied pressure. As for the differences between the 3 manufacturing

methods detailed in Table 4.4, while the thread angle should be consistent at 60 degrees across all screws, minor discrepancies were observed in all methods (machining, thread rolling, and die). The variation in angle measurements can be attributed to defects caused by surface roughness on the thread's side surfaces, which interfere with accurate angle assessment. This surface roughness complication can result in errors when drawing the line for angle measurement, as illustrated in Figures 4.3-4.8. Consequently, it would be a misrepresentation to suggest that the thread angle varies based on the production method. (Armentia et al., 2021) observed variations in the thread angle between machined and thread rolled prosthetic screws. These discrepancies mirror the ones we encountered in our analysis.

The surface roughness parameters presented in Table 4.5 suggest that the machined screws might have a rougher surface compared to the other samples, due to their higher surface parameters. The discrepancies observed between the surface roughness parameters (Ra, Rq, and Rz) and the findings from the profilograms can be attributed to the numerous surface irregularities and micro-imperfections identified on the rounded crest of the machined screws, as shown in marked areas in Figure 4.16M2. These irregularities, which appear as sharp edges and varying-sized protrusions termed as burrs, are likely responsible for the high surface roughness parameters. Such imperfections could also impact the functional behavior of the screws.

In fact, these parameters are typically derived from measurements along a single line (path) across the surface. While this approach is practical due to measurement equipment constraints, it may not fully capture the 3-dimensional complexities of the surface texture. This can lead to potential overlooking of features not intersected by the line or an inability to measure features oriented parallel to the line. This limitation could lead to potential inaccuracies, depending on how representative the selected line is of the entire surface. Thus, while these parameters offer valuable insights into aspects of surface roughness, they should be interpreted with care. For a more thorough understanding of the surface texture, scanning electron microscopy (SEM) imaging was utilized. The SEM analysis afforded a more accurate understanding of the surface roughness at a micro level that cannot be obtained with the contour measuring device. Insights into surface irregularities, imperfections, and the overall micro-texture, which might impact the performance of the screw, particularly in relation to potential loosening, were revealed through this process

(Figure 4.17). Similarly, the findings of (Armentia et al., 2021) revealed that surface roughness parameters for machined screws were consistently higher than those for thread rolled screws, although the SEM images in their study portrayed a contrasting scenario. The machined screws appeared to exhibit a lower surface roughness under SEM examination, a result that aligns seamlessly with the observations of this study.

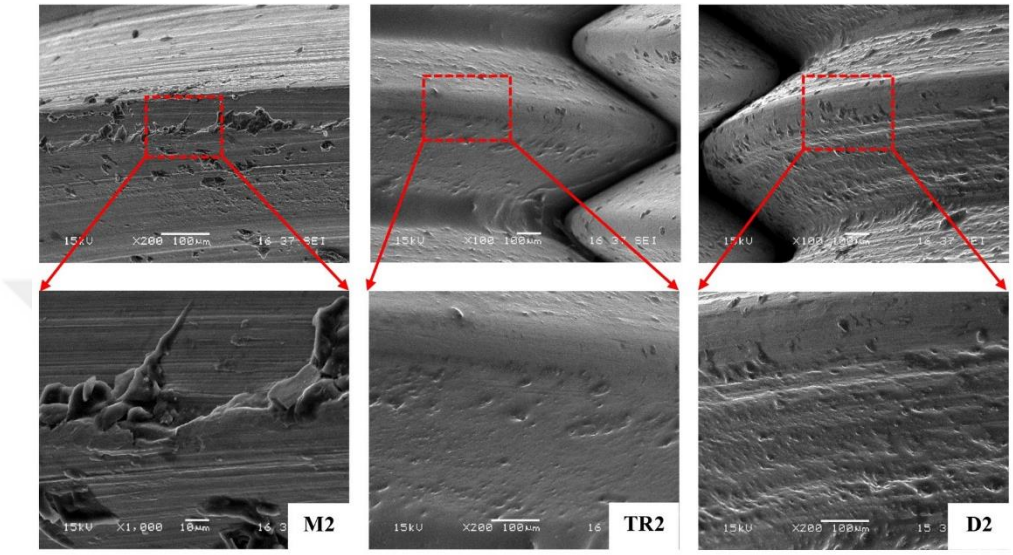


Figure 4.16. Surface irregularities and micro-imperfections on the rounded crest of screw M1, Machined screw. TR1, Thread-rolled screw. D1, Die screw.

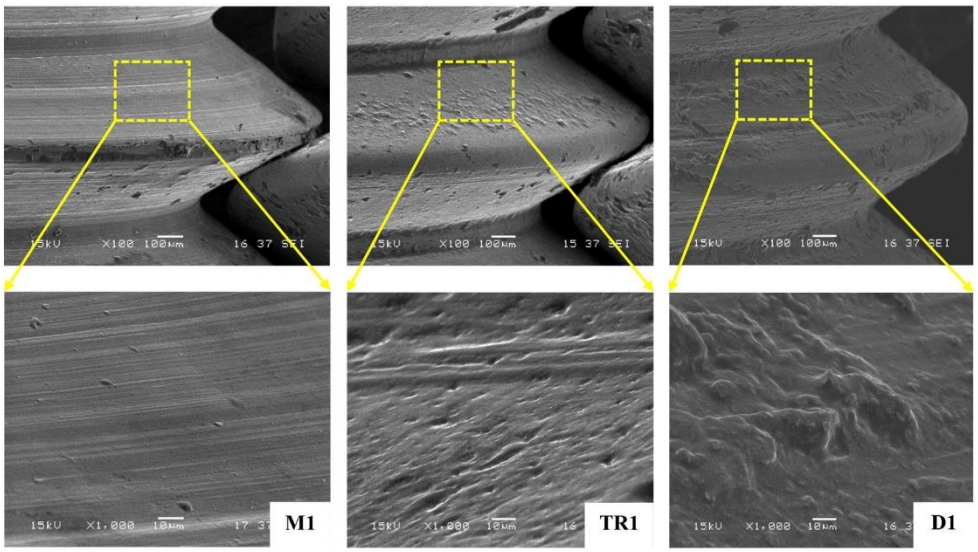


Figure 4.17. SEM images revealing different surface irregularities on screw surface. M1, Machined screw. TR1, Thread-rolled screw. D1, Die screw.

From Tables 4.6 and 4.7, it can be observed that the machined screws, regardless of whether they were paired with machined or thread-rolled implants, exhibited torque

losses both before and after the vibration test. However, the average total torque loss was somewhat higher for machined screws paired with machined implants (3.51%) compared to those paired with thread-rolled implants (2.42%). The total torque loss is a significant measure of screw loosening; therefore, based on these observations, it can be inferred that the pairing of machined screws with machined implants may result in a higher propensity for screw loosening compared to the pairing of machined screws with thread-rolled implants.

Similarly, based on the results presented in Tables 4.10 and 4.11, die screws paired with machined implants exhibited a higher average total torque loss of 7.53% compared to those paired with thread-rolled implants which had an average total torque loss of 6.27%. This suggests a higher propensity for screw loosening in the die screws when paired with machined implants. These findings corroborate earlier observations that machined screws paired with machined implants were also prone to a higher degree of screw loosening compared to when paired with thread-rolled implants.

When calculating these average values, any extremely high or negative total torque loss (%) values were excluded. The decision to exclude certain outlier values from the average total torque loss calculations was made based on their significant deviation from the expected trend, ensuring a fair comparison and to eliminate any potential deviation in the data. These values might result from experimental errors or unique circumstances that require further investigation.

5. CONCLUSIONS AND RECOMMENDATIONS

5.1. Conclusions

Based on the findings derived from this combined 3D Finite Element Analysis (FEA) and experimental study, the following conclusions were drawn:

1. The abutment implant angle and the abutment screw head diameter significantly affected the stresses of dental implant components, total deformation, and natural frequency of dental implants. This, in turn, may influence the mechanical stability of the screw joint and the likelihood of screw loosening in dental implants.
2. The abutment screw length had no significant effect on the dependent variables studied.
3. Upon analyzing the results from surface roughness measurements, torque and vibration tests, and SEM imaging, it was evident that each manufacturing method used in this study produces a unique surface roughness. This variation in surface roughness correspondingly influences the degree of screw loosening. Therefore, a significant correlation can be concluded between screw loosening and screw surface roughness.
4. The machined screws demonstrated less loosening compared to both thread-rolled screws and die screws. This might be attributed to the lower surface roughness of machined screws compared to the other types.
5. The type of screw (machined, thread-rolled, and die) significantly affected the total torque loss ($P<.05$). In addition, the type of implant (whether machined or thread-rolled) had a significant effect on the torque loss values before and after the vibration test ($P<.05$).

5.2. Recommendations

1. Further research might be required to fully understand the role of the abutment screw length in the mechanical stability of dental implants.
2. While this study mainly focused on the impact of surface roughness on screw loosening, it is recommended to conduct further research into other factors that might contribute to screw loosening, such as the impact of material properties, the design of

the implant or screw, and the influence of biological factors.

3. This study found that different manufacturing methods resulted in different levels of surface roughness, which subsequently influenced screw loosening. It is recommended to explore additional manufacturing processes and their effect on surface roughness and screw loosening.
4. The screws used in this study were of metric 4 size, which differs from the sizes typically used in dental implants. Nevertheless, the findings on the correlation between manufacturing process, surface roughness, and screw loosening are fundamentally valuable. To make these findings directly applicable to clinical practice, similar studies should be performed using screws of sizes typically used in dental implants. Therefore, it is recommended to replicate these experiments using a range of screw sizes that are commonly used in dental implants to validate and expand the applicability of the findings of this study.
5. The influence of various coating and surface treatment processes on surface roughness and screw loosening can be investigated. This might offer potential solutions to reduce screw loosening by modifying surface characteristics.

REFERENCES

Aboyoussef, H., Weiner, S., & Ehrenberg, D. (2000). Effect of an antirotation resistance form on screw loosening for single implant-supported crowns. *The Journal of prosthetic dentistry*, *83*(4), 450-455. https://doi.org/10.1016/S0022-3913(00)70040-0

Aktas, S. E. R. K. A. N., Kelebekler, E. R. S. O. Y., Ayaz, M. U. R. A. T., & Kisioglu, Y. A. S. İ. N. (2022). Development of a new universal test bench for endosseous dental implants. *Experimental Techniques*, *46*(4), 595-606. https://doi.org/10.1007/s40799-021-00499-5

Aktas, S., & Kisioglu, Y. (2020). Effects of thread rolling processing parameters on mechanical properties and microstructures of high-strength bolts. *Materials Testing*, *62*(10), 1017-1024. https://doi.org/10.3139/120.111579

Alonso-Pérez, R., Bartolomé, J. F., Ferreiroa, A., Salido, M. P., & Pradíes, G. (2018). Original vs. non-original abutments for screw-retained single implant crowns: An in vitro evaluation of internal fit, mechanical behaviour and screw loosening. *Clinical Oral Implants Research*, *29*(12), 1230-1238. https://doi.org/10.1111/clr.13390

Al-Sanea, A., Mutlu, I., Kişioğlu, Y., & Mohamed, E. (2023). The Effect of V-Thread and Square Thread Dental Implants on Bone Stresses. *Journal of Biomimetics, Biomaterials and Biomedical Engineering*, *60*, 83-96. https://doi.org/10.4028/p-3qasy2

Armentia, M., Abasolo, M., Coria, I., Albizuri, J., & Aguirrebeitia, J. (2021). Fatigue performance of prosthetic screws used in dental implant restorations: Rolled versus cut threads. *The Journal of Prosthetic Dentistry*, *126*(3), 406-e1. https://doi.org/10.1016/j.prosdent.2021.06.035

Arnetzl, G. V., Payer, M., Falkensammer, F., & Arnetzl, G. (2016). Effect of double conical abutment screw on implant preload. *Clinical Oral Implants Research*, *27*(5), 553-557. https://doi.org/10.1111/clr.12623

Arshad, M., Mahgoli, H., & Payaminia, L. (2018). Effect of Repeated Screw Joint Closing and Opening Cycles and Cyclic Loading on Abutment Screw Removal Torque and Screw Thread Morphology: Scanning Electron Microscopy Evaluation. *International Journal of Oral & Maxillofacial Implants*, *33*(1), 31-40.

Assenza, B., Scarano, A., Leghissa, G., Carusi, G., Thams, U., Roman, F. S., & Piattelli, A. (2005). Screw-vs Cement-implant–retained Restorations: An Experimental Study in the Beagle. Part 1. Screw and Abutment Loosening. *Journal of oral Implantology*, *31*(5), 242-246. https://doi.org/10.1563/1548-1336(2005)31[242:SVCRAE]2.0.CO;2

Barbosa, G. S., Silva-Neto, J. P. D., Simamoto-Júnior, P. C., Neves, F. D. D., Mattos, M. D. G. C. D., & Ribeiro, R. F. (2011). Evaluation of screw loosening on new abutment screws and after successive tightening. *Brazilian Dental Journal*, *22*, 51-55. https://doi.org/10.1590/S0103-64402011000100009

Bhushan, B. (2000). *Modern tribology handbook*, two volume set. CRC press.

Boemio, G., Rizzo, P., & De Nardo, L. (2011). Assessment of dental implant stability by means of the electromechanical impedance method. *Smart Materials and Structures*, *20*(4), 045008. https://doi.org/10.1088/0964-1726/20/4/045008

Brägger, U., Aeschlimann, S., Bürgin, W., Hämmerle, C. H., & Lang, N. P. (2001). Biological and technical complications and failures with fixed partial dentures (FPD) on implants and teeth after four to five years of function. *Clinical oral implants research*, *12*(1), 26-34. https://doi.org/10.1034/j.1600-0501.2001.012001026.x

Bulaqi, H. A., Barzegar, A., Paknejad, M., & Safari, H. (2019). Assessment of preload, remaining torque, and removal torque in abutment screws under different frictional conditions: A finite element analysis. *The Journal of Prosthetic Dentistry*, *121*(3), 548-e1. https://doi.org/10.1016/j.prosdent.2018.10.035

Bulaqi, H. A., Mashhadi, M. M., Safari, H., Samandari, M. M., & Geramipanah, F. (2015). Dynamic nature of abutment screw retightening: finite element study of the effect of retightening on the settling effect. *The Journal of prosthetic dentistry*, *113*(5), 412-419. https://doi.org/10.1016/j.prosdent.2014.09.017

Butkevica, A., Nathanson, D., Pober, R., & Strating, H. (2018). Measurements of repeated tightening and loosening torque of seven different implant/abutment connection designs and their modifications: An in vitro study. *Journal of Prosthodontics*, *27*(2), 153-161. https://doi.org/10.1111/jopr.12467

Cavazos Jr, E., & Bell, F. A. (1996). Preventing loosening of implant abutment screws. *The Journal of prosthetic dentistry*, *75*(5), 566-569. https://doi.org/10.1016/S0022-3913(96)90464-3

Chen, G., Chen, Y., Chen, Y., & Ji, S. (2020). Dynamics modeling and experimental modal analysis of bolt loosening for lightning rod. *Journal of Vibroengineering*, *22*(3), 657-671. https://doi.org/10.21595/jve.2019.20918

Chen, J., Wang, L., Yang, L., Zhang, X., Huang, B., & Li, J. (2021). The prosthetic screw loosening of two-implant supported screw-retained fixed dental prostheses in the posterior region: a retrospective evaluation and finite element analysis. *Journal of Biomechanics*, *122*, 110423. https://doi.org/10.1016/j.jbiomech.2021.110423

Chen, X., Ma, R., Min, J., Li, Z., Yu, P., & Yu, H. (2020). Effect of PEEK and PTFE coatings in fatigue performance of dental implant retaining screw joint: An in vitro

study. *Journal of the Mechanical Behavior of Biomedical Materials*, *103*, 103530. https://doi.org/10.1016/j.jmbbm.2019.103530

Cho, S. C., Small, P. N., Elian, N., & Tarnow, D. (2004). Screw loosening for standard and wide diameter implants in partially edentulous cases: 3-to 7-year longitudinal data. *Implant dentistry*, *13*(3), 245-250. https://doi.org/10.1097/01.id.0000140459.87333.f8

Coppedê, A. R., Faria, A. C. L., Mattos, M. D. G. C. D., Rodrigues, R. C. S., Shibli, J. A., & Ribeiro, R. F. (2013). Mechanical comparison of experimental conical-head abutment screws with conventional flat-head abutment screws for external-hex and internal tri-channel implant connections: an in vitro evaluation of loosening torque. *International Journal of Oral & Maxillofacial Implants*, *28*(6).

de Moura, M. B., Rodrigues, R. B., Pinto, L. M., de Araújo, C. A., Novais, V. R., & Júnior, P. C. S. (2017). Influence of screw surface treatment on retention of implant-supported fixed partial dentures. *Journal of Oral Implantology*, *43*(4), 254-260. https://doi.org/10.1563/aaid-joi-D-16-00145

Dixon, D. L., Breeding, L. C., Sadler, J. P., & McKay, M. L. (1995). Comparison of screw loosening, rotation, and deflection among three implant designs. *The Journal of prosthetic dentistry*, *74*(3), 270-278. https://doi.org/10.1016/S0022-3913(05)80134-9

Domblesky, J. P., & Feng, F. (2002). A parametric study of process parameters in external thread rolling. *Journal of Materials Processing Technology*, *121*(2-3), 341-349. https://doi.org/10.1016/S0924-0136(01)01223-7

Duncan, J. P., Nazarova, E., Vogiatzi, T., & Taylor, T. D. (2003). Prosthodontic complications in a prospective clinical trial of single-stage implants at 36 months. *International Journal of Oral & Maxillofacial Implants*, *18*(4), 561-565.

Elias, C. N., Figueira, D. C., & Rios, P. R. (2006). Influence of the coating material on the loosing of dental implant abutment screw joints. *Materials Science and Engineering: C*, *26*(8), 1361-1366. https://doi.org/10.1016/j.msec.2005.08.011

Eraslan, O., & İnan, Ö. (2010). The effect of thread design on stress distribution in a solid screw implant: a 3D finite element analysis. *Clinical oral investigations*, *14*, 411-416. https://doi.org/10.1007/s00784-009-0305-1

Faria, A. C. L., Bordin, A. R. D. V., Pedrazzi, V., Rodrigues, R. C. S., & Ribeiro, R. F. (2012). Effect of whitening toothpaste on titanium and titanium alloy surfaces. *Brazilian Oral Research*, *26*, 498-504. https://doi.org/10.1590/S1806-83242012005000014

Farina, A. P., Spazzin, A. O., Consani, R. L. X., & Mesquita, M. F. (2014). Screw joint stability after the application of retorque in implant-supported dentures under

simulated masticatory conditions. *The Journal of prosthetic dentistry*, *111*(6), 499-504. https://doi.org/10.1016/j.prosdent.2013.07.024

Farina, A. P., Spazzin, A. O., Maria Costa Nuñez Pantoja, J., Leonardo Xediek Consani, R., & Mesquita, M. F. (2012). An in vitro comparison of joint stability of implant-supported fixed prosthetic suprastructures retained with different prosthetic screws and levels of fit under masticatory simulation conditions. *International Journal of Oral & Maxillofacial Implants*, *27*(4), 833-838.

Goodacre, C. J., Bernal, G., Rungcharassaeng, K., & Kan, J. Y. (2003). Clinical complications with implants and implant prostheses. *The Journal of prosthetic dentistry*, *90*(2), 121-132. https://doi.org/10.1016/S0022-3913(03)00212-9

Guda, T., Ross, T. A., Lang, L. A., & Millwater, H. R. (2008). Probabilistic analysis of preload in the abutment screw of a dental implant complex. *The Journal of prosthetic dentistry*, *100*(3), 183-193. https://doi.org/10.1016/S0022-3913(08)60177-8

Guzaitis, K. L., Knoernschild, K. L., & Viana, M. A. (2011). Effect of repeated screw joint closing and opening cycles on implant prosthetic screw reverse torque and implant and screw thread morphology. *The Journal of prosthetic dentistry*, *106*(3), 159-169. https://doi.org/10.1016/S0022-3913(11)60115-7

Ha, C. Y., Lim, Y. J., Kim, M. J., & Choi, J. H. (2011). The influence of abutment angulation on screw loosening of implants in the anterior maxilla. *International Journal of Oral & Maxillofacial Implants*, *26*(1), 45-55.

Hench, L. L., & Wilson, J. (1993). *An introduction to bioceramics* (Vol. 1). Singapore: World Scientific.

Hotinski, E., & Dudley, J. (2019). Abutment screw loosening in angulation-correcting implants: an in vitro study. *The Journal of Prosthetic Dentistry*, *121*(1), 151-155. https://doi.org/10.1016/j.prosdent.2018.03.005

Jemt, T. (1990). A 3-year follow-up study of early single implant restorations and modum Branemark. *Int. J. Periodont. Rest. Dent.*, *10*, 341-349.

Jemt, T., Laney, W. R., Harris, D., Henry, P. J., Krogh Jr, P. H., Polizzi, G., ... & Herrmann, I. (1991). Osseointegrated implants for single tooth replacement: a 1-year report from a multicenter prospective study. *International Journal of Oral & Maxillofacial Implants*, *6*(1), 24-37.

Jeng, M. D., Lin, Y. S., & Lin, C. L. (2020). Biomechanical evaluation of the effects of implant neck wall thickness and abutment screw size: A 3D nonlinear finite element analysis. *Applied Sciences*, *10*(10), 3471. https://doi.org/10.3390/app10103471

Jeong, Y. H., Lee, C. H., Chung, C. H., Son, M. K., & Choe, H. C. (2014). Effects of TiN and WC coating on the fatigue characteristics of dental implant. *Surface and Coatings Technology*, *243*, 71-81. https://doi.org/10.1016/j.surfcoat.2012.02.046

Jörn, D., Kohorst, P., Besdo, S., Rücker, M., Stiesch, M., & Borchers, L. (2014). Influence of lubricant on screw preload and stresses in a finite element model for a dental implant. *The Journal of prosthetic dentistry*, *112*(2), 340-348. https://doi.org/10.1016/j.prosdent.2013.10.016

Jung, R. E., Pjetursson, B. E., Glauser, R., Zembic, A., Zwahlen, M., & Lang, N. P. (2008). A systematic review of the 5-year survival and complication rates of implant-supported single crowns. *Clinical oral implants research*, *19*(2), 119-130. https://doi.org/10.1111/j.1600-0501.2007.01453.x

Kanneganti, K. C., Vinnakota, D. N., Pottem, S. R., & Pulagam, M. (2018). Comparative effect of implant-abutment connections, abutment angulations, and screw lengths on preloaded abutment screw using three-dimensional finite element analysis: An in vitro study. *The Journal of the Indian Prosthodontic Society*, *18*(2), 161-167. https://doi.org/10.4103%2Fjips.jips_219_17

Khraisat, A., Hashimoto, A., Nomura, S., & Miyakawa, O. (2004). Effect of lateral cyclic loading on abutment screw loosening of an external hexagon implant system. *The Journal of prosthetic dentistry*, *91*(4), 326-334. https://doi.org/10.1016/j.prosdent.2004.01.001

Kim, K. S., & Lim, Y. J. (2020). Axial displacements and removal torque changes of five different implant-abutment connections under static vertical loading. *Materials*, *13*(3), 699. https://doi.org/10.3390/ma13030699

Kim, S. K., Koak, J. Y., Heo, S. J., Taylor, T. D., Ryoo, S., & Lee, S. Y. (2012). Screw loosening with interchangeable abutments in internally connected implants after cyclic loading. *International Journal of Oral & Maxillofacial Implants*, *27*(1), 42-47.

Kitagawa, T., Tanimoto, Y., Odaki, M., Nemoto, K., & Aida, M. (2005). Influence of implant/abutment joint designs on abutment screw loosening in a dental implant system. *Journal of Biomedical Materials Research Part B: Applied Biomaterials: An Official Journal of The Society for Biomaterials, The Japanese Society for Biomaterials, and The Australian Society for Biomaterials and the Korean Society for Biomaterials*, *75*(2), 457-463. https://doi.org/10.1002/jbm.b.30328

Kofron, M. D., Carstens, M., Fu, C., & Wen, H. B. (2019). In vitro assessment of connection strength and stability of internal implant-abutment connections. *Clinical Biomechanics*, *65*, 92-99. https://doi.org/10.1016/j.clinbiomech.2019.03.007

Koosha, S., Toraji, S., & Mostafavi, A. S. (2020). Effect of fluid contamination on the reverse torque values of abutment screws at implant-abutment connections. *The*

Journal of prosthetic dentistry, *123*(4), 618-621. https://doi.org/10.1016/j.prosdent.2019.05.001

Korioth, T. W., Cardoso, A. C., & Versluis, A. (1999). Effect of washers on reverse torque displacement of dental implant gold retaining screws. *The Journal of prosthetic dentistry*, *82*(3), 312-316. https://doi.org/10.1016/S0022-3913(99)70086-7

Kreissl, M. E., Gerds, T., Muche, R., Heydecke, G., & Strub, J. R. (2007). Technical complications of implant-supported fixed partial dentures in partially edentulous cases after an average observation period of 5 years. *Clinical oral implants research*, *18*(6), 720-726. https://doi.org/10.1111/j.1600-0501.2007.01414.x

Lang, L. A., Kang, B., Wang, R. F., & Lang, B. R. (2003). Finite element analysis to determine implant preload. *The Journal of prosthetic dentistry*, *90*(6), 539-546. https://doi.org/10.1016/j.prosdent.2003.09.012

Lee, J. H., & Cha, H. S. (2018). Screw loosening and changes in removal torque relative to abutment screw length in a dental implant with external abutment connection after oblique cyclic loading. *The Journal of Advanced Prosthodontics*, *10*(6), 415-421. https://doi.org/10.4047/jap.2018.10.6.415

Lee, J., Kim, Y. S., Kim, C. W., & Han, J. S. (2002). Wave analysis of implant screw loosening using an air cylindrical cyclic loading device. *The Journal of prosthetic dentistry*, *88*(4), 402-408. https://doi.org/10.1067/mpr.2002.128099

Lee, K. Y., Shin, K. S., Jung, J. H., Cho, H. W., Kwon, K. H., & Kim, Y. L. (2020). Clinical study on screw loosening in dental implant prostheses: a 6-year retrospective study. *Journal of the Korean Association of Oral and Maxillofacial Surgeons*, *46*(2), 133-142. https://doi.org/10.5125%2Fjkaoms.2020.46.2.133

Londhe, S. M., Gowda, E. M., Mandlik, V. B., & Shashidhar, M. P. (2020). Factors associated with abutment screw loosening in single implant supported crowns: A cross-sectional study. *medical journal armed forces india*, *76*(1), 37-40. https://doi.org/10.1016/j.mjafi.2018.06.011

Ma, S., & Fenton, A. (2015). Screw-versus cement-retained implant prostheses: a systematic review of prosthodontic maintenance and complications. *International Journal of Prosthodontics*, *28*(2), 127-145.

Noureddine, D., Serier, B., & Bachir Bouiadjra, B. A. (2017). Stress distribution of the variable dynamic loading in the dental implant: A three-dimensional finite element analysis. *Journal of Biomimetics, Biomaterials and Biomedical Engineering*, *31*, 44-52. https://doi.org/10.4028/www.scientific.net/JBBBE.31.44

Osman, R. B., & Swain, M. V. (2015). A critical review of dental implant materials with an emphasis on titanium versus zirconia. *Materials*, *8*(3), 932-958. https://doi.org/10.3390/ma8030932

Park, J. M., Baek, C. H., Heo, S. J., Kim, S. K., Koak, J. Y., Kim, S. K., & Belser, U. C. (2017). An In Vitro Evaluation of the Loosening of Different Interchangeable Abutments in Internal-Connection-Type Implants. *International Journal of Oral & Maxillofacial Implants*, *32*(2), 350-355.

Patterson, E. A., & Johns, R. (1992). Theoretical analysis of the fatigue life of fixture screws in osseointegrated dental implants. *The International journal of oral & maxillofacial implants*, *7*(1), 26-33.

Pjetursson, B. E., Tan, K., Lang, N. P., Brägger, U., Egger, M., & Zwahlen, M. (2004). A systematic review of the survival and complication rates of fixed partial dentures (FPDs) after an observation period of at least 5 years: I. Implant-supported FPDs. *Clinical oral implants research*, *15*(6), 625-642. https://doi.org/10.1111/j.1600-0501.2004.01117.x

Pournasrollah, A., Negahdari, R., Gharekhani, V., Torab, A., & Ataei, S. J. (2019). Investigating the effect of abutment–implant connection type on abutment screw loosening in a dental implant system using finite element methods. *Journal of Dental Research, Dental Clinics, Dental Prospects*, *13*(4), 289-297. https://doi.org/10.15171%2Fjoddd.2019.044

Quaranta, A., Lim, Z. W., Tang, J., Perrotti, V., & Leichter, J. (2017). The impact of residual subgingival cement on biological complications around dental implants: A systematic review. *Implant dentistry*, *26*(3), 465-474. https://doi.org/10.1097/ID.0000000000000593

Resnik, R. (2020). *Misch's contemporary implant dentistry* (4th ed.). Elsevier Health Sciences.

Sahin, C., & Ayyildiz, S. (2014). Correlation between microleakage and screw loosening at implant-abutment connection. *The journal of advanced prosthodontics*, *6*(1), 35-38. https://doi.org/10.4047/jap.2014.6.1.35

Sammour, S. R., El-Sheikh, M. M., & El-Gendy, A. A. (2019). Effect of implant abutment connection designs, and implant diameters on screw loosening before and after cyclic loading: in-vitro study. *Dental Materials*, *35*(11), e265-e271. https://doi.org/10.1016/j.dental.2019.07.026

Siadat, H., Najafi, H., Alikhasi, M., Falahi, B., Beyabanaki, E., & Zayeri, F. (2018). Effect of lateral oblique cyclic loading on microleakage and screw loosening of implants with different connections. *Journal of Dental Research, Dental Clinics, Dental Prospects*, *12*(3), 183-189. https://doi.org/10.15171%2Fjoddd.2018.028

Siadat, H., Pirmoazen, S., Beyabanaki, E., & Alikhasi, M. (2015). Does abutment collar length affect abutment screw loosening after cyclic loading?. *Journal of Oral Implantology*, *41*(S1), 346-351. https://doi.org/10.1563/AAID-JOI-D-D-14-00021

Siamos, G., Winkler, S., & Boberick, K. G. (2002). The relationship between implant preload and screw loosening on implant-supported prostheses. *Journal of Oral Implantology*, *28*(2), 67-73. https://doi.org/10.1563/1548-1336(2002)028%3C0067:TRBIPA%3E2.3.CO;2

Staubli, N., Walter, C., Schmidt, J. C., Weiger, R., & Zitzmann, N. U. (2017). Excess cement and the risk of peri-implant disease–a systematic review. *Clinical oral implants research*, *28*(10), 1278-1290. https://doi.org/10.1111/clr.12954

Stüker, R. A., Teixeira, E. R., Beck, J. C. P., & Costa, N. P. D. (2008). Preload and torque removal evaluation of three different abutment screws for single standing implant restorations. *Journal of Applied Oral Science*, *16*, 55-58. https://doi.org/10.1590/S1678-77572008000100011

Sun, F., Wang, L., Li, X. C., Cheng, W., Lin, Z., Ba, D. C., ... & Sun, C. S. (2020). Effect of surface modification on the long-term stability of dental implant abutment screws by plasma nitriding treatment. *Surface and Coatings Technology*, *399*, 126089. https://doi.org/10.1016/j.surfcoat.2020.126089

von Krammer, R. (1997). A simple antirotational device for implant abutment screws. *Journal of Prosthetic Dentistry*, *78*(5), 529. https://doi.org/10.1016/S0022-3913(97)70072-6

von Krammer, R. (1999). Procedure for obturating the access canal and preventing the loosening of the abutment screw in an implant-retained fixed prosthesis. *The Journal of prosthetic dentistry*, *81*(2), 234-236. https://doi.org/10.1016/S0022-3913(99)70255-6

Wang, R. R., & Fenton, A. (1996). Titanium for prosthodontic applications: a review of the literature. *Quintessence international*, *27*(6), 401-408.

Weiss, E. I., Kozak, D., Gross, M. D., & Maurice, T. (2000). Effect of repeated closures on opening torque values in seven abutment-implant systems. *The Journal of prosthetic dentistry*, *84*(2), 194-199. https://doi.org/10.1067/mpr.2000.108069

Wu, T., Fan, H., Ma, R., Chen, H., Li, Z., & Yu, H. (2017). Effect of lubricant on the reliability of dental implant abutment screw joint: An in vitro laboratory and three-dimension finite element analysis. *Materials Science and Engineering: C*, *75*, 297-304. https://doi.org/10.1016/j.msec.2016.11.041

Xiao, H., Yang, Y., Liu, Z., & Taylor, T. D. (2017). Opinions Regarding Reuse or Replacement of Implant Prosthesis Retaining Screws: A Systematic Review. *International Journal of Oral & Maxillofacial Implants*, *32*(5), 985-991.

Yao, K. T., Chen, C. S., Cheng, C. K., Fang, H. W., Huang, C. H., Kao, H. C., & Hsu, M. L. (2018). Optimization of the Conical Angle Design in Conical Implant–Abutment Connections: A Pilot Study Based on the Finite Element Method. *Journal of Oral Implantology*, *44*(1), 26-35. https://doi.org/10.1563/aaid-joi-D-17-00149

Yeo, I. S., Lee, J. H., Kang, T. J., Kim, S. K., Heo, S. J., Koak, J. Y., ... & Lee, S. Y. (2014). The effect of abutment screw length on screw loosening in dental implants with external abutment connections after thermocycling. *International Journal of Oral & Maxillofacial Implants*, *29*(1), 59-62.

Yodrux, A., Yodpijit, N., & Jongprasithpornt, M. (2019). Stress and displacement analysis of dental implant threads using three-dimensional finite element analysis. *Applied Science and Engineering Progress*, *12*(3), 216-222.

APPENDIXES

APPENDIXE A

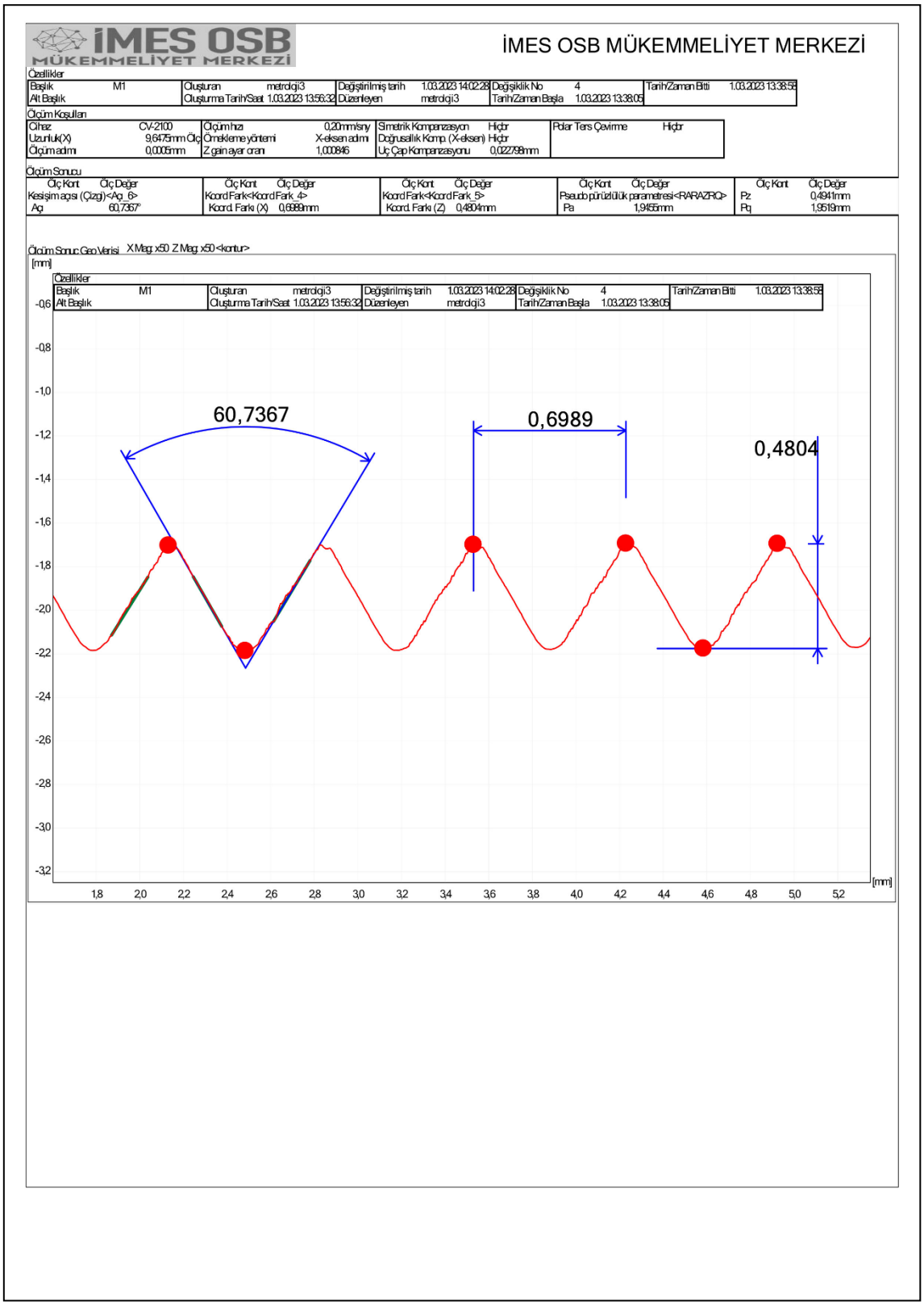


Figure A.1. Surface roughness parameters of machined screw sample 1 (M1).

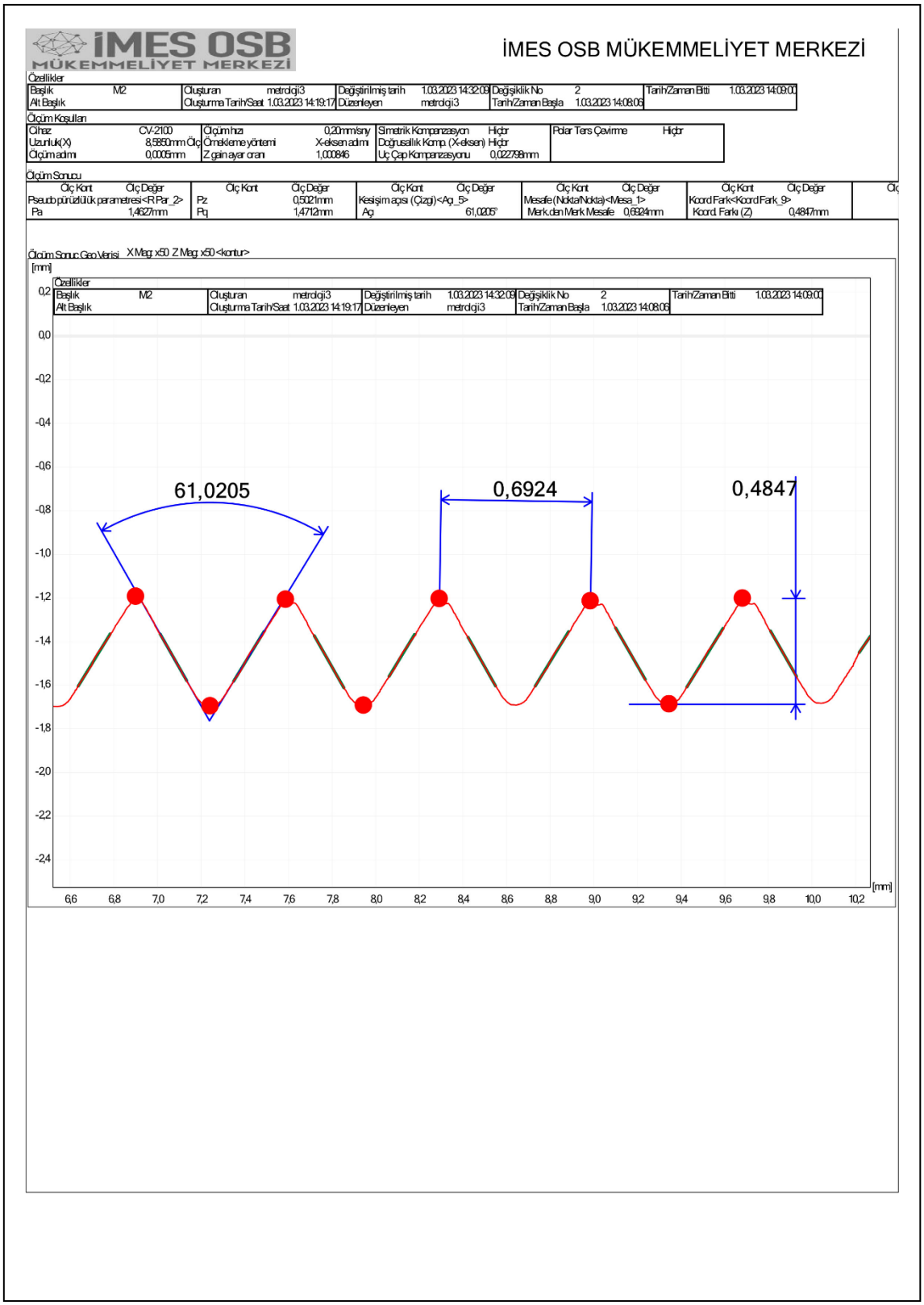


Figure A.2. Surface roughness parameters of machined screw sample 2 (M2).

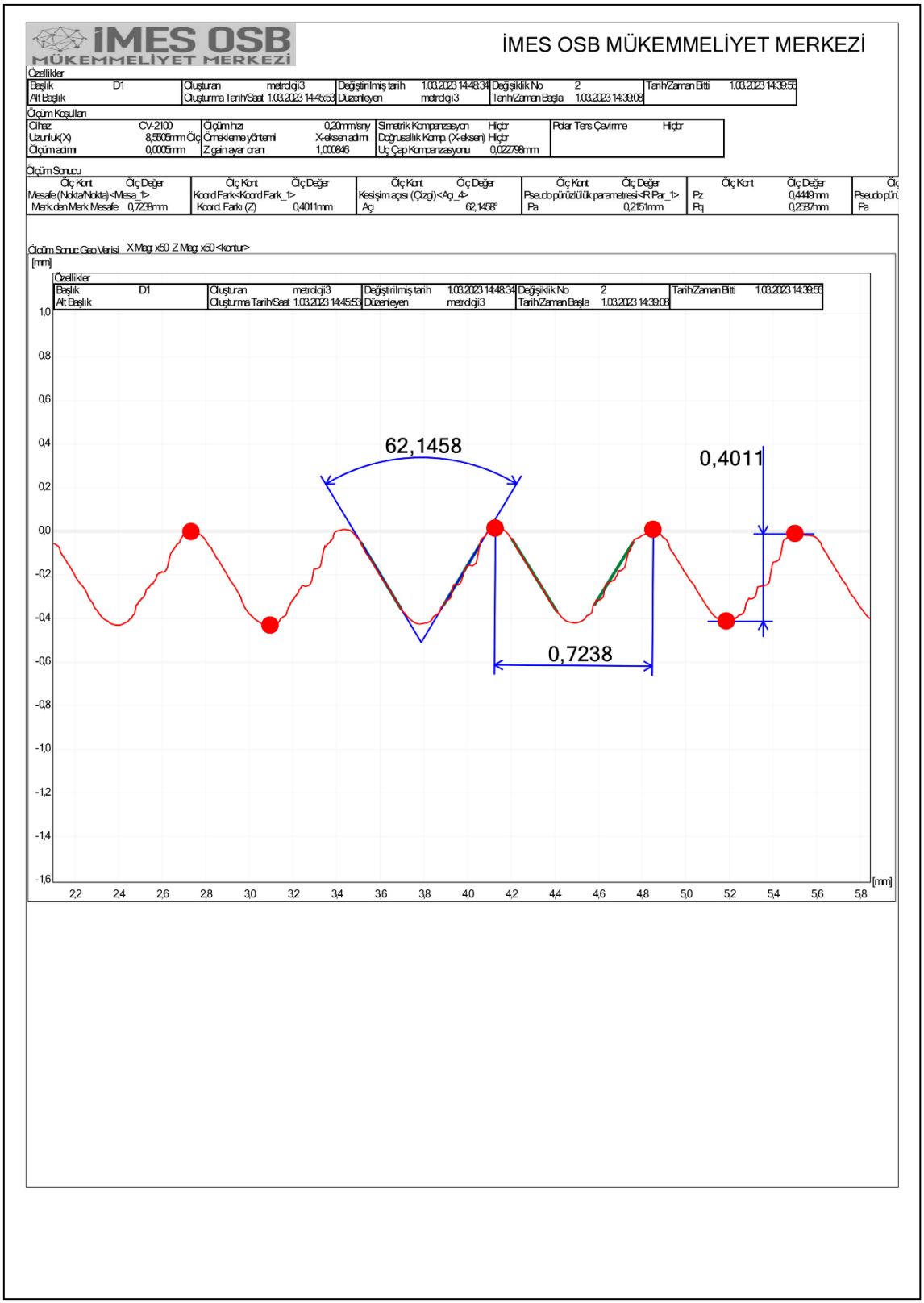


Figure A.3. Surface roughness parameters of die screw sample 1 (D1).

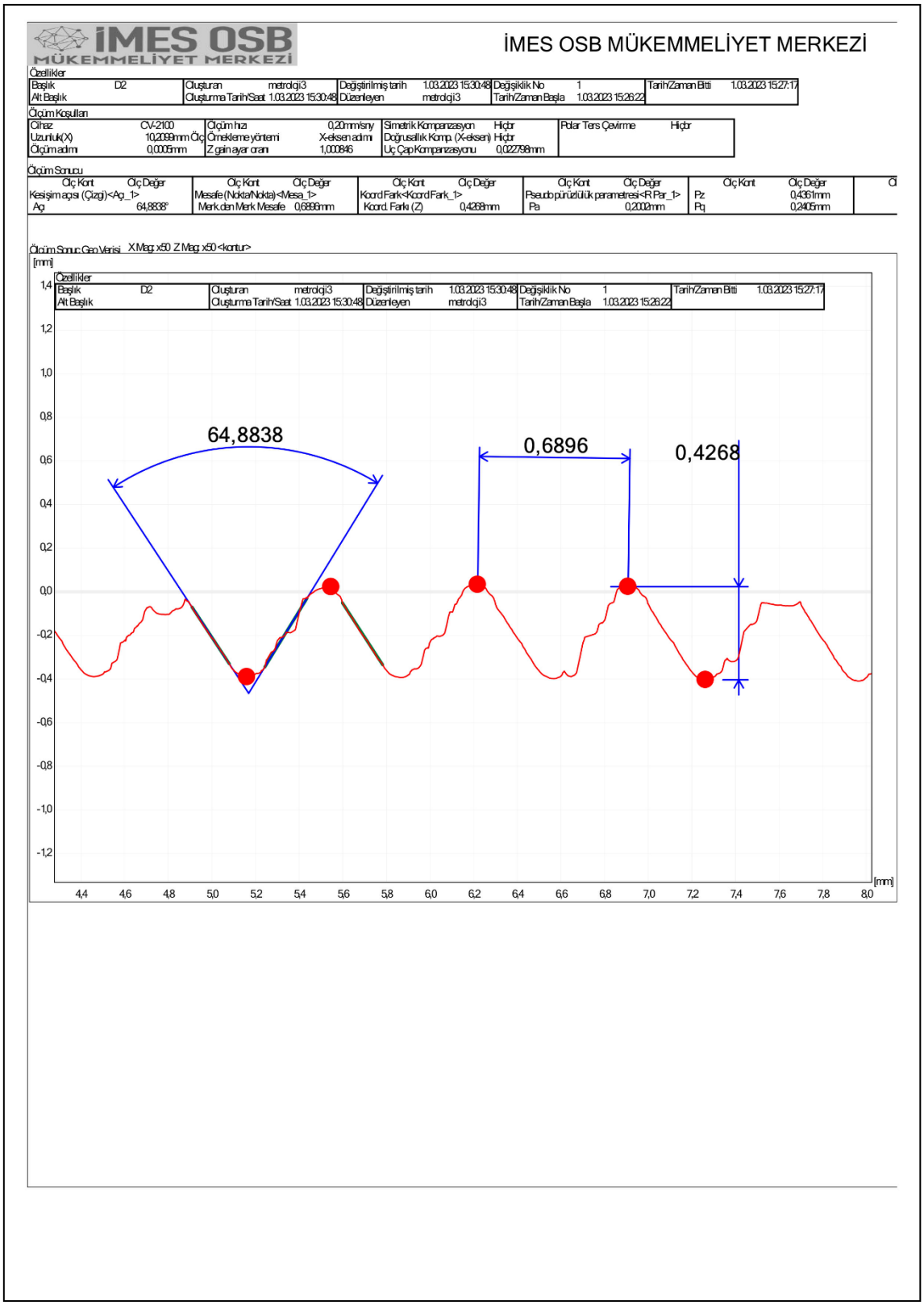


Figure A.4. Surface roughness parameters of die screw sample 2 (D2).

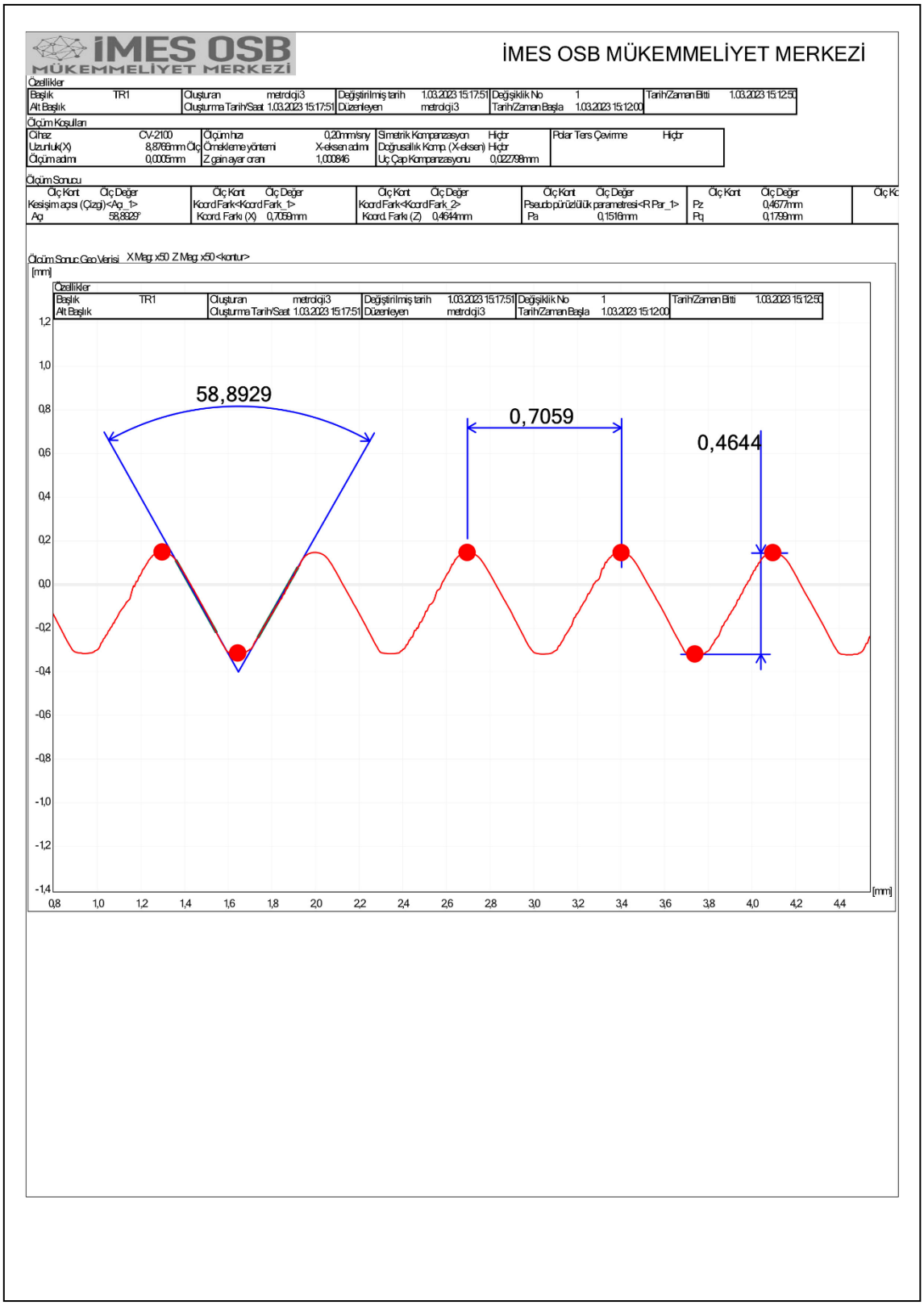


Figure A.5. Surface roughness parameters of thread-rolled screw sample 1 (TR1).

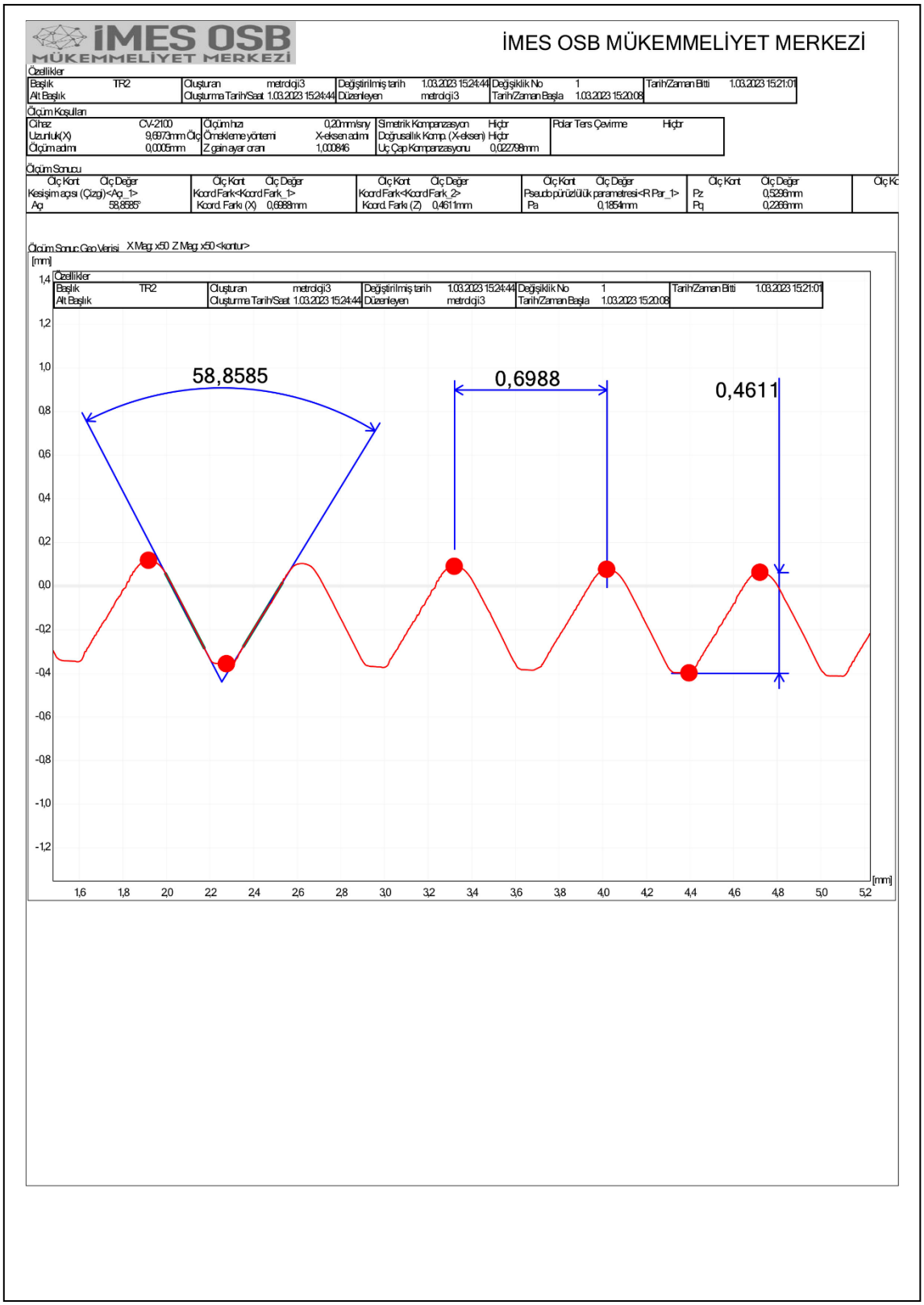


Figure A.6. Surface roughness parameters of thread-rolled screw sample 2 (TR2).

PUBLICATIONS AND WORKS

AL-sanea, A., Aktaş, S., Çelik, T., & Kişioğlu, Y. (2023). Investigation of Dental Implant Abutment Screw Surface Roughness Effects on Screw Loosening. *The Journal of prosthetic dentistry*.

AL-sanea, A., Aktaş, S., Çelik, T., & Kişioğlu, Y. (2023). Effects of the Internal Contact Surfaces of Dental Implants on Screw Loosening: A 3D Finite Element Analysis. *The Journal of prosthetic dentistry*.

AL-sanea, A., Mutlu, I., Kişioğlu, Y., & Mohamed, E. (2023). The Effect of V-Thread and Square Thread Dental Implants on Bone Stresses. *Journal of Biomimetics, Biomaterials and Biomedical Engineering, 60,* 83-96. https://doi.org/10.4028/p-3qasy2

AL-sanea, A., Çelik, T., Aktaş, S., & Kişioğlu, Y. (2023). Comparative Analysis of Torque Loss in Dental Implant Abutment Screws Manufactured Using Machining, Die, and Thread Rolling Methods. *International Marmara Sciences Congress (IMASCON 2023 SPRING)*, Kocaeli, Turkey, 9-10 June 2023.

AL-sanea, A., Çelik, T., Aktaş, S., & Kişioğlu, Y. (2022). Evaluation of the Effect of Friction Coefficient between Dental Implant Components on Dental Implant Stability Using Modal Analysis. *International Marmara Sciences Congress (IMASCON 2022 AUTUMN)*, Kocaeli, Turkey, 9-10 December 2022.

AL-sanea, A., Eltayeb, M., & Naresh Kumar, N. (2018). Simulation and Analysis of Artificial Hip Joint Using Software Modeling. *International Conference on Computer, Control, Electrical, and Electronics Engineering (ICCCEEE)*, Khartoum, Sudan, 12-14 August 2018. https://doi.org/10.1109/ICCCEEE.2018.8515835

AL-sanea, **A.**, Hussein**,** E. M., Amer, R., & Omer, A. (2018). Non-Invasive System for Detecting Malaria Parasites. *International Conference on Computer, Control, Electrical, and Electronics Engineering (ICCCEEE)*, Khartoum, Sudan, 12-14 August 2018. https://doi.org/10.1109/ICCCEEE.2018.8515814

BIOGRAPHY

Abdulrahman AL-sanea completed his primary and secondary education in his hometown, Ibb-Yemen, before setting out on an academic journey in the field of biomedical engineering. He earned his Bachelor's degree with First Class Honors from Sudan University of Science and Technology in 2017. His undergraduate thesis was titled "A Non-Invasive System for Detecting Malaria Parasites". After his graduation, AL-sanea worked roughly for two years as a teaching assistant in the Biomedical Engineering Department at the Sudan University of Science and Technology. Concurrently, he also worked in a similar capacity at Hayat University College in Khartoum. Following his undergraduate studies, Abdulrahman furthered his education by pursuing two master's degrees in biomedical engineering. He received his first master's degree from the University of Medical Sciences and Technology (UMST) in Sudan, 2022, achieving a grade of distinction. His thesis focused on the Influence of Implant Thread Design on Stress Distribution in Surrounding Bone. AL-sanea completed his second master's degree in biomedical engineering, track of biomechanics, at Kocaeli University with a thesis titled "Effects of Internal Contact Surfaces of Dental Implants and Abutment Screw Surface Roughness on Screw Loosening".